

ScreeNOT: Exact MSE-Optimal Singular Value Thresholding in Correlated Noise

David L. Donoho *

Matan Gavish †

Elad Romanov †

Abstract

We derive a formula for optimal hard thresholding of the singular value decomposition in the presence of correlated additive noise; although it nominally involves unobservables, we show how to apply it even where the noise covariance structure is not a-priori known or is not independently estimable.

The proposed method, which we call **ScreeNOT**, is a mathematically solid alternative to Cattell’s ever-popular but vague Scree Plot heuristic from 1966.

ScreeNOT has a surprising oracle property: it typically achieves *exactly*, in large finite samples, the lowest possible MSE for matrix recovery, on each given problem instance – i.e. the specific threshold it selects gives exactly the smallest achievable MSE loss among all possible threshold choices for *that* noisy dataset and *that* unknown underlying true low rank model. The method is computationally efficient and robust against perturbations of the underlying covariance structure.

Our results depend on the assumption that the singular values of the noise have a limiting empirical distribution of compact support; this model, which is standard in random matrix theory, is satisfied by many models exhibiting either cross-row correlation structure or cross-column correlation structure, and also by many situations where there is inter-element correlation structure. Simulations demonstrate the effectiveness of the method even at moderate matrix sizes. The paper is supplemented by ready-to-use software packages implementing the proposed algorithm.

Key Words. Singular value thresholding, Optimal threshold, Scree Plot, Low-rank matrix denoising

Code Supplement. Implementation of the proposed algorithm, scripts generating all figures in this paper, and many additional simulations are available at the code supplement [Donoho et al., 2020] and permanently deposited at the Stanford Digital Repository¹. Note that Python, R and Matlab packages implementing the ScreeNOT algorithm have been published, see the code supplement for more information.

Acknowledgements. This research was made possible by the United States – Israel Binational Science Foundation (BSF) Grant 2016201 “Frontiers of Matrix Recovery” and partially supported by NSF DMS grants no. 1407813, 1418362, and 1811614. ER was supported by Israel Science Foundation grant no. 1523/16 and an Einstein-Kaye Fellowship from the Hebrew University of Jerusalem.

*Department of Statistics, Stanford University

†School of Computer Science and Engineering, Hebrew University of Jerusalem

¹<https://purl.stanford.edu/py196rk3919>

Contents

1	Introduction	3
2	The ScreeNOT Procedure: User-level description	6
2.1	Procedure API	6
2.1.1	Inputs	6
2.1.2	Outputs	6
2.2	Example in a stylized application	6
2.3	Internals of the Procedure	7
2.4	How the procedure works on the stylized application	8
3	Setup and background from random matrix theory	9
3.1	Background from random matrix theory	11
3.2	Noise matrices with correlated columns	14
4	Results	16
4.1	A theory for optimal singular value thresholding	16
4.2	The ScreeNOT algorithm	18
4.3	Stability of ScreeNOT	21
5	Numerical experiments	21
6	Proofs	24
6.1	The asymptotic loss at a fixed threshold	24
6.2	Achieving oracle loss	27
6.3	Estimating $T_\gamma(F_Z)$	29
A	Proof of Lemma 8	34
B	Proof of Proposition 2	34
C	Additional numerical experiments	36
C.1	Noise distributions	36
C.2	Description of experiments	37
C.3	Distribution: Marcenko-Pastur, $\gamma = 1.0$	39
C.4	Distribution: Chi10, $\gamma = 0.5$	43
C.5	Distribution: Chi10, $\gamma = 1.0$	47
C.6	Distribution: Fisher3n, $\gamma = 0.5$	51
C.7	Distribution: Fisher3n, $\gamma = 1.0$	55
C.8	Distribution: Mix2, $\gamma = 0.5$	59
C.9	Distribution: Mix2, $\gamma = 1.0$	63
C.10	Distribution: Unif[1,10], $\gamma = 0.5$	67
C.11	Distribution: Unif[1,10], $\gamma = 1.0$	71
C.12	Distribution: PaddedIdentity, $\gamma = 0.5$	75
C.13	Distribution: PaddedIdentity, $\gamma = 1.0$	79

1 Introduction

Across a wide variety of scientific and technical fields, practitioners have found many valuable applications of *singular value thresholding* (SVT). This procedure starts from the singular value decomposition (SVD), which represents the data matrix Y as

$$Y = \sum_{i=1}^{\min(n,p)} y_i \cdot \mathbf{u}_i \mathbf{v}_i^\top, \quad (1)$$

using the empirical singular values $\{y_i\}_{i=1}^{\min(n,p)}$, and the empirical left- and right- singular vectors of Y , denoted here \mathbf{u}_i and \mathbf{v}_i .

In such applications, it is generally claimed that the small singular values represent ‘noise’ and the large singular values ‘signal’; practitioners attempt to separate signal from noise by setting a threshold θ (say), and using, in place of Y , the partial reconstruction containing only would-be signal components:

$$\hat{X}_\theta = \sum_i y_i \mathbb{1}_{\{y_i > \theta\}} \cdot \mathbf{u}_i \mathbf{v}_i^\top. \quad (2)$$

How do practitioners determine the threshold θ ? Often, by eye. They plot the ordered singular values and spot ‘elbows’. Sometimes, they give this a scholarly veneer by saying they are using the ‘scree-plot method’; they might even formally cite the originator of this folk-tradition, [Cattell, 1966] which still gets more than 1000 citations yearly. According to the method prescribed in that paper, the practitioner plots the values $\{y_i\}$ and uses her *eyes* to distinguish between ‘signal’ and ‘noise’ singular values of Y .

How *should* they determine the threshold? Relevant theory and methodology literature spans multiple disciplines over multiple decades; we mention only a few entry points, including: [Wold, 1978, Jackson, 1993, Lagerlund et al., 1997, Edfors and Sandell, 1998, Alter et al., 2000, Achlioptas and McSherry, 2001, Azar et al., 2001, Jolliffe, 2005, Price et al., 2006, Hoff, 2006, Bickel and Levina, 2008, Owen and Perry, 2009, Perry, 2009, Chatterjee, 2015, Gavish and Donoho, 2014]. Progress has been made in our understanding of the underlying problem, and many valuable quantitative approaches have been developed - to which we here add one more. Our contribution relies on recent advances in random matrix theory which point, we think convincingly, to the method introduced here. This method typically offers the exact optimal loss available on each specific, finite dataset Y .

Our task formalization supposes that: (a) there is an underlying matrix X of fixed rank r - though X and even its rank r are unknown to us; (b) only a potentially loose upper bound on the signal rank r is known; (c) the data matrix Y has the signal+noise form $Y = X + Z$, where Z is a noise matrix with a general covariance structure - also unknown to us; (d) we use hard thresholding of singular values, exactly as in (2) above²; (e) we adopt squared error *loss*³:

$$\text{SE}[X|\theta] = \|\hat{X}_\theta - X\|_F^2. \quad (3)$$

As goal, we literally aim to choose a loss-minimizing value $\theta_{\text{opt}} = \theta_{\text{opt}}(Y|X)$ solving:

$$\text{SE}[X|\theta_{\text{opt}}] = \min_{\theta} \text{SE}[X|\theta]. \quad (4)$$

²And not some variant, such as soft thresholding or a more general shrinkage.

³ $\|X\|_F^2 = \sum_{i,j} X_{i,j}^2$ denotes the squared Frobenius norm.

Aiming for $\theta_{\text{opt}}(Y|X)$ may seem overambitious, as we know only the data matrix Y , and not X . Wait and see.

Essentially this problem was studied previously by two of the authors in the special case of white noise. [Gavish and Donoho, 2014] supposed that the underlying noise Z matrix has i.i.d Gaussian zero-mean entries and the problem is scaled so that the columns of Z have unit Euclidean squared norm in expectation, and considered a sequence of increasingly large problems. In the square case, when Y has as many rows as columns: the authors found results⁴ which, in light of our results below, say that, with eventually overwhelming probability, we have $\theta_{\text{opt}} = 4/\sqrt{3}$. Their analysis relied on then-recent advances in the ‘Johnstone spiked model’ of random matrix theory [Johnstone, 2001]; they proposed a method for white noise with unknown variance, where the threshold formula became $\theta_{\text{opt}} \approx 4/\sqrt{3} \cdot \frac{y_{\text{med}}}{\sqrt{n \cdot .6528}}$, where y_{med} denotes the median empirical singular value of Y .⁵

Understanding the white noise case cannot be the end of the story. Practitioners ordinarily don’t know that their noise is white, and in fact realistic noise models can include correlations between columns, rows, or even general row-column combinations. Fortunately, a broad range of noise models can be studied using appropriate advances that have been made in random matrix theory. In this broader context, as we show, a more general formula for the optimal threshold can be given, which of course reduces to $4/\sqrt{3}$ in the above ‘square-matrix in white noise’ case, but which is inevitably quite a bit more sophisticated in general.

Section 2 below describes ScreeNOT, our proposed deployment of this formula on actual data. The acronym NOT stands for *Noise-adaptive Optimal Thresholding*; ‘adaptive’ refers to the algorithm’s optimality across a wide range of unknown noise covariances. The prefix ‘Scree’ reminds us that, still today, in many cases, the alternative would simply be ‘eyeballing’ the Scree Plot [Cattell, 1966]. Cattell and his many followers clearly believed that *something*, some information, in the scree plot – namely, in the collection of data singular values $\{y_i\}$ – could tell us where the noise stopped and the signal began. But what exactly? In a very concrete sense, the ScreeNOT algorithm shows that the information needed to separate signal from noise truly been there in the distribution of empirical singular values, where they all hoped it was - the information now being clearly identified as specific functional of the singular values.

The method, once implemented, surprised us by the *finite-sample* optimality it exhibited; in simulations at reasonable problem sizes it typically achieves the exact minimal loss (4) for the given dataset, even though the method is not entitled to know the underlying low-rank model X or specifics of the noise model on Z ; we initially expected a weaker and more ‘asymptotic’ optimality property, perhaps similar to the one shown in [Gavish and Donoho, 2014]. Our analysis below proves typicality of such exact optimality in finite samples. This strong optimality is partly due to the penetrating nature of random matrix theory; but also to the very specific task: minimizing squared error loss (3) of singular value thresholding (2).

Underlying Analysis. Hoping to make the paper helpful to prospective users of the proposed method, we have made the Introduction and also Section 2 mostly independent of the analysis to come; however, we now very briefly offer mathematically-oriented readers some

⁴That is, the authors of [Gavish and Donoho, 2014] adopted a slightly different viewpoint involving asymptotic MSE, and showed that $4/\sqrt{3}$ is optimal, whereas we consider here exact finite sample MSE loss, and show that with eventually overwhelming probability, $4/\sqrt{3}$ is exactly optimal *on each typical realization*.

⁵ $\sqrt{.6528}$ is approximately the median of the standard quarter-circle law; see the original paper.

insight about the approach being followed in later sections and the tools being developed there.

At heart, this paper concerns the asymptotic analysis of a sequence of matrix recovery problems where the problem sizes n and p grow to ∞ in a proportional fashion. We assume that the matrix X has r nonzero singular values x_1, \dots, x_r which are fixed independently of n and p . About the sequence of random noise matrices $Z = Z_{n,p}$, we assume that the sequence of empirical cumulative distribution functions (CDF's) of noise singular values converges to a compactly supported distribution F_Z with certain qualitative restrictions at boundary of the support.

Using results of Benaych-Georges and Nadakuditi [Benaych-Georges and Nadakuditi, 2012a], we obtain an expression for an asymptotically optimal hard threshold, as a *functional* $T(\cdot)$ of the limiting CDF of noise singular values F_Z . The functional is continuous and even differentiable in certain senses.

Admittedly, the limiting CDF of noise singular values F_Z is not observable to the statistician, as we only observe a sample of the signal+noise singular values mixed together. Performing a kind of amputation and prosthetic extension on the CDF F_Y of singular values of Y , which we do observe, we construct a modified empirical CDF \hat{F}_n which consistently estimates the limiting CDF of noise-only singular values. Applying the hard threshold selection functional to this modified empirical CDF \hat{F}_n gives our proposed method, in the form $\hat{\theta} = T(\hat{F}_n)$. As we show in Section 2, there is a quite explicit and computationally tractable algorithm for computing $T(\hat{F}_n)$, which we label **ScreeNOT**.

Owing to the continuity of the hard threshold functional $T(\cdot)$, and the consistency of the constructed CDF, the resulting method is a consistent estimator of the underlying asymptotically optimal threshold $T(F_Z)$. We also prove a finite-sample optimality of the method. Specifically, the ScreeNOT algorithm is shown to be exactly optimal for squared error loss with high probability, in large-enough finite samples, under very general model assumptions. For generic configurations of signal singular values $(x_i)_{i=1}^r$, there is, in large finite samples, an *optimal interval* of thresholds, all achieving the optimal MSE at that realization; the consistency of the optimal threshold estimator implies that eventually for large-enough n , with overwhelming probability, the proposed method achieves the exact optimal MSE loss.

Outline. This paper is organized as follows. In Section 2 we offer a practical, succinct description of the ScreeNOT algorithm, for the convenience of prospective users. In Section 3 we introduce the signal+noise model used and survey relevant results from random matrix theory. In Section 4 we state our main results regarding the optimality and stability properties of ScreeNOT, both in finite matrix size and asymptotically as the matrix size grows to infinity. In Section 5 we demonstrate the mathematical results in various simulations and numerical examples; for space considerations only a handful of figures are shown, with most simulation results deferred to Appendix C and available in the code supplement [Donoho et al., 2020]. The results are proved in Section 6, with some proofs referred to Appendix A and Appendix B.

Reproducibility advisory. Implementation of the proposed algorithm, scripts generating all figures in this paper, and many additional simulations have been permanently deposited and are available at the code supplement [Donoho et al., 2020].

2 The ScreeNOT Procedure: User-level description

In this section we give a brief self-contained description of our proposed procedure. Note that Python, R and Matlab packages implementing the ScreeNOT algorithm have been published, see the code supplement [Donoho et al., 2020] for more information.

2.1 Procedure API

ScreeNOT selects a hard threshold for singular values, which can in finite samples give the optimal MSE approximation of a low rank matrix from a noisy version; the noise may be correlated, and the threshold will adapt to that appropriately.

2.1.1 Inputs

The user provides these inputs to ScreeNOT :

- y:** the singular values $y_1 \dots, y_{\min(n,p)}$ of the data matrix Y ;
- n, p :** size parameters of the data matrix Y .
- k :** upper bound on the rank r of the underlying unknown signal matrix X which is to be recovered. This upper bound may be very loose.

2.1.2 Outputs

ScreeNOT returns $\hat{\theta} = \hat{\theta}(Y)$, the value to be used in singular value thresholding.

To use the threshold, the user should reconstruct an approximation to the underlying signal matrix X using the empirical singular values y_i and the empirical singular vectors \mathbf{u}_i and \mathbf{v}_i as follows:

$$\hat{X}_n = \sum_i y_i \mathbb{1}_{\{y_i > \hat{\theta}\}} \cdot \mathbf{u}_i \mathbf{v}_i^\top.$$

In this reconstruction, the singular values smaller than $\hat{\theta}$ are judged to be noise and the corresponding singular decomposition components are ignored.

2.2 Example in a stylized application

We next construct a synthetic-data example, in which we know ground truth for demonstration purposes. The synthetic data $Y = X + Z$ and the invocation of ScreeNOT are based on these ingredients.

Signal X : The underlying signal matrix, unbeknownst to the hypothetical user, has rank 4, with singular values $(x_1, \dots, x_4) = (4, 3, 2, 1)$.

Noise Z : The underlying noise, unbeknownst to the hypothetical user, follows an $AR(1)$ process in the row index, within each column. The $AR(1)$ process has parameter $\rho = .2$, and additionally each entry is divided by \sqrt{n} , so to have variance $1/n$.⁶

Problem Size: $n = p = 500$

Rank bound: $k = 12$. The user specifies a bound of $k = 12$ on the possible rank of the signal.

Figure 1 shows a so-called scree plot [Cattell, 1966] of the first 30 empirical singular values y_i . For this particular instance, it is verified (by exhaustive search) that the minimal loss is attained by retaining the first three principal components of Y ; in other words, thresholding at any point $\theta \in (y_3, y_4)$ is optimal. The threshold $\hat{\theta}$ returned by the ScreeNOT procedure is indicated by the green horizontal line, and, indeed, it falls inside the optimal interval.

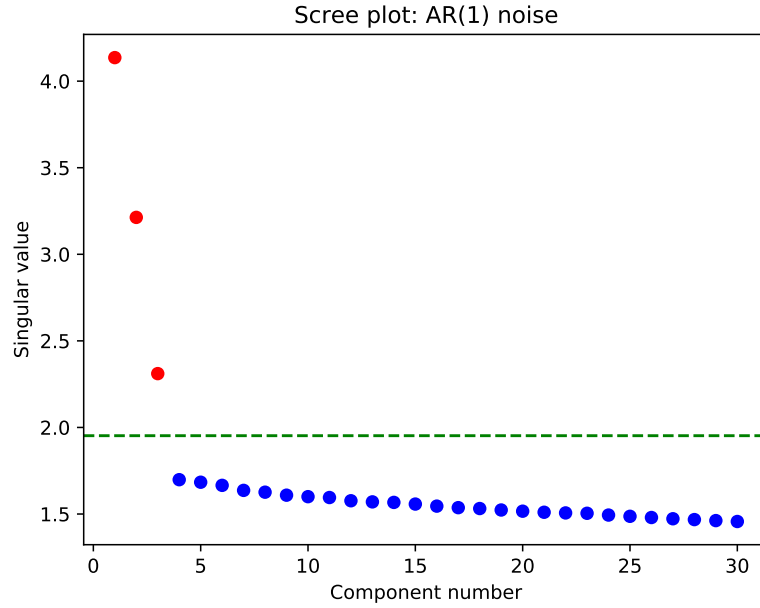


Figure 1: Scree plot for the stylized example of Section 2.2. Horizontal axis: singular value index, where the singular values y_i of the data matrix Y are sorted in decreasing order. Vertical axis: singular values y_i . Dashed green line: the optimal threshold calculated by ScreeNOT.

2.3 Internals of the Procedure

We briefly describe the computational task performed by ScreeNOT.

Step 1. Sort the singular values in non-increasing order: $y_1 \geq \dots \geq y_p$.

Step 2. Compute the “pseudo singular values”:

$$\tilde{y}_i = y_{k+1} + \frac{1 - \left(\frac{i-1}{k}\right)^{2/3}}{2^{2/3} - 1} (y_{k+1} - y_{2k+1}) \quad \text{for } i = 1, \dots, k,$$

⁶That is, the columns of Z are independent and distributed as \mathbf{z}/\sqrt{n} , where the random vector \mathbf{z} has entries:

$$z_1 = \varepsilon_1, \quad z_i = \rho \cdot z_{i-1} + (1 - \rho) \cdot \varepsilon_i \quad \text{for } 2 \leq i \leq p,$$

where $\varepsilon_1, \dots, \varepsilon_p \stackrel{\text{iid}}{\sim} \mathcal{N}(0, 1)$.

and set $\tilde{y}_i = y_i$ for $i = k + 1, \dots, p$.⁷

Step 3. Define the four scalar functions $\varphi, \tilde{\varphi}, \varphi', \tilde{\varphi}'$ by

$$\varphi(y) = \frac{1}{p} \sum_{i=1}^n \frac{y}{y^2 - \tilde{y}_i^2}, \quad \varphi'(y) = -\frac{1}{p} \sum_{i=1}^n \frac{y^2 + \tilde{y}_i^2}{(y^2 - \tilde{y}_i^2)^2},$$

and

$$\tilde{\varphi}(y) = \gamma \varphi(y) + \frac{1 - \gamma}{y}, \quad \tilde{\varphi}'(y) = \gamma \varphi'(y) - \frac{1 - \gamma}{y^2}.$$

Now define

$$\Psi(y) = y \cdot \left(\frac{\varphi'(y)}{\varphi(y)} + \frac{\tilde{\varphi}'(y)}{\tilde{\varphi}(y)} \right).$$

Step 4. Assuming that $\tilde{y}_1, \dots, \tilde{y}_p$ are not all zero, the function $y \mapsto \Psi(y)$ can be shown to be continuous and strictly increasing for $y > \tilde{y}_1$. Moreover, $\lim_{y \searrow \tilde{y}_1} \Psi = -\infty$ and $\Psi(\infty) = -2$. The computed hard threshold is the unique value $\hat{\theta}$ satisfying

$$\Psi(\hat{\theta}) = -4. \tag{5}$$

This equation is then solved numerically (by binary search, say).

Step 5. The algorithm returns the value $\hat{\theta}$.

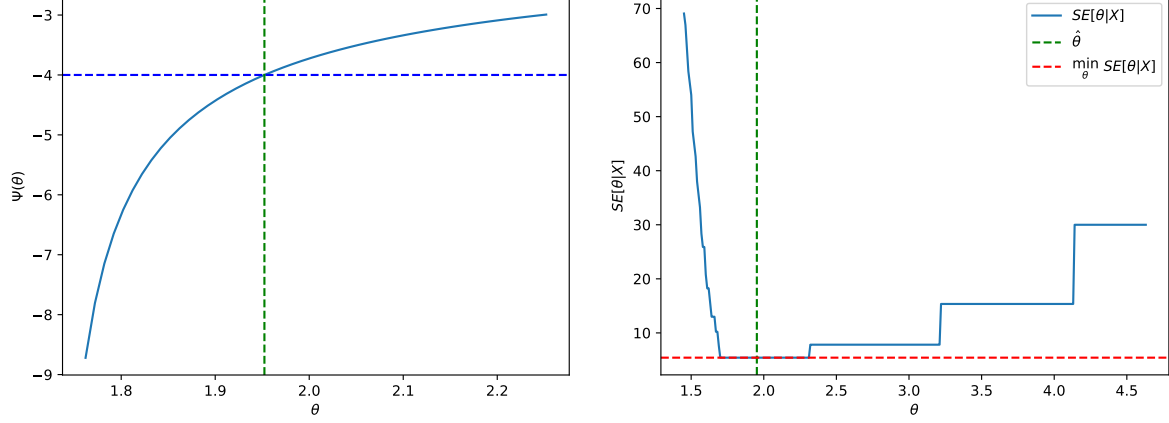
Evidently, the procedure as stated costs $O(n \log(n))$ flops; the dominant cost is sorting the singular values; ordinarily of course, sorting is performed anyway as part of a standard SVD. In that situation, the additional computational effort is $O(n)$, which is unimportant compared to the cost of the underlying SVD.

2.4 How the procedure works on the stylized application

Figure 2(a) shows a plot of $\Psi(\theta)$ as a function of θ . The horizontal blue line indicates the desired level -4 . The vertical green line indicates the crossing point, $\hat{\theta}$, which is the value returned by ScreeNOT.

Figure 2(b) shows a plot of the loss $\text{SE}[\theta|X]$ versus θ . The red horizontal line shows the optimum achievable loss. The green vertical line shows the threshold selected by the procedure. It intersects the loss curve within the optimal level and the achieved loss is therefore optimal.

⁷We assume that $2k + 1 < p$. Our proposed estimator is expected to perform poorly when k is large compared to p .



(a) Solving the master equation (5)

(b) MSE loss $SE[\theta|X]$ over θ

Figure 2: Calculation of the optimal threshold $\hat{\theta}$ on the stylized example of Section 2.2. (a) *Left panel*: Horizontal axis: candidate thresholds θ . Vertical axis: The function $\Psi(\theta)$. The ScreeNOT algorithm solves the equation $\Psi(\theta) = -4$ for θ . Vertical green line shows the solution, denoted by $\hat{\theta}$. This is the value returned by ScreeNOT. (b) *Right panel*: The MSE loss function $SE[\theta|X]$ for the stylized example of Section 2.2, plotted over candidate thresholds θ . There is an interval of values θ all achieving the lowest possible loss; The threshold $\hat{\theta}$ returned by ScreeNOT (shown by the vertical green line) is located inside this optimal interval.

3 Setup and background from random matrix theory

The rest of this paper is dedicated to formal analysis of the ScreeNOT algorithm. To that end, we now define a precise signal+noise model and set up the necessary notation.

An asymptotic model for low-rank matrices observed in additive noise. To recap, let X_n be an unknown n -by- p matrix, to be estimated. We observe a noisy measurement of X_n , $Y_n = X_n + Z_n$, where Z_n is a noise matrix, which is statistically independent of X_n . Our analysis employs an asymptotic framework originating in Random Matrix Theory, and considers a sequence of such problems $n, p \rightarrow \infty$, with the following generative assumptions.

1. **Limiting shape:** the dimensions n, p tend to infinity together at a fixed ratio $p/n \rightarrow \gamma$. More concretely, fix $\gamma \in (0, 1]$ and set $p = p_n = \lceil \gamma n \rceil$. Denoting $\gamma_n = p_n/n$, of course, $\gamma \leq \gamma_n < \gamma + \frac{1}{n}$ and $\gamma_n \rightarrow \gamma$ as $n \rightarrow \infty$.
2. **Fixed signal rank and singular values:** The matrix X_n has fixed rank $r = \text{rank}(X_n)$ and fixed singular values. Specifically, let r be constant, and fix r positive and distinct numbers $x_1 > \dots > x_r > 0$. X_n is the matrix

$$X_n = \sum_{i=1}^r x_i \mathbf{a}_{i,n} \mathbf{b}_{i,n}^\top,$$

where $\mathbf{a}_{i,n} \in \mathbb{R}^n$ (resp. $\mathbf{b}_{i,n} \in \mathbb{R}^p$) for $i = 1, \dots, r$ are sequences of left (resp. right) singular vectors of X_n , obeying a generative assumption as described next. We let $\mathbf{x} = (x_1, \dots, x_r)$ denote the vector of singular values and we refer to either the matrix X or just \mathbf{x} as the *signal*. We refer to the vector of singular values $\mathbf{x} = (x_1, \dots, x_r)$ as the *signal*.

3. **Incoherent signal singular vectors.** The vectors $\mathbf{a}_{1,n}, \dots, \mathbf{a}_{r,n}$ (resp. $\mathbf{b}_{i,n}$) constitute a random, uniformly distributed orthonormal r -frame in \mathbb{R}^n (resp. in \mathbb{R}^p).⁸
4. **Compactly supported, limiting bulk distribution of noise singular values.** Each matrix Z_n is statistically independent of X_n . Let $z_{1,n}, \dots, z_{p,n}$ denote its singular values, with empirical CDF F_{Z_n} , $F_{Z_n}(z) = p^{-1} \sum_{i=1}^p \mathbf{1}_{\{z_{i,n} \leq z\}}$. There is a *limiting empirical CDF* (LECDF) F_Z such that $F_{Z_n} \rightarrow F_Z$ a.s. at continuity points.

Moreover, we assume that F_Z is compactly supported⁹ and denote the upper edge of the support (sometimes called the *noise bulk edge*) by

$$\mathcal{Z}_+ \equiv \mathcal{Z}_+(F_Z) = \sup \{z : F_Z(z) < 1\}.$$

We also assume that F_Z is nontrivial (dF_Z is not a single atom at $z = 0$), in other words, $\mathcal{Z}_+(F_Z) > 0$. Note that neither the distribution F_Z nor its bulk edge $\mathcal{Z}_+(F_Z)$ are assumed to be known to the statistician.

5. **No outliers straying from the bulk.** Asymptotically, no singular values of Z_n can be found above the bulk edge:

$$z_{1,n} = \|Z_n\| \xrightarrow{a.s.} \mathcal{Z}_+(F_Z).$$

6. **Thickness of the bulk edge.** The following condition holds:

$$\lim_{y \rightarrow \mathcal{Z}_+(F_Z)} \int (y - z)^{-2} dF_Z(z) = \infty,$$

where the limit is taken from the right. That is, F_Z puts “sufficient” mass near the upper edge of its support. Under this condition, when the signal singular values x_i are sufficiently small, the amount of “information” one can obtain about the corresponding singular vectors $\mathbf{a}_{i,n} \mathbf{b}_{i,n}^\top$ from the leading singular vectors of Y_n also vanishes.

This assumption is by no means esoteric. For example, suppose that F_Z has a continuous density f_Z in a neighborhood of $z_+ = \mathcal{Z}_+(F_Z)$, where it behaves like $f_Z(z) \sim C(z - z_+)^{\alpha}$ as $z \rightarrow z_+$; here $\alpha > 0$ is some exponent. Then this condition holds whenever $\alpha \leq 1$. In Section 3.2, we mention a broad class of noise matrices Z_n for which this property holds with $\alpha = 1/2$.

Class of estimators and performance measure. Our goal is to estimate X_n . We consider the family of singular value hard-thresholding estimators: $\hat{X}_\theta = \hat{X}_\theta(Y_n)$, where

$$\hat{X}_\theta = \sum_{i=1}^p y_{i,n} \mathbf{1}_{\{y_{i,n} > \theta\}} \cdot \mathbf{u}_{i,n} \mathbf{v}_{i,n}^\top, \quad (6)$$

where $Y_n = \sum_{i=1}^p y_{i,n} \mathbf{u}_{i,n} \mathbf{v}_{i,n}^\top$ is an SVD. We measure the error with respect to Frobenius norm (squared error)¹⁰, where we denote:

$$\text{SE}_n[\mathbf{x}|\theta] = \|X_n - \hat{X}_\theta(Y_n)\|_F^2. \quad (7)$$

⁸In other words, $\mathbf{a}_{1,n}, \dots, \mathbf{a}_{r,n}$ are sampled from the $O(n)$ -invariant distribution on the Stiefel manifold $V_r(\mathbb{R}^n)$. Equivalently, one can assume that $\mathbf{a}_{i,n}$ and $\mathbf{b}_{i,n}$ are any arbitrary sequences of orthonormal r -frames, and the distribution of Z_n is invariant to multiplication by $O(n)$ to the left and by $O(p)$ to the right.

⁹This will seem strange to many statisticians when they first encounter it; but note that if Z_n is a standard Gaussian white noise, then even though the distribution of matrix entries is not compactly supported, the limiting bulk distribution of singular values is compactly supported, in $[(1 - \sqrt{\gamma}), (1 + \sqrt{\gamma})]$.

¹⁰Recall that for a matrix A , $\|A\|_F^2 = \sum_{i,j} |A_{i,j}|^2$.

Our task is to choose θ , so as to make $\text{SE}_n[\mathbf{x}|\theta]$ as small as possible, in an appropriate sense (note that $\text{SE}_n[\mathbf{x}|\theta]$ is a random variable - we *do not* take the expectation of X_n and Y_n). The best possible performance is given by the **Oracle Loss**

$$\text{SE}_n^*[\mathbf{x}] = \min_{\theta \geq 0} \text{SE}_n[\mathbf{x}|\theta], \quad (8)$$

which is the best loss one can achieve over the family of singular value hard-threshold estimators, *even knowing the true signal* X_n . Our goal in this paper is to develop a threshold selector that, “typically for large n ”, attains the oracle loss $\text{SE}_n^*[\mathbf{x}]$. Note that the oracle loss $\text{SE}_n^*[\mathbf{x}]$ is also a random variable, and it is not a priori clear how to estimate it. An important observation is that the (random) function $\theta \mapsto \text{SE}_n[\mathbf{x}|\theta]$ is piecewise constant, with finitely many jumps (specifically, these are at the singular values of Y_n : $y_{1,n}, \dots, y_{p,n}$). In particular, the minimum of $\text{SE}_n[\mathbf{x}|\theta]$ is attained not strictly at a point, but on an *interval* (or a union of intervals).

3.1 Background from random matrix theory

The Spiked Model. Our perspective on the matrix denoising problem extends the one proposed by Perry [Perry, 2009] and Shabalin and Nobel [Shabalin and Nobel, 2013]. In the model they proposed, which was inspired by Johnstone’s Spiked Covariance model [Johnstone, 2001], one works under the same model $Y_n = X_n + Z_n$ as described above, but specifically assumes that the noise matrix Z_n is column-normalized and white, namely, that its entries are properly scaled *i.i.d* random variables. This model’s close sibling, the Spiked Model for high-dimensional covariance, has been extensively studied in the probability and statistics literature, to such an extent that we cannot point to all of the existing literature here. Seminal works such as [Bai and Yao, 2008, Baik and Silverstein, 2006, Paul, 2007] and others have shown that the randomness in the Spiked Model can be neatly described in terms of the so-called BBP phase transition, similar to the one discovered in [Baik et al., 2005]; and of the displacement of the sample eigenvalues relative to the population eigenvalues; and of the rotation of the sample eigenvectors relative to the populations eigenvectors.

In the matrix denoising setup we consider here, the model described by our assumptions above has been studied in [Benaych-Georges and Nadakuditi, 2012b], and the same three underlying phenomena were identified and quantified:

1. **BBP phase transition:** Let $z_+ = \mathcal{Z}_+(F_Z)$ denote the noise bulk edge. There is a functional $\mathcal{X}_+(F_Z, \gamma)$ that depends on the LECDF F_Z and the asymptotic shape γ that defines an important threshold phenomenon in the behavior of limiting empirical singular values. Setting $x_+ = \mathcal{X}_+(F_Z, \gamma)$, then for any $i = 1, \dots, r$ where $x_i \leq x_+$,

$$y_{i,n} \xrightarrow{a.s.} z_+, \quad n \rightarrow \infty. \quad (9)$$

In short, *sufficiently small signal singular values* x_i *do not produce outliers beyond the noise bulk edge*. As we are about to see, the situation for $x_i > x_+$ is quite different. The split between $x_i \gtrless x_+$ is sometimes called the Baik-Ben Arous-Péché (BBP) phase transition, after the original example of this type [Baik et al., 2005].

2. **Limiting location of outlier singular values:** The limiting value of $y_{n,i}$ is *not* its underlying population counterpart x_i . There is instead a functional $\mathcal{Y}(x; F_Z, \gamma)$, depending on F_Z and γ , describing this limiting behavior. The function of x obtained by fixing F_Z , and γ

- $\mathcal{Y}(x) \equiv \mathcal{Y}(x; F_Z, \gamma)$ - explains how the asymptotic limit varies with theoretical singular value x . For any $i = 1, \dots, r$ where $x_i \geq x_+ \equiv \mathcal{X}_+$,

$$y_{i,n} \xrightarrow{a.s.} y_{i,\infty} = \mathcal{Y}(x_i), \quad n \rightarrow \infty. \quad (10)$$

The function $x \mapsto \mathcal{Y}(x)$ is strictly increasing and one-to-one between $[x_+, \infty)$ and $[z_+, \infty)$.

3. **No limiting cross-correlation of non-corresponding principal subspaces:** For $i \neq j$, empirical dyad $\mathbf{u}_{n,i} \mathbf{v}_{n,i}^T$ ultimately decorrelates from each of the non-corresponding population dyads $\mathbf{a}_{n,j} \mathbf{b}_{n,j}^T$. For any $i, j = 1, \dots, r$ such that $i \neq j$,

$$\langle \mathbf{a}_{n,i}, \mathbf{u}_{n,i} \rangle \cdot \langle \mathbf{b}_{n,j}, \mathbf{v}_{n,j} \rangle \xrightarrow{a.s.} 0, \quad n \rightarrow \infty. \quad (11)$$

4. **Limiting cross-correlation of corresponding principal subspaces:** Suppose the signal singular values $(x_i)_{i=1}^r$ are distinct. The empirical dyad $\mathbf{u}_{n,i} \mathbf{v}_{n,i}^T$ does correlate with its theoretical counterpart $\mathbf{a}_{n,i} \mathbf{b}_{n,i}^T$, but not perfectly. The limit is described by a functional $\mathcal{C}(x; F_Z, \gamma)$ depending on x, F_Z and γ . Fixing once again F_Z and γ , we get a function of x , $\mathcal{C}(x) \equiv \mathcal{C}(x; F_Z, \gamma)$, such that, with $x_+ = \mathcal{X}_+(F_Z, \gamma)$,

$$\langle \mathbf{a}_{n,i}, \mathbf{u}_{n,i} \rangle \cdot \langle \mathbf{b}_{n,i}, \mathbf{v}_{n,i} \rangle \xrightarrow{a.s.} \begin{cases} \mathcal{C}(x_i) & x_i > x_+ \\ 0 & x_i \leq x_+ \end{cases}. \quad (12)$$

We now give formulas for \mathcal{X}_+ and the mappings $\mathcal{Y}(\cdot)$ and $\mathcal{C}(\cdot)$, as computed in [Benaych-Georges and Nadakuditi, 2012b]. For a CDF H , let

$$\varphi(y; H) = \int \frac{y}{y^2 - z^2} dH(z), \quad (13)$$

which defines a smooth function on $y > \mathcal{Z}_+(H)$. Its derivative is

$$\varphi'(y; H) = - \int \frac{y^2 + z^2}{(y^2 - z^2)^2} dH(z). \quad (14)$$

Also define

$$\tilde{\varphi}_\gamma(y; H) = \gamma \varphi(y; H) + \frac{(1 - \gamma)}{y}, \quad \tilde{\varphi}'_\gamma(y; H) = \gamma \varphi'(y; H) - \frac{1 - \gamma}{y^2}. \quad (15)$$

Note that $\tilde{\varphi}_\gamma(y; H)$ is simply $\varphi(y; \tilde{H}_\gamma)$, where $\tilde{H}_\gamma(z) = \gamma H(z) + (1 - \gamma) \mathbb{1}_{\{z \geq 0\}}$. This so-called *companion CDF* \tilde{H}_γ describes the same distribution of nonzero singular values as H , diluted by ‘zero padding’ and has the following interpretation: if Z_n is a sequence of n -by- p matrices with a limiting singular value distribution H , then Z_n^\top has a limiting singular value distribution \tilde{H}_γ ¹¹. Let

$$\begin{aligned} \mathcal{D}_\gamma(y; H) &\equiv \varphi(y; H) \cdot \tilde{\varphi}_\gamma(y; H), \\ \mathcal{D}'_\gamma(y; H) &\equiv \varphi'(y; H) \cdot \tilde{\varphi}_\gamma(y; H) + \varphi(y; H) \cdot \tilde{\varphi}'_\gamma(y; H). \end{aligned} \quad (16)$$

¹¹Practitioners will recognize that computer software often offers two options for SVD outputs, a ‘fat’ output with zero padding and a ‘thin’ output with those superfluous zeros stripped away. If H denotes the LECDF of the ‘thin’ output singular values, then \tilde{H} is the corresponding LECDF of the fat outputs.

To ease the notation in coming paragraphs, we put for short $\mathcal{D}_\gamma(y) = \mathcal{D}_\gamma(y; F_Z, \gamma)$, and similarly for $\varphi(y)$, $\tilde{\varphi}_\gamma(y)$. Let $z_+ = \mathcal{Z}_+(F_Z)$ denote the bulk edge. The BBP phase transition location $x_+ = \mathcal{X}_+(F_Z, \gamma)$ is given by

$$x_+ = \lim_{y \rightarrow z_+} (\mathcal{D}_\gamma(y))^{-1/2}, \quad (17)$$

equivalently, $1/x_+^2 = \lim_{y \rightarrow z_+} \mathcal{D}_\gamma(y)$. It is easy to verify that $\varphi(y)$, $\tilde{\varphi}_\gamma(y)$ and $\mathcal{D}_\gamma(y)$ are non-negative, strictly decreasing functions of $y > z_+$, each tending to 0 as $y \rightarrow \infty$. Thus, $\mathcal{D}_\gamma(\cdot)$ maps the interval (z_+, ∞) bijectively into $(x_+, 0)$; denote by $\mathcal{D}_\gamma^{-1}(\cdot) \equiv \mathcal{D}_\gamma^{-1}(\cdot; F_Z)$ the inverse mapping.

We finally can give formulas for the fundamental phenomenological limits described earlier. The limiting empirical signal singular value $y_{i,\infty} = \mathcal{Y}(x_i) \equiv \mathcal{Y}(x_i; F_Z, \gamma)$ obeys

$$\mathcal{Y}(x) = \mathcal{D}_\gamma^{-1}\left(\frac{1}{x^2}\right), \quad \text{for } x > x_+, \quad (18)$$

equivalently, $\mathcal{D}_\gamma(\mathcal{Y}(x)) = 1/x^2$. The asymptotic cosine $\mathcal{C}(x) \equiv \mathcal{C}(x; F_Z, \gamma)$ is given by

$$\mathcal{C}(x) = -\frac{2}{x^3} \cdot \frac{1}{\mathcal{D}'_\gamma(\mathcal{Y}(x))}, \quad \text{for } x > x_+. \quad (19)$$

We sometimes adopt the implicit parameterization of $\mathcal{C}(x)$ in terms of $y = \mathcal{Y}(x)$:

$$\mathcal{C}(x) = -2 \cdot \frac{(\mathcal{D}_\gamma(y))^{3/2}}{\mathcal{D}'_\gamma(y)}, \quad \text{where } y = \mathcal{Y}(x) \text{ and } x > x_+. \quad (20)$$

Existence of a BBP phase transition. Recall that $x_+ = \mathcal{X}_+(F_Z, \gamma)$ gives the threshold such that whenever $x_i \leq x_+$, one *does not* observe an outlier singular value away from the bulk of Y . Not all noise distributions display this phase transition phenomenon, i.e. they may not exhibit $x_+ > 0$: indeed, by Eq. (17), $\mathcal{X}_+ > 0$ if and only if $\lim_{y \rightarrow \mathcal{Z}_+(F_Z)} \mathcal{D}_\gamma(y; F_Z) < \infty$, equivalently, $\lim_{y \rightarrow \mathcal{Z}_+(F_Z)} \int (y - z)^{-1} dF_Z(z) < \infty$. This condition entails that near its own bulk edge, F_Z is not “thick”. For example, when F_Z has a density in a neighborhood of $z_+ = \mathcal{Z}_+(F_Z)$ that behaves as $f_Z(z) \sim C(z - z_+)^{\alpha}$, this condition is satisfied whenever $\alpha > 0$. For example, the family of noise distributions described in Section 3.2 is of this type (with $\alpha = 1/2$); they all display a BBP phase transition. Moreover, Assumption 6 gives $\lim_{y \rightarrow z_+} \mathcal{D}'_\gamma(y; F_Z) = -\infty$. From Eq. (20), this means that if $x_+ \equiv \mathcal{X}_+(F_Z, \gamma) > 0$, then $\mathcal{C}(x_+) = 0$ as $x \rightarrow x_+$ from the right. Curiously, when $x_+ = 0$, this does not have to be the case. For instance, when $dF_Z = \delta_1$ and $\gamma = 1$, an easy computation shows $x_+ = 0$ and $\mathcal{C}(x) = \frac{y^3}{y(y^2+1)}$, where $y = \mathcal{Y}(x)$ and $\mathcal{Z}_+(F_Z) = 1$. We see that $\lim_{x \rightarrow x_+} \mathcal{C}(x) = 1/2$: this means that an *arbitrarily small* signal already creates a very strong bias in the direction of the principal singular vectors of Y_n .

Notation. We use throughout the paper the notation

$$y_{i,\infty} = \begin{cases} \mathcal{Y}(x_i) & \text{when } x_i > \mathcal{X}_+, \\ \mathcal{Z}_+(F_Z) & \text{when } x_i \leq \mathcal{X}_+. \end{cases}$$

By the results of [Benaych-Georges and Nadakuditi, 2012b], the singular values of Y_n , $y_{1,n} \geq \dots \geq y_{p,n}$, satisfy $y_{i,n} \xrightarrow{a.s.} y_{i,\infty}$ for any fixed index i (for $i > r$ this is an easy consequence of the interlacing inequality for singular values).

3.2 Noise matrices with correlated columns

We conclude this section by mentioning an important family of noise matrices satisfying our assumptions, namely, noise matrices with independent rows, having cross-column correlations. We consider noise matrices of the form $Z_n = W_n S_n^{1/2}$, where (W_n) and (S_n) are sequences of matrices obeying:

- W_n is an n -by- p matrix with i.i.d elements. Specifically, let W denote a random variable with moments

$$\mathbb{E}(W) = 0, \quad \mathbb{E}(W^2) = 1, \quad \mathbb{E}(W^4) < \infty.$$

The entries of W_n are i.i.d, and has the law $(W_n)_{ij} \stackrel{d}{=} n^{-1/2}W$, that is, scaled so to have variance $1/n$. Finiteness of the fourth moment of W is essential; see [Bai et al., 1998].

- (S_n) is a sequence of non-random p -by- p matrices. Let $\lambda_1(S_n) \geq \dots \geq \lambda_p(S_n)$ be the eigenvalues of S_n , and denote by $F_{S_n}(\lambda) = p^{-1} \sum_{i=1}^p \mathbb{1}_{\{\lambda_i(S_n) \leq \lambda\}}$ the empirical CDF of its eigenvalues. We assume that the sequence (F_{S_n}) converges to a compactly supported LECDF F_S . Moreover, denoting the upper and lower edges of the support by

$$\lambda_+(F_S) = \sup\{\lambda : F_S(\lambda) < 1\}, \quad \lambda_-(F_S) = \inf\{\lambda : F_S(\lambda) > 0\},$$

we assume that $\lambda_1(S_n) \rightarrow \lambda_+(F_S)$ and $\lambda_p(S_n) \rightarrow \lambda_-(F_S)$.

We refer to a random matrix ensemble of the form above as a **noise matrix with correlated columns**. They appear, for example, in the following scenario: We observe n i.i.d p -dimensional samples $\mathbf{y}_i = \mathbf{x}_i + \mathbf{z}_i$, where \mathbf{x}_i are instances of a signal vector, assumed to be supported in an r -dimensional subspace, and $\mathbf{z}_i = S_n^{1/2} \mathbf{w}_i$ is a vector of correlated noise, with covariance $\text{Cov}(\mathbf{w}_i) = S_n$. Let Y_n be the n -by- p matrix, whose rows are $n^{-1/2} \mathbf{y}_i^\top$ (define X_n , W_n and Z_n similarly). Then $Y_n = X_n + Z_n = X_n + W_n S_n^{1/2}$, where observe that $\text{rank}(X_n) \leq r$, by assumption. For any estimator $\hat{X} = \hat{X}(Y_n)$, let $\hat{\mathbf{x}}_1, \dots, \hat{\mathbf{x}}_n$ be the rows of the matrix $n \cdot \hat{X}$. Then the Frobenius loss is just the average L^2 loss in estimating the signal samples \mathbf{x}_i by the vectors $\hat{\mathbf{x}}_i$: $\|X_n - \hat{X}(Y_n)\|_F^2 = n^{-1} \sum_{i=1}^n \|\mathbf{x}_i - \hat{\mathbf{x}}_i\|_2^2$.

Much is known about the singular values of Z_n :

1. **Limiting singular value distribution:** F_{Z_n} converges weakly almost surely to a compactly supported law F_Z . This limiting law is defined in terms of its Stieltjes transform¹², $m(y) = \int (z^2 - y)^{-1} dF_Z(z)$; $m(y)$ is the unique Stieltjes transform satisfying the equation

$$m(y) = \int \frac{1}{t(1 - \gamma - \gamma y m(y)) - y} dF_S(t), \quad \text{for all } y \in \mathbb{C} \setminus \mathbb{R}.$$

2. **Extreme singular values:** The largest and smallest singular values of Z_n converge almost surely to the upper and lower edges of the support of the limiting law F_Z :

$$\mathcal{Z}_+(F_{Z_n}) \xrightarrow{a.s.} \mathcal{Z}_+(F_Z), \quad \mathcal{Z}_-(F_{Z_n}) \xrightarrow{a.s.} \mathcal{Z}_-(F_Z).$$

¹² $m(y)$ is in fact the Stieltjes transform of the limiting eigenvalue distribution of $Z^\top Z$:

$$m(y) = \int (z - y)^{-1} dF_{Z^\top Z}(z) = \int (z^2 - y) dF_Z(z).$$

3. **Behavior at the edge of the bulk:** On $\mathbb{R} \setminus \{0\}$, the limiting law F_Z is absolutely continuous with respect to Lebesgue measure. Denoting by f_Z the corresponding density, it behaves like $f_Z(z) \sim C(z - \mathcal{Z}_+(F_Z))^{1/2}$ as $z \rightarrow \mathcal{Z}_+(F_Z)$. This is the same behavior as a Marcenko-Pastur law, corresponding to $S_n = I$. This edge behavior will motivate one of our strategies for estimating F_{Z_n} from the observed singular values F_{Y_n} (*imputation*, see Section 4.2); this is an important step in the ScreenNOT algorithm. Also, note that in particular, the limiting noise CDF F_Z satisfies Assumption 6.

4. **CLT for linear spectral statistics:** Denote

$$\underline{y} = (1 - \sqrt{\gamma})^2 \cdot \liminf_{n \rightarrow \infty} \lambda_p(S_n), \quad \bar{y} = (1 + \sqrt{\gamma})^2 \cdot \limsup_{n \rightarrow \infty} \lambda_1(S_n).$$

Note that $\bar{y}^{1/2} \leq y_-(F_Z) \leq \mathcal{Z}_+(F_Z) \leq \bar{y}^{1/2}$. Let g be analytic on an open domain in \mathbb{C} containing the closed interval $[\underline{y}, \bar{y}]$. Set

$$\Phi_n[g] = \int g(z^2) (dF_Z - dF_{Z_n})(z),$$

which is a random variable.¹³ Then the sequence $p \cdot \Phi_n[g]$ is tight. If, moreover, $\mathbb{E}(W^4) = 3$, then $p \cdot \Phi_n[g]$ converges in law to a Gaussian random variable.

For properties (1) and (2), we refer to [Bai et al., 1998] and the references therein (see also the book [Bai and Silverstein, 2010]). Property (3) is proved in [Silverstein and Choi, 1995]. Property (4) is proved in [Bai and Silverstein, 2004].

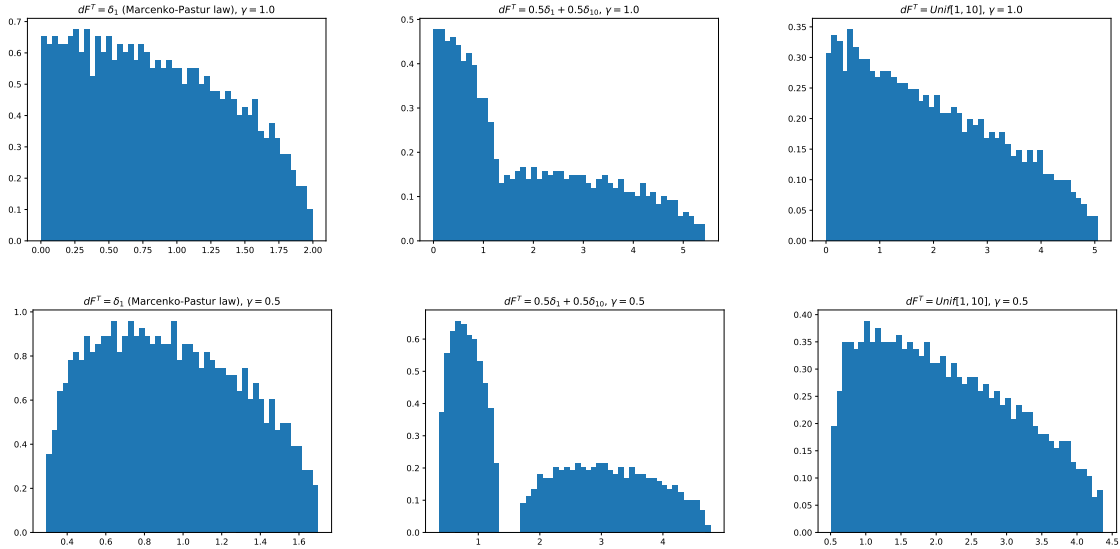


Figure 3: Several empirical noise singular value distributions that come from the model in Section 3.2. Left to right: covariance eigenvalue distribution: (i) $dF_S = \delta_1$ (giving a Marcenko-Pastur bulk); (ii) An equal mix of two atoms, $dF_S = \frac{1}{2}\delta_1 + \frac{1}{2}\delta_{10}$; (iii) F_S uniform on $[1, 10]$. Top: shape $\gamma = 1$; bottom: $\gamma = 0.5$. Each plot is the histogram of singular values from a single random $n \times p$ matrix, with $p = 1000$ and $n = p/\gamma$.

As a final remark, we mention that when the covariance matrix S_n is invertible and known (or can be consistently estimated with respect to operator norm), estimating X_n using the leading

¹³A random variable of the form $\int h(z)F_{Z_n}(z) = p^{-1} \sum_{i=1}^n h(z_{i,n})$ is called a linear spectral statistic.

singular vectors of Y_n is sub-optimal. Instead, it is better to first “whiten” the noise, that is, compute $Y_n^w = Y_n S_n^{-1/2} = X_n S_n^{-1/2} + W_n$. Letting $\mathbf{u}_{i,n}^w$ and $\mathbf{v}_{i,n}^w$ be respectively the left and right singular vectors of Y_n , we “re-color” the right singular vectors, $\mathbf{v}_{i,n}^c = S_n^{1/2} \mathbf{v}_{i,n}^w / \|S_n^{1/2} \mathbf{v}_{i,n}^w\|$. Under a uniform prior on the signal singular vectors, as we assume in this paper, and when W_n is i.i.d Gaussian, the correlations between the signal singular vectors and empirical singular vectors can be shown to be *stronger* in the whiten-then-recolor scheme:

$$\lim_{n \rightarrow \infty} \langle \mathbf{a}_{i,n}, \mathbf{u}_{i,n}^w \rangle \langle \mathbf{b}_{i,n}, \mathbf{v}_{i,n}^c \rangle \geq \lim_{n \rightarrow \infty} \langle \mathbf{a}_{i,n}, \mathbf{u}_{i,n} \rangle \langle \mathbf{b}_{i,n}, \mathbf{v}_{i,n} \rangle.$$

For details see [Leeb and Romanov, 2018, Hong et al., 2018].

4 Results

Outline. We start by developing a theory for optimal hard thresholding, under the assumption that the noise singular value distribution F_Z is known. We show that there is an asymptotically uniquely admissible hard threshold $T_\gamma(F_Z)$, which is given as a certain functional T_γ of the asymptotic aspect ratio γ and the limiting noise CDF F_Z . Relying on the fact that $\text{SE}_n[\mathbf{x}|\theta]$ can only take a finite number of values as θ varies, we show that thresholding at $T_\gamma(F_Z)$ has rather strong optimality properties: it in fact attains oracle loss, at finite n , with probability increasing to 1 as $n \rightarrow \infty$. We then move on to the practical setting of interest, in which F_Z is unknown. We propose a method for consistently estimating $T_\gamma(F_Z)$ from the observed data Y_n . We do this by applying the optimal threshold functional $T_{p/n}(\cdot)$ on a judiciously transformed version of F_{Y_n} , the empirical singular value distribution of Y_n . The continuity of the functional with respect to the CDF and the shape parameter then implies that the resulting quantity is a consistent estimator for $T_\gamma(F_Z)$; the optimality properties of the adaptive algorithm then follow from the previously developed theory. Unless otherwise stated, we always operate under assumptions (1)-(6) of Section 3.

4.1 A theory for optimal singular value thresholding

Consider the function $\theta \mapsto \text{ASE}[\mathbf{x}|\theta]$ defined for $\theta > 0$ by

$$\text{ASE}[\mathbf{x}|\theta] = \sum_{i=1}^r R(x_i|\theta), \quad \text{where} \quad R(x_i|\theta) = \mathbb{1}_{\{y_{i,\infty} \leq \theta\}} \cdot R_0(x_i) + \mathbb{1}_{\{y_{i,\infty} > \theta\}} \cdot R_1(x_i), \quad (21)$$

and

$$R_0(x) = x^2, \quad R_1(x) = x^2 + \mathcal{Y}(x)^2 - 2x\mathcal{Y}(x)\mathcal{C}(x), \quad (22)$$

and recall that $y_{i,\infty} = z_+ (\equiv \mathcal{Z}_+(F_Z))$ when $x_i \leq x_+ (= \mathcal{X}_+(F_Z, \gamma))$ and $y_{i,\infty} = \mathcal{Y}(x_i)$ when $x > x_+$. Define also

$$\text{ASE}^*[\mathbf{x}] = \sum_{i=1}^r R^*(x_i), \quad \text{where} \quad R^*(x_i) = \begin{cases} R_0(x_i) & \text{when } x_i < x_+, \\ \min\{R_0(x_i), R_1(x_i)\} & \text{when } x_i \geq x_+. \end{cases} \quad (23)$$

Clearly, $R^*(x) \leq R(x|\theta)$ for any x and θ , which means $\text{ASE}^*[\mathbf{x}] \leq \text{ASE}[\mathbf{x}|\theta]$.

It is easy to verify that for almost every $\theta > \mathcal{Z}_+(F_Z)$, the loss of thresholding at the fixed point θ converges: $\lim_{n \rightarrow \infty} \text{SE}_n[\mathbf{x}|\theta] = \text{ASE}[\mathbf{x}|\theta]$ almost surely; see Lemma 7 for a precise statement. We start by finding the threshold that attains minimum asymptotic loss.

Definition 1 (Optimal threshold functional). For a compactly supported CDF H and $\gamma \in (0, 1]$, let

$$\Psi_\gamma(y; H) = y \cdot \frac{\mathcal{D}'_\gamma(y; H)}{\mathcal{D}_\gamma(y; H)} = y \cdot \left(\frac{\varphi'(y; H)}{\varphi(y; H)} + \frac{\tilde{\varphi}'_\gamma(y; H)}{\tilde{\varphi}_\gamma(y; H)} \right); \quad (24)$$

this is well-defined for $y > \mathcal{Z}_+(H)$. Define the functional of H

$$T_\gamma(H) = \inf \{y : y > \mathcal{Z}_+(H) \text{ and } \Psi_\gamma(y; H) \geq -4\}. \quad (25)$$

we call this the **optimal threshold functional**.

Lemma 1. The following holds:

1. For any H and γ , $y \mapsto \Psi_\gamma(y; H)$ is negative and increasing, with $\Psi_\gamma(\infty) = -2$.
2. Assume that H is compactly supported and satisfies $\lim_{y \rightarrow \mathcal{Z}_+(H)} \int (y - z)^{-2} dH(z) = \infty$ (note that, by assumption, $H = F_Z$ satisfies this). Then $T_\gamma(H)$ is the unique number $> \mathcal{Z}_+(H)$ satisfying $\Psi_\gamma(T_\gamma(H); H) = -4$.
3. Thresholding at $\theta^* = T_\gamma(F_Z)$ universally minimizes the asymptotic loss:

$$\text{ASE}[\mathbf{x}|\theta^*] = \min_{\theta} \text{ASE}[\mathbf{x}|\theta] = \text{ASE}^*[\mathbf{x}].$$

Moreover, θ^* is the unique threshold for which the above holds **universally**, for all signals \mathbf{x} .

Lemma 1 is proved in Section 6.1.

Note that $\theta \mapsto \text{ASE}[\mathbf{x}|\theta]$ is piecewise constant, with jumps at $y_{1,\infty}, \dots, y_{r,\infty}$. This means that its minimum is actually attained on an *interval*:

Definition 2 (The asymptotic optimal interval). Let

$$\underline{\Theta}(\mathbf{x}) = \max \{y_{i,\infty} : y_{i,\infty} < T_\gamma(F_Z)\}, \quad \overline{\Theta}(\mathbf{x}) = \min \{y_{i,\infty} : y_{i,\infty} > T_\gamma(F_Z)\}. \quad (26)$$

Note that since $T_\gamma(F_Z) > z_+ = \mathcal{Z}_+(F_Z, \gamma)$ and $y_{r+1,\infty} = z_+$, we always have, by definition, $\underline{\Theta}(\mathbf{x}) \geq z_+$. Moreover, if $y_{1,\infty} \leq T_\gamma(F_Z)$ then we define $\overline{\Theta}(\mathbf{x}) = \infty$.

Lemma 2. 1. Throughout the interval $\theta \in (\underline{\Theta}(\mathbf{x}), \overline{\Theta}(\mathbf{x}))$, $\text{ASE}[\mathbf{x}|\theta]$ is constant. Moreover, it attains its minimum there; if $\theta_0 \in (\underline{\Theta}(\mathbf{x}), \overline{\Theta}(\mathbf{x}))$, then

$$\text{ASE}[\mathbf{x}|\theta_0] = \min_{\theta \geq 0} \text{ASE}[\mathbf{x}|\theta] = \text{ASE}^*[\mathbf{x}].$$

2. Any $\theta_1 > \mathcal{Z}_+(F_Z)$ **outside** $[\underline{\Theta}(\mathbf{x}), \overline{\Theta}(\mathbf{x})]$ has

$$\text{ASE}[\mathbf{x}|\theta_1] > \text{ASE}^*[\mathbf{x}].$$

3. **Unique asymptotic admissibility:** $T_\gamma(F_Z)$ is in the interior of the asymptotic optimal interval. In fact, it is the only threshold which has optimal asymptotic loss simultaneously for all signals \mathbf{x} :

$$\bigcap_{\mathbf{x} \text{ signal}} (\underline{\Theta}(\mathbf{x}), \overline{\Theta}(\mathbf{x})) = \{T_\gamma(F_Z)\}.$$

Lemma 2 is proved in Section 6.1.

It is clear at this point that thresholding at any point in the interior of the asymptotic optimal interval achieves the best asymptotic loss, among all other fixed hard thresholds. Our main result states that, remarkably, one **cannot** come up with a consistently better thresholding strategy, even if given access to the true unknown signal X_n :

Theorem 1. 1. Almost surely,

$$\lim_{n \rightarrow \infty} \text{SE}_n^*[\mathbf{x}] = \text{ASE}^*[\mathbf{x}].$$

2. Let $\theta \in (\underline{\Theta}(\mathbf{x}), \overline{\Theta}(\mathbf{x}))$ be in the interior of the asymptotic optimal interval, and θ_n be any sequence of thresholds (possibly depending on Y_n) such that $\theta_n \xrightarrow{a.s.} \theta$. Then

$$\text{SE}_n[\mathbf{x}|\theta_n] \xrightarrow{a.s.} \text{ASE}^*[\mathbf{x}].$$

Our next result states that thresholding inside the asymptotic optimal interval in fact achieves oracle risk with high probability, **for finite n** :

Theorem 2. Suppose that $T_\gamma(F_Z) \notin \{y_{1,\infty}, \dots, y_{r,\infty}\}$.¹⁴ Then:

1. Let $\theta_0 \in (\underline{\Theta}(\mathbf{x}), \overline{\Theta}(\mathbf{x}))$ and θ_n be a sequence with $\theta_n \xrightarrow{a.s.} \theta_0$. Then

$$\mathbb{P} \{ \exists N \text{ s.t. } \forall n \geq N : \text{SE}_n[\mathbf{x}|\theta_n] = \text{SE}_n^*[\mathbf{x}] \} = 1.$$

2. Let $\theta_1 \notin [\underline{\Theta}(\mathbf{x}), \overline{\Theta}(\mathbf{x})]$ and $\theta_n \xrightarrow{a.s.} \theta_1$. There exists $\delta > 0$, $\delta = \delta(\mathbf{x}; F_Z, \gamma)$ such that

$$\mathbb{P} \{ \exists N \text{ s.t. } \forall n \geq N : \text{SE}_n[\mathbf{x}|\theta_n] > \text{SE}_n^*[\mathbf{x}] + \delta \} = 1.$$

Theorems 1 and 2 are proved in Section 6.2.

4.2 The ScreeNOT algorithm

In practice, the noise distribution F_Z is generally unknown to the statistician. Theorems 1 and 2, along with the unique admissibility property of Lemma 2, tell us that our goal should be to estimate the optimal threshold $T_\gamma(F_Z)$.

We start by showing that the functional $(\gamma, H) \mapsto T_\gamma(H)$ is continuous with respect to weak convergence of CDFs, with the additional requirement that the edge of the support converges as well:

Lemma 3 (Continuity of the optimal threshold functional). Suppose that H is compactly supported and satisfies the condition $\lim_{y \rightarrow \mathcal{Z}_+(H)} \int (y - z)^{-2} dH(z) = \infty$. Let H_n be a sequence of CDFs such that

1. H_n converges weakly to H , denoted $H_n \xrightarrow{d} H$.

2. $\mathcal{Z}_+(H_n) \rightarrow \mathcal{Z}_+(H)$.

Then $T_{p/n}(H_n) \rightarrow T_\gamma(H)$.

Lemma 3 is proved in Section 6.3.

Recall that the empirical singular value distribution of the noise matrix, F_{Z_n} , converges, by assumption, weakly almost surely to F_Z , with $\mathcal{Z}_+(F_{Z_n}) \xrightarrow{a.s.} \mathcal{Z}_+(F_Z)$. The matrix noise Z_n , and consequently F_{Z_n} , is of course unknown to the statistician. However, since Y_n is a rank- r additive perturbation of Z_n , the interlacing inequalities for singular values imply for example the

¹⁴If $y_{i,\infty} = T_\gamma(F_Z)$ for some i , thresholding either slightly above or below $y_{i,n}$ (but still inside the asymptotic optimal interval) will achieve the same (optimal) asymptotic risk. However, we cannot deduce that for finite n , one option is consistently better than the other.

convergence of CDF's in Kolmogorov-Smirnov distance $\|F_{Y_n} - F_{Z_n}\|_{KS} \rightarrow 0$ (by the same arguments used in Lemma 4 below) and hence also in weak convergence. The obstacle preventing the would-be use of $T_{p/n}(F_{Y_n})$ to estimate $T_\gamma(F_Z)$ lies with the fact that T is not continuous in Kolmogorov-Smirnov metric convergence or other topologies involving CDF convergence such as weak convergence. More concretely, $T_{p/n}(F_{Y_n})$ can be very different than $T_\gamma(F_Z)$ because the top masspoints of F_{Y_n} don't converge to the bulk edge F_Z .¹⁵ Indeed, recall that $\mathcal{Z}_+(F_{Y_n}) = y_{1,n} \xrightarrow{a.s.} y_{1,\infty}$, which is $> \mathcal{Z}_+(F_Z)$ when $x_i > \mathcal{X}_+$.

To get a reasonable simulacrum of F_{Z_n} built from knowledge only of F_{Y_n} we perform “surgery” on F_{Y_n} , “amputating” the top k masspoints and fitting a “prosthesis” to replace them. Post-surgery, we get an estimate for the unknown empirical noise CDF F_{Z_n} .

As indicated in Section 2 above, the user of our proposed procedure supplies an upper bound (which can be potentially very loose) $k \geq r$ on the rank of the unknown low-rank matrix.

We could, in principle, propose any one of the following “pseudo-noise” CDFs, derived from F_{Y_n} :

- **Transport to zero:** We construct a CDF, $F_{n,k}^0$, obtained by removing the k largest singular values of Y_n , and adding k additional zeros. That is,

$$F_{n,k}^0(y) = \frac{1}{p} \sum_{i=k+1}^p \mathbb{1}_{\{y_{i,n} \leq y\}} + \frac{k}{p} \mathbb{1}_{\{y \geq 0\}}.$$

- **“Winsorization” (clipping):** As in the previous construction, we remove the leading k singular values. Instead of adding k zeroes, we add k copies of $y_{k+1,n}$. Equivalently, we “clip” the large singular values of Y_n to be at most the size of $y_{n,k+1}$. That is,

$$F_{n,k}^w(y) = \frac{1}{p} \sum_{i=k+1}^p \mathbb{1}_{\{y_{i,n} \leq y\}} + \frac{k}{p} \mathbb{1}_{\{y_{n,k+1} \leq y\}}.$$

- **“Imputation” (reconstruction of the missing upper tail):** After removing the top k singular values of Y_n , we try to construct the noise tail in a principled way. Recall that when Z_n is a noise matrix with correlated columns, as described in Section 3.2, F_Z has a density near $z_+ = \mathcal{Z}_+(F_Z)$ that behaves as $f_Z(z) \sim C(z_+ - z)^{1/2}$ as $z \rightarrow z_+$ ([Silverstein and Choi, 1995]). Using the heuristic

$$\frac{\ell - 1}{p} \approx \int_{z_{\ell,n}}^{z_+(F_Z)} f_Z(z) dz \approx \int_{z_{\ell,n}}^{z_+} C(z_+ - z)^{1/2} dz = C'(z_+ - z_{\ell,n})^{3/2},$$

we can estimate the distance between singular values in the upper tail as

$$z_{\ell,n} - z_{t,n} \approx C'' \left[\left(\frac{t-1}{p} \right)^{2/3} - \left(\frac{\ell-1}{p} \right)^{2/3} \right].$$

Taking $y_{\ell,n} \approx z_{\ell,n}$ for $\ell \geq r+1$, we propose to estimate the unknown constant as:

$$C'' = \frac{y_{2k+1,n} - y_{k+1,n}}{(2k/p)^{2/3} - (k/p)^{2/3}},$$

¹⁵Of course, this does not prevent convergence of ECDFs. Recall that $F_{Y_n} \xrightarrow{d} F_Z$ means that for **bounded and continuous** functions f , $\int f(z) dF_{Y_n}(z) \rightarrow \int f(z) dF_Z(z)$.

assuming $2k + 1 < p$ (when k is not very small compared to p , there is no reason to believe this heuristic should give good results). We “reconstruct” the missing upper tail as

$$\tilde{y}_{i,n} = y_{k+1,n} + C'' \left[\left(\frac{k}{p} \right)^{2/3} - \left(\frac{i-1}{p} \right)^{2/3} \right] = y_{k+1,n} + \frac{1 - \left(\frac{i-1}{k} \right)^{2/3}}{2^{2/3} - 1} (y_{2k+1,n} - y_{k+1,n}) .$$

The CDF we use is then

$$F_{n,k}^i(y) = \frac{1}{p} \sum_{i=k+1}^p \mathbb{1}_{\{y_{i,n} \leq y\}} + \frac{1}{p} \sum_{i=1}^k \mathbb{1}_{\{\tilde{y}_{i,n} \leq y\}} .$$

The label i on $F_{n,k}^i$ stands for ‘imputation’, a standard terminology in statistical practice for filling in utterly missing data with plausible pseudo-data. Numerical results in Section 5 suggest that in many cases, the ‘imputation’ method gives significantly better results than truncation or Winsorization at finite n . It is also more psychologically “supportive”, which is why we recommended it to practitioners in Section 2 above. However, our formal results hold for all three methods

Lemma 4. *Suppose that $k = k_n$ satisfies $k_n \geq r$ and $k_n/p \rightarrow 0$ (in particular, k can be any constant $\geq r$). Then for any choice $\star \in \{0, w, i\}$:*

1. *Almost surely, $F_{n,k}^\star \xrightarrow{d} F_Z$.*
2. *$\mathcal{Z}_+(F_{n,k}^\star) \xrightarrow{a.s.} \mathcal{Z}_+(F_Z)$.*
3. *We have the following bound on the Kolmogorov-Smirnov distance between $F_{n,k}^\star$ and F_{Z_n} :*

$$\|F_{n,k}^\star - F_Z\|_{\text{KS}} = \sup_z |F_{n,k}^\star(z) - F_{Z_n}(z)| \leq \frac{k}{p} .$$

Lemma 4 is proved in Section 6.3.

The following theorem states the optimality properties of the proposed ScreeNOT algorithm. It is an immediate corollary of Theorems 1, 2 and Lemma 4:

Theorem 3. *Suppose that $k = k_n$ satisfies $k_n \geq r$ and $k_n/p \rightarrow 0$. For any $\star \in \{0, w, i\}$, $\hat{\theta}_n = T_{p/n}(F_{n,k}^\star)$ satisfies:*

1. *$\hat{\theta}_n \xrightarrow{a.s.} T_\gamma(F_Z)$.*
2. *$\text{SE}_n[\mathbf{x}|\hat{\theta}_n] \xrightarrow{a.s.} \text{ASE}^*[\mathbf{x}]$.*
3. *Assume that $T_\gamma(F_Z) \notin \{y_{1,\infty}, \dots, y_{r,\infty}\}$. Then*

$$\mathbb{P} \{ \exists N \text{ s.t. } \forall n \geq N : \text{SE}_n[\mathbf{x}|\theta_n] = \text{SE}_n^*[\mathbf{x}] \} = 1 .$$

Regarding the assumption in item 3 above, we note the following.

Lemma 5. *The condition $T_\gamma(F_Z) \notin \{y_{1,\infty}, \dots, y_{r,\infty}\}$ is **generic**, i.e. in the space of possible singular value r -vectors \mathbf{x} this condition holds on an open dense set.*

Fix the noise bulk F_Z ; then $\theta^* = T_\gamma(F_Z)$ is a constant not varying as the underlying signal \mathbf{x} changes. Moreover, it always strictly exceeds the bulk edge $\mathcal{Z}_+(F_Z)$. So $x^* = \mathcal{Y}^{-1}(\theta^*; F_Z, \gamma)$ is a uniquely defined constant which exceeds $\mathcal{X}_+(F_Z, \gamma)$. The set of vectors \mathbf{x} with all entries distinct from x^* is open and dense.

4.3 Stability of ScreeNOT

A natural question is how fast $T_{p/n}(F_{n,k}^*)$ converges to the limit $T_\gamma(F_Z)$. We show that in the case of noise matrices with correlated columns, the noise model described in Section 3.2, the typical deviations are of order $\mathcal{O}(k/p)$.

We start with a “quantitative” version of Lemma 3:

Lemma 6. *Adopt the setting of Lemma 3. Set*

$$\Delta_{1,n} = |\varphi(T_\gamma(H); H) - \varphi(T_\gamma(H); H_n)|, \quad \Delta_{2,n} = |\varphi'(T_\gamma(H); H) - \varphi'(T_\gamma(H); H_n)|,$$

where φ and φ' are given in Eqs (13) and (14). Then

$$|T_\gamma(H) - T_{p/n}(H_n)| = \mathcal{O}\left(\Delta_{1,n} + \Delta_{2,n} + \left|\frac{p}{n} - \gamma\right|\right).$$

Lemma 6, along with the Kolmogorov-Smirnov distance bound from Lemma 4 and the tightness result for linear spectral statistics from [Bai and Silverstein, 2004] (see Section 3.2), gives the following:

Proposition 1. *Suppose that (Z_n) is a sequence of noise matrices with correlated columns, as described in Section 3.2; and let F_S denote the LECDF of eigenevalues of the cross-column covariances S_n . Assume, in addition, that $T_\gamma(F_Z) > \bar{y}^{1/2} = (1 + \sqrt{\gamma}) \cdot \sqrt{\lambda_+(F_S)}$.¹⁶ Suppose that $k \geq r$ with $k/p \rightarrow 0$. Then for any $\star \in \{0, w, i\}$,*

$$|T_\gamma(F_Z) - T_{p/n}(F_{n,k}^*)| = \mathcal{O}_P\left(\frac{k+1}{p}\right).$$

Lemma 6 and Proposition 1 are proved in Section 6.3.

5 Numerical experiments

Appendix C contains comprehensive experiments conducted on a large variety of noise distributions. For space considerations we include here results for the white noise (Marcenko-Pastur) case with $\gamma = 0.5$. Simulation results and code reproducing all figures here and in Appendix C is permanently available at [Donoho et al., 2020]. See Appendix C for full details on each experiment reported here.

¹⁶This additional assumption is used due to a technical requirement in the results of [Bai and Silverstein, 2004]. We suspect that it can be removed.

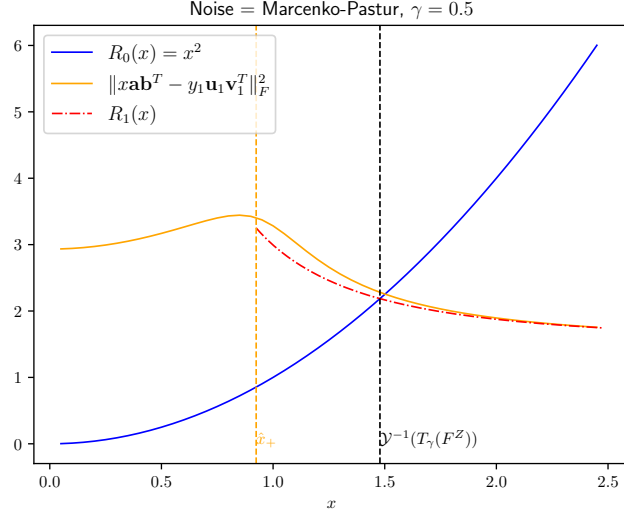


Figure 4: The functions $R_0(x)$ and $R_1(x)$ from Lemma 8. Observe that $x^* = \mathcal{Y}^{-1}(T_\gamma(F_Z))$ is their unique crossing point $x > x_+$. Here, $\gamma = 0.5$, $p = 500$ and $n = p/\gamma$.

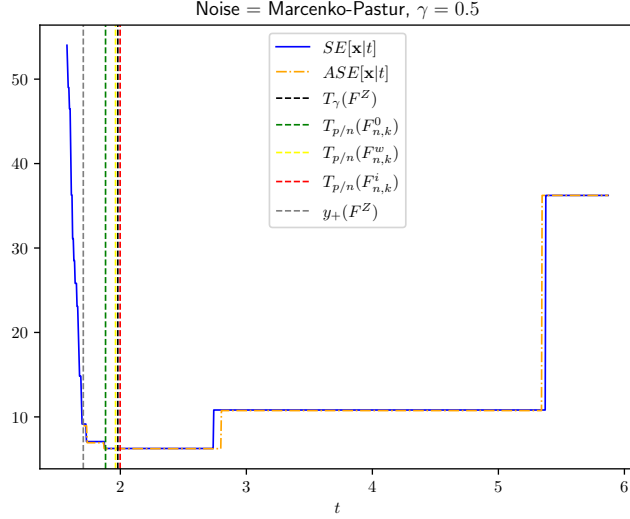


Figure 5: A single problem instance, corresponding to the rank $r = 5$ signal $\mathbf{x} = (0.5, 1.0, 1.3, 2.5, 5.2)$. Shown are the functions $SE_n[\mathbf{x}|t]$ and $ASE[\mathbf{x}|t]$ on top of each other. Here $\gamma = 0.5$, $p = 500$ and $n = p/\gamma$. We indicate the locations of \mathcal{Z}_+ , $T_\gamma(F_Z)$ and the estimates $T_{p/n}(F_{n,k}^\star)$ for $\star \in \{0, w, i\}$, with $k = 4r = 20$.

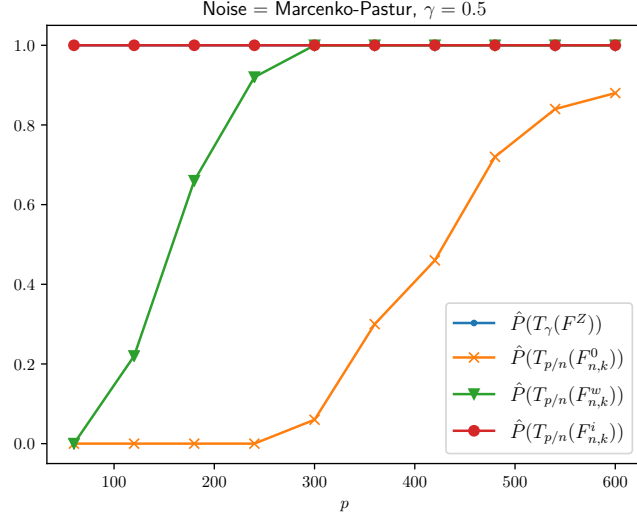


Figure 6: For various choices of p , and $T = 50$ denoising experiments, shown are the fraction of experiments where each threshold $\in \{T_\gamma(F_Z), T_{p/n}(F_{n,k}^0), T_{p/n}(F_{n,k}^w), T_{p/n}(F_{n,k}^i)\}$ attains oracle loss. Here, $\mathbf{x} = (0.5, 1.0, 1.3, 2.5, 5.2)$ so that $r = 5$ and $k = 4r = 20$.

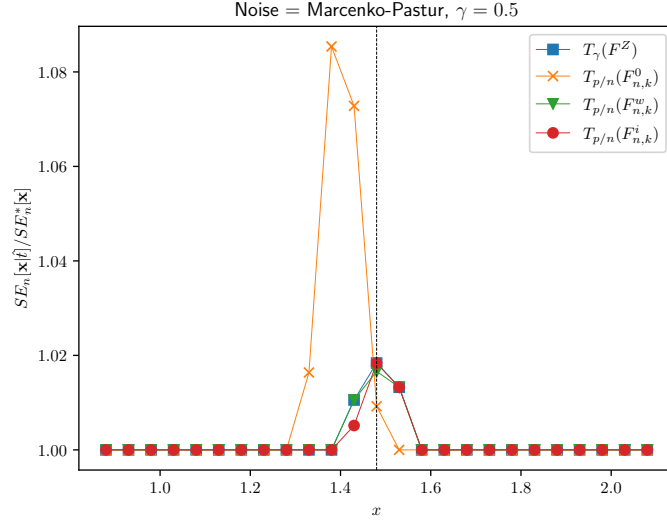


Figure 7: Oracle loss $SE_n^*[\mathbf{x}]$ compared with $SE_n[\mathbf{x}|\hat{t}]$ for the choices $\hat{t} \in \{T_\gamma(F_Z), T_{p/n}(F_{n,k}^0), T_{p/n}(F_{n,k}^w), T_{p/n}(F_{n,k}^i)\}$, for a single spike. We let the spike intensity x vary and plot $SE_n[\mathbf{x}|\hat{t}]/SE_n^*[\mathbf{x}]$ for each choice of estimator. The ratios shown are averages across $T = 20$ experiments.

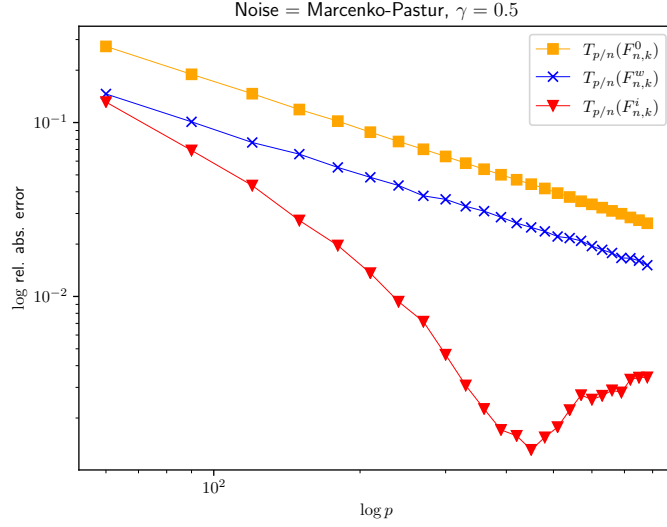


Figure 8: Rate of convergence of $T_{p/n}(F_{n,k}^*)$ towards $T_{\gamma}(F_Z)$. Here, $r = 10$ with $x = (1, \dots, 10)$, set $k = 20$. Shown is the relative absolute error $|T_{p/n}(F_{n,k}^*) - T_{\gamma}(F_Z)| / T_{\gamma}(F_Z)$ as p varies and $n = p/\gamma$. A logarithmic scale is used to observe the polynomial rate of decay in p . All points are generated by averaging the error of $T = 50$ experiments.

6 Proofs

6.1 The asymptotic loss at a fixed threshold

Throughout this section, F_Z and γ will be held fixed, and we will leave them implicit where possible, so as to make the notation less cumbersome. In particular, we set $z_+ = \mathcal{Z}_+(F_Z)$, $x_+ = \mathcal{X}_+(F_Z, \gamma)$ throughout and we suppress mention of F_Z and γ in entities like \mathcal{C} , \mathcal{Y} , \mathcal{D} .

We start by investigating $\lim_{n \rightarrow \infty} \text{SE}_n[\mathbf{x}|\theta]$ for fixed θ . Note that when $\theta < z_+$, it is clear that $\lim_{n \rightarrow \infty} \text{SE}_n[\mathbf{x}|\theta] = \infty$; the reason being that, for small enough $\epsilon > 0$, with probability 1, $(1 - F_Z(t + \epsilon)) \cdot n = \Omega(n)$ empirical singular values $y_{i,n}$ pass the threshold t , so that $\text{rank}(\hat{X}_t(Y_n))$ increases indefinitely (this argument will be made more precise later).

The following is an easy calculation:

Lemma 7. *For any $\theta > z_+$, almost surely:*

1.

$$\liminf_{n \rightarrow \infty} \text{SE}_n[\mathbf{x}|\theta] \geq \text{ASE}^*[\mathbf{x}].$$

2. *If, in addition, $\theta \notin \{y_{1,\infty}, \dots, y_{r,\infty}\}$, then*

$$\lim_{n \rightarrow \infty} \text{SE}_n[\mathbf{x}|\theta] = \text{ASE}[\mathbf{x}|\theta].$$

The quantities $\text{ASE}[\mathbf{x}|\theta]$ and $\text{ASE}^*[\mathbf{x}]$ appear in Eqs. (21) and (23) respectively.

Proof. Since $y > z_+$ and $y_{r+1,\infty} \xrightarrow{a.s.} z_+$, we see that with probability 1, for large enough n , $\hat{X}_t(Y_n) = \sum_{i=1}^r y_{i,n} \mathbb{1}_{\{y_{i,n} > \theta\}} \cdot \mathbf{u}_{i,n} \mathbf{v}_{i,n}^\top$. Thus, for large enough n ,

$$\begin{aligned} \text{SE}_n[\mathbf{x}|t] &= \left\| \sum_{i=1}^r x_i \cdot \mathbf{a}_{i,n} \mathbf{b}_{i,n}^\top - \sum_{i=1}^r y_{i,n} \mathbb{1}_{\{y_{i,n} > \theta\}} \cdot \mathbf{u}_{i,n} \mathbf{v}_{i,n}^\top \right\|_F^2 \\ &= \sum_{i=1}^r \sum_{j=1}^r x_i y_{j,n} \mathbb{1}_{\{y_{i,n} > \theta\}} \cdot \langle \mathbf{a}_{i,n}, \mathbf{u}_{j,n} \rangle \langle \mathbf{b}_{i,n}, \mathbf{v}_{j,n} \rangle. \end{aligned}$$

The lemma follows by recalling that $y_{i,n} \xrightarrow{a.s.} y_{i,\infty}$ for all $i = 1, \dots, r$, where $y_{i,\infty} = \mathcal{Y}(x_i)$ if $x_i > x_+$ and $y_{i,\infty} = z_+ < \theta$ whenever $x_i \leq x_+$, and that

$$\langle \mathbf{a}_{i,n}, \mathbf{u}_{j,n} \rangle \langle \mathbf{b}_{i,n}, \mathbf{v}_{j,n} \rangle \rightarrow \begin{cases} \mathcal{C}(x_i) & \text{when } i = j \text{ and } x_i > x_+, \\ 0 & \text{otherwise} \end{cases},$$

and also the fact that $\mathbb{1}_{\{y_{i,n} > \theta\}} \xrightarrow{a.s.} \mathbb{1}_{\{y_{i,\infty} > \theta\}}$ whenever $\theta \neq y_{i,\infty}$. \square

Our goal for the moment is to characterize the minimum of $\text{ASE}[\mathbf{x}|\theta]$ with respect to thresholds θ strictly above the noise bulk edge, $\theta > z_+$. This will give us the optimal *fixed* threshold, in the sense of minimal asymptotic loss (though, at this point, we cannot exclude the possibility that thresholding precisely at $\theta = z_+$ might achieve better asymptotic risk).

Recall, by Eqs. (21) and (23), that the asymptotic loss decouples across the signal spikes as

$$\text{ASE}[\mathbf{x}|\theta] = \sum_{i=1}^r R(x_i|\theta), \quad \text{ASE}^*[\mathbf{x}] = \sum_{i=1}^r R^*(x_i),$$

where $R(x|\theta) = R^*(x) = x^2$ when $x \leq x_+$, and for $x > x_+$,

$$R(x|\theta) = \mathbb{1}_{\{\mathcal{Y}(x) \leq \theta\}} \cdot R_0(x) + \mathbb{1}_{\{\mathcal{Y}(x) > \theta\}} \cdot R_1(x), \quad R^*(x) = \min(R_0(x), R_1(x)),$$

with

$$R_0(x) = x^2, \quad R_1(x) = x^2 + \mathcal{Y}(x)^2 - 2x\mathcal{Y}(x)\mathcal{C}(x).$$

If we were able to find $\theta > z_+$ such that $R(x|\theta) = R^*(x)$ for all $x > x_+$, then, clearly, it achieves minimal asymptotic loss. To do that, it is convenient to introduce a re-parameterization $y = \mathcal{Y}(x)$, where recall that $\mathcal{Y}(\cdot)$ is an increasing bijection, mapping (x_+, ∞) to (z_+, ∞) . Using Eqs. (18) and (19), assuming $x > x_+$, we get

$$x^2 = (\mathcal{D}(y))^{-1}, \quad \mathcal{C}(x) = -2 \frac{(\mathcal{D}(y))^{3/2}}{\mathcal{D}'(y)},$$

so that

$$R_1(x) - R_0(x) = y^2 - 2xy\mathcal{C}(x) = y^2 + 4y \cdot \frac{\mathcal{D}(y)}{\mathcal{D}'(y)} = y^2 \left(1 + \frac{4}{\Psi_\gamma(y)} \right),$$

where

$$\Psi_\gamma(y) = y \cdot \frac{\mathcal{D}'(y)}{\mathcal{D}(y)}$$

is as defined in Eq. (24). Since $\Psi_\gamma(\cdot)$ is negative (\mathcal{D} is positive and decreasing), we conclude that

$$R^*(x) = \mathbb{1}_{\{\Psi_\gamma(y) \leq -4\}} \cdot R_0(x) + \mathbb{1}_{\{\Psi_\gamma(y) > -4\}} \cdot R_1(x). \quad (27)$$

The next lemma establishes some essential properties of $\Psi_\gamma(y)$:

Lemma 8. Let H be a compactly supported CDF, with $\mathcal{Z}_+(H) > 0$. Let $\gamma \in (0, 1]$, and let $\Psi_\gamma(y; H)$ be defined as in Eq. (24). Then

1. The function $y \mapsto \Psi_\gamma(y; H)$ is strictly increasing on $y \in (\mathcal{Z}_+(H), \infty)$, with $\lim_{y \rightarrow \infty} \Psi_\gamma(y; H) = -2$.
2. Assume that

$$\lim_{y \rightarrow \mathcal{Z}_+(F_Z)} \int (y - z)^{-2} dH(z) = \infty.$$

(This is Assumption 6 for $H = F_Z$). Then $\lim_{y \rightarrow \mathcal{Z}_+(H)} \Psi_\gamma(y; H) = -\infty$, and there is a unique point $y^* \in (\mathcal{Z}_+(F_Z), \infty)$ such that $\Psi_\gamma(y; H) = -4$.

The proof of Lemma 8 is deferred to the Appendix, Section A.

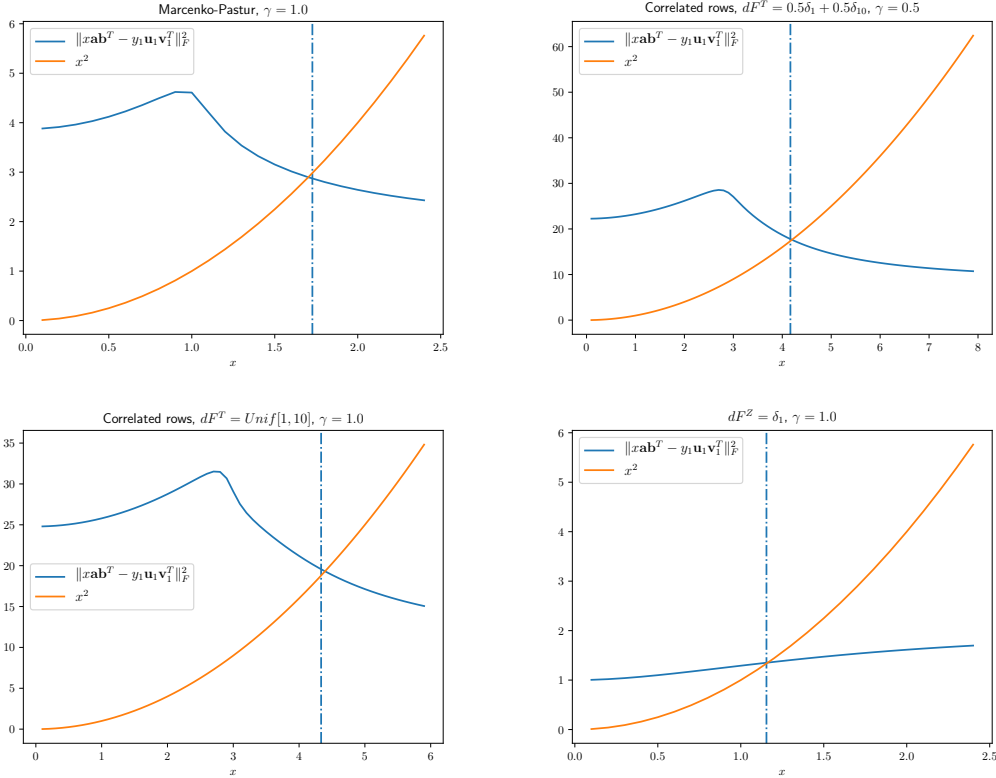


Figure 9: A numerical illustration of Lemma 8 and its consequences. Assuming a rank-1 signal $X = x \cdot \mathbf{a}_{1,n} \mathbf{b}_{1,n}^\top$, set $R_0(x) = \|X\|_F^2 = x^2$ and $R_1(x) = \lim_{n \rightarrow \infty} \|X - y_{1,n} \mathbf{a}_{1,n} \mathbf{b}_{1,n}^\top\|_F^2$. The point $x^* = \mathcal{Y}^{-1}(T_\gamma(F_Z))$ is the unique crossing point $R_0(x^*) = R_1(x^*)$. When $x < x^*$, the principal components of Y are “too noisy”, so that estimating $\hat{X} = 0$ gives better squared error; when $x > x^*$, the situation reverses. At each plot, $R_0(x)$ and $R_1(x)$ are plotted as x varies, for finite n , fixed signal components $\mathbf{a}_{1,n} \mathbf{b}_{1,n}^\top$ and a single instance of Z_n . The dashed vertical line is an estimate of x^* , obtained by applying the functional $T_{p/n}(\cdot)$ on F_{Z_n} , as well as computing the inverse map $\mathcal{Y}^{-1}(T_{p/n}(F_{Z_n}))$ numerically from F_{Z_n} . In all cases, $p = 500$ and $n = p/\gamma$. From left to right, top to bottom: (i) Marcenko-Pastur law with shape $\gamma = 1$; (ii) Noise matrix with correlated columns, with $F_S = \frac{1}{2}\delta_1 + \frac{1}{2}\delta_{10}$ and $\gamma = 0.5$; (iii) Likewise, with $F_S = \text{Unif}[1, 10]$; (iv) $F_Z = \delta_1$ and $\gamma = 1$ (specifically, $Z_n = I$).

Proof of Lemma 1. The lemma follows as a straightforward corollary of Lemma 8. Lemma 8 implies that there is a unique number $T_\gamma(F_Z) > \mathcal{Z}_+(F_Z)$ such that $\Psi_\gamma(T_\gamma(F_Z); F_Z) = -4$. Since $y \mapsto \Psi_\gamma(y; F_Z)$ is increasing, plugging into Eq. (27),

$$R^*(x) = R(x|T_\gamma(F_Z)) = \mathbb{1}_{\{y \leq T_\gamma(F_Z)\}} \cdot R_0(x) + \mathbb{1}_{\{y > T_\gamma(F_Z)\}} \cdot R_1(x), \quad (28)$$

where $x > \mathcal{X}_+$ and $y = \mathcal{Y}(x)$. We conclude that $\text{ASE}^*[\mathbf{x}] = \text{ASE}[\mathbf{x}|T_\gamma(F_Z)]$. This is the minimum of $\text{ASE}[\mathbf{x}|\theta]$ over all $\theta \geq 0$ since, clearly, $\text{ASE}[\mathbf{x}|\theta] \geq \text{ASE}^*[\mathbf{x}]$ by definition. Moreover, for any $\theta \neq T_\gamma(F_Z)$, we can find some $y > \mathcal{Z}_+(F_Z)$ such that either $\theta < y < T_\gamma(F_Z)$ or $T_\gamma(F_Z) < y < \theta$. Taking $x = \mathcal{Y}^{-1}(y)$, we find that $R(x|\theta) > R(x|T_\gamma(F_Z)) = R^*(x)$, since there is a **unique** crossing point $x > \mathcal{X}_+$ with $R_0(x) = R_1(x)$ (this is because $y \mapsto \Psi_\gamma(y; F_Z)$ is strictly increasing). Thus, we can construct a signal \mathbf{x} for which $\text{ASE}[\mathbf{x}|\theta] > \text{ASE}^*[\mathbf{x}]$; we conclude that $T_\gamma(F_Z)$ is the unique threshold which minimizes $\text{ASE}[\mathbf{x}|\theta]$ universally for all \mathbf{x} .

Proof of Lemma 2. Part (1) of the Lemma follows from Lemma 1, along with the observation that if $\mathcal{Y}(x) = T_\gamma(F_Z)$, then $R_0(x) = R_1(x) = R^*(x)$; this means that regardless of whether we threshold slightly above or below $\mathcal{Y}(x)$, we get the same asymptotic loss. Part (2) follows by the same argument as in the proof of Lemma 3, in the paragraph above. Finally, part (3) follows right from the definition of $\underline{\Theta}(\mathbf{x})$ and $\overline{\Theta}(\mathbf{x})$.

6.2 Achieving oracle loss

We move on to study the oracle loss $\text{SE}_n^*[\mathbf{x}]$. This random variable depends on both X_n and the noise Z_n .

Denote

$$\hat{X}_{[k]} = \sum_{i=1}^k y_{n,i} \mathbf{u}_{i,n} \mathbf{v}_{i,n}^\top, \quad k = 0, \dots, p. \quad (29)$$

That is, $\hat{X}_{[k]}$ is obtained from Y by keeping only the top $k = 0, \dots, p$ singular values (equivalently, hard thresholding at $t = y_{k+1,n}$). Any hard thresholding estimator \hat{X}_θ obviously corresponds to some $\hat{X}_{[k]}$, specifically, $y_{k,n} > \theta \geq y_{k+1,n}$ (for notational consistency, set $y_{0,n} = \infty$). Thus,

$$\text{SE}_n^*[\mathbf{x}] = \min_{0 \leq k \leq p} \|X - \hat{X}_{[k]}\|_F^2.$$

We first show that keeping too many singular values is consistently sub-optimal:

Lemma 9. Set $M = r + 1 + \left\lceil \frac{\text{ASE}^*[\mathbf{x}]}{z_+} \right\rceil$. Then

$$\mathbb{P} \left\{ \exists N \text{ s.t. } \forall n \geq N : \text{SE}_n^*[\mathbf{x}] < \min_{k \geq M} \|X - \hat{X}_{[k]}\|_F^2 \right\} = 1.$$

Proof. Recall that for any matrix $A \in \mathbb{R}^{n \times p}$ with SVD $A = \sum_{i=1}^p \sigma_i \mathbf{u}_i \mathbf{v}_i^\top$, its best rank- r approximation with respect to Frobenius norm is obtained by taking its r leading principal components. Since X has rank r , for any $k \geq M$,

$$\|X - \hat{X}_{[k]}\|_F^2 \geq \min_{\text{rank}(B)=r} \|B - \hat{X}_{[k]}\|_F^2 = \sum_{i=r+1}^k y_{i,n}^2 \geq \sum_{i=r+1}^M y_{i,n}^2.$$

Recall that any fixed $i \geq r + 1$ satisfies $y_{i,n} \xrightarrow{a.s.} y_{i,\infty} = z_+$. Since M is constant, and satisfies $M > r + \text{ASE}^*[\mathbf{x}]/z_+$, we obtain that

$$\sum_{i=r+1}^M y_{i,n}^2 \xrightarrow{a.s.} (M - r)z_+ > \text{ASE}^*[\mathbf{x}].$$

Since $\text{SE}_n^*[\mathbf{x}] \leq \text{SE}_n[\mathbf{x}|T_\gamma(F_Z)] \xrightarrow{a.s.} \text{ASE}^*[\mathbf{x}]$, we conclude that almost surely, for all large enough n , $\text{SE}_n^*[\mathbf{x}] < \min_{k \geq M} \|X - \hat{X}_{[k]}\|_F^2$. \square

Lemma 9 tells us that to study the oracle loss $\text{SE}_n^*[\mathbf{x}]$ as $n \rightarrow \infty$, we only need, essentially, to study the risk of a bounded number of estimators; specifically, $X_{[k]}$ for $0 \leq k < M$. In order to obtain formulas for $\lim_{n \rightarrow \infty} \|X_n - \hat{X}_{[k]}\|_F^2$, we need to compute the limiting correlations between the underlying signal dyads, $\mathbf{a}_{1,n}\mathbf{b}_{1,n}^\top, \dots, \mathbf{a}_{r,n}\mathbf{b}_{r,n}^\top$ and the corresponding empirical dyads $\mathbf{u}_{i,n}\mathbf{v}_{i,n}^\top$, for all $1 \leq i < M$. For empirical spikes up to $i = r$, these limiting correlations are computed in [Benaych-Georges and Nadakuditi, 2012a] (recall Eq. (12)).

The next result shows that, as one would expect, the j -th singular vectors of Y , for any bounded $j \geq r + 1$, are asymptotically uncorrelated with the signal singular vectors:

Proposition 2. *For any $1 \leq i \leq r$ and fixed $j \neq i$ (not necessarily $j \leq r$), one has*

$$\langle \mathbf{a}_{n,i}, \mathbf{u}_{n,j} \rangle \cdot \langle \mathbf{b}_{n,i}, \mathbf{v}_{n,j} \rangle \xrightarrow{a.s.} 0.$$

We provide a proof of Proposition 2, assuming that $r = 1$. This restriction is due to our proof technique, and numerical results indicate that this results holds generally in the multi-spiked case. The proof is technical, and provided in Section B.

The following Lemma is an immediate corollary of Proposition 2:

Lemma 10. *For any $k \geq r$,*

$$\|X - \hat{X}_{[k]}\|_F^2 \xrightarrow{a.s.} \sum_{i=1}^r [x_i^2 + y_{i,\infty}^2 - 2x_i \cdot y_{i,\infty} \cdot \mathcal{C}(x_i)] + (k - r)z_+,$$

where, by way of notation, we use $\mathcal{C}(x_i) = 0$ for $x_i \leq x_+$. In particular,

$$\mathbb{P} \left\{ \exists N \text{ s.t. } \forall n \geq N : \text{SE}_n^*[\mathbf{x}] < \min_{k \geq r+1} \|X - \hat{X}_{[k]}\|_F^2 \right\} = 1.$$

Proof. The calculation is straightforward, as in the proof of Lemma 7. For the last part, simply recall that

$$\text{SE}_n[\mathbf{x}|T_\gamma(F_Z)] \xrightarrow{a.s.} \text{ASE}^*[\mathbf{x}] \leq \sum_{i=1}^r [x_i^2 + y_{i,\infty}^2 - 2x_i \cdot y_{i,\infty} \cdot \mathcal{C}(x_i)].$$

\square

We are ready to prove Theorems 1 and 2.

Proof of Theorem 1. By Lemmas 9 and 10, almost surely, there exists N such that $\forall n \geq N$,

$$\text{SE}_n^*[\mathbf{x}] = \min_{0 \leq k \leq r} \|X - \hat{X}_{[k]}\|_F^2.$$

Part (1) then follows from the observation that $\min_{0 \leq k \leq r} \|X - \hat{X}_{[k]}\|_F^2 \xrightarrow{a.s.} \text{ASE}^*[\mathbf{x}]$, as can be deduced from the calculations of Section 6.1. We now prove (2). Let's assume, for ease of notation, that $T_\gamma(F_Z) \notin \{y_{1,\infty}, \dots, y_{r,\infty}\}$. In that case, the asymptotic optimal interval is just the interval between some two consecutive spikes, say,

$$\underline{\Theta}(\mathbf{x}) = y_{k^*+1,\infty}, \quad \overline{\Theta}(\mathbf{x}) = y_{k^*,\infty},$$

with the notation $y_{0,\infty} = \infty$. With probability one, for large enough n , $X_{\theta_n} = \hat{X}_{[k^*]}$. Now, recall that $\|X_n - \hat{X}_{[k^*]}\|_F^2 \xrightarrow{a.s.} \text{ASE}^*[\mathbf{x}]$.

Proof of Theorem 2. Let k^* be as in the proof of Theorem 1. We know, from Lemmas 9, 10 and the definition of the asymptotic optimal interval, that $\|X - \hat{X}_{[k^*]}\|_F^2 \xrightarrow{a.s.} \text{ASE}^*[\mathbf{x}]$ and that almost surely, $\liminf_{n \rightarrow \infty} \min_{k \neq k^*} \|X - \hat{X}_{[k]}\|_F^2 > \text{ASE}^*[\mathbf{x}]$ (here we assume that there is no $y_{i,\infty}$ that equals $T_\gamma(F_Z)$). Thus,

$$\mathbb{P} \left\{ \exists N \text{ s.t. } \forall n \geq N : \text{SE}_n^*[\mathbf{x}] = \|X - \hat{X}_{[k^*]}\|_F^2 < \min_{k \neq k^*} \|X - \hat{X}_{[k]}\|_F^2 \right\} = 1.$$

The proof follows by noting that: (i) If $\theta \in (\underline{\Theta}(\mathbf{x}), \overline{\Theta}(\mathbf{x}))$, then with probability 1, for all large enough n , $\hat{X}_{\theta_n} = \hat{X}_{[k^*]}$; (ii) If $\theta \notin [\underline{\Theta}(\mathbf{x}), \overline{\Theta}(\mathbf{x})]$ then with probability 1, for large enough n , $\hat{X}_{\theta_n} \neq \hat{X}_{[k^*]}$.

6.3 Estimating $T_\gamma(F_Z)$

Proof of Lemma 3. Let $\epsilon > 0$ be small. By assumption, $T_\gamma(H) > \mathcal{Z}_+(H)$, and it is the unique number satisfying $\Psi_\gamma(T_\gamma(H); H) = -4$. Let $y_1 = T_\gamma(H) - \epsilon/2$, $y_2 = T_\gamma(H) + \epsilon/2$, where ϵ was chosen small enough so that $\mathcal{Z}_+(H) < y_1 < y_2$. Note that $\Psi_\gamma(y_1; H) < -4 < \Psi_\gamma(y_2; H)$. Since $H_n \xrightarrow{d} H$ (and $|p/n - \gamma| \leq 1/n \rightarrow 0$) we find that for all large enough n , $\Psi_{p/n}(y_1; H_n) < -4 < \Psi_{p/n}(y_2; H_n)$. Since also $\mathcal{Z}_+(H_n) \rightarrow \mathcal{Z}_+(H) < y_1$, we deduce that for large enough n , $y_1 < T_{p/n}(H_n) < y_2$, that is, $|T_{p/n}(H_n) - T_\gamma(H)| < \epsilon$.

Proof of Lemma 4. Part (1) will follow from (3), since convergence in KS distance implies weak convergence, and $F_{Z_n} \xrightarrow{d} F_Z$ almost surely. For part (3), denote by $z_{i,n}$, $i = 1, \dots, p$, the singular values of Z_n . By Weyl's interlacing inequality, since $Y_n = X_n + Z_n$ and $\text{rank}(X) = r \leq k$,

$$z_{i,n} \leq y_{i,n} \leq z_{i-k,n}, \quad \text{for } i = k+1, \dots, p.$$

Fix some y , and let j be the smallest index $j \geq k+1$ such that $y_{j,n} \leq y$ (set $j = 0$ if no such index exists). The interlacing inequality states that $z_{j,n} \leq y$ as well. If $j = k+1$, then at worst the interval contains all of $z_{k,n}, \dots, z_{1,n}$, and none of the additional "pseudo-singular values" we have introduced. Hence, in that case, $|F_{Z_n}(y) - F_{n,k}^*| \leq k/p$. Now, suppose that $j > k+1$. Since $y_{j+1,n} > y$, the interlacing inequality gives $z_{j+1-k,n} \geq y_{j+1,n} > y$, hence in addition to $z_{p,n}, \dots, z_{j,n}$, the interval $(-\infty, y]$ contains at most k additional singular values of

Z_n , specifically $z_{j+1,n}, \dots, z_{j-k}$. In the worst case, we have added no “pseudo-singular values” with $\leq y$, hence again $|F_{Z_n}(y) - F_{n,k}^*| \leq k/p$. Lastly, to prove (2), note that for any $\epsilon > 0$, $F_Z(\mathcal{Z}_+(F_Z) - \epsilon) < 1$, which means that almost surely, for large enough n there are $\Omega(n)$ singular values of Z_n bigger than $\mathcal{Z}_+(F_Z) - \epsilon$. By interlacing, for any $m_n = o(n)$ with $m_n < r$, $y_{m_n,n} \geq z_{m_n,n}$, and $z_{m_n,n}$ must eventually be among those singular values bigger than $\mathcal{Z}_+(F_Z) - \epsilon$. But this is true for any $\epsilon > 0$, meaning that $y_{m_n} \xrightarrow{a.s.} \mathcal{Z}_+(F_Z)$ whenever $r < m_n = o(n)$.

Proof of Lemma 6. Fix any a satisfying $\mathcal{Z}_+(H) < a < T_\gamma(H)$. Observe that one can find a neighborhood \mathcal{N} of $T_\gamma(H)$ and $c_1, c_2 > 0$ such that $c_2 < \Psi'_{\gamma'}(y; G) < c_1$ for any distribution G supported on $[0, a]$ and γ' (to see this, simply follow calculations in the proof of Lemma 8). Thus, since $T_{p/n}(H_n) \rightarrow T_\gamma(H)$, for all large enough n ,

$$c_2(T_{p/n}(H_n) - T_\gamma(H)) < \Psi_{p/n}(T_{p/n}(H_n); H_n) - \Psi_{p/n}(T_\gamma(H); H_n) \leq c_1(T_{p/n}(H_n) - T_\gamma(H)).$$

Using $\Psi_\gamma(T_\gamma(H); H) = \Psi_{p/n}(T_{p/n}(H_n); H_n) = -4$, and the fact that Ψ is increasing, we conclude that

$$\begin{aligned} |T_{p/n}(H_n) - T_\gamma(H)| &\leq \max(1/c_1, 1/c_2) \cdot |\Psi_{p/n}(T_{p/n}(H_n); H_n) - \Psi_{p/n}(T_\gamma(H); H_n)| \\ &= \max(1/c_1, 1/c_2) \cdot |\Psi_\gamma(T_\gamma(H_n); H) - \Psi_{p/n}(T_\gamma(H); H_n)|. \end{aligned}$$

The right-hand-side is now $\mathcal{O}(\Delta_{1,n} + \Delta_{2,n} + |p/n - \gamma|)$.

Proof of Proposition 1. By Lemma 6, we need to show that

$$|\varphi(T_\gamma(F_Z); F_Z) - \varphi(T_\gamma(F_Z); F_{n,k}^*)|, |\varphi'(T_\gamma(F_Z); F_Z) - \varphi'(T_\gamma(H); F_{n,k}^*)| = \mathcal{O}_{\mathbb{P}}(k/p)$$

(by definition, $|\gamma_n - \gamma| \leq 1/n$). Write

$$\begin{aligned} \varphi(T_\gamma(F_Z); F_Z) - \varphi(T_\gamma(F_Z); F_{n,k}^*) &= [\varphi(T_\gamma(F_Z); F_Z) - \varphi(T_\gamma(F_Z); F_{Z_n})] \\ &\quad + [\varphi(T_\gamma(F_Z); F_{Z_n}) - \varphi(T_\gamma(F_Z); F_{n,k}^*)], \end{aligned}$$

we bound each bracket separately (the argument when φ is replaced by φ' is the same). The expression $\varphi(T_\gamma(F_Z); F_Z) = \int \frac{T_\gamma(F_Z)}{T_\gamma(F_Z)^2 - z^2} dF_Z(z)$ is a linear spectral statistic, and satisfies the requirement of [Bai and Silverstein, 2004], by assumption - see Section 3.2. Hence,

$$|\varphi(T_\gamma(F_Z); F_Z) - \varphi(T_\gamma(F_Z); F_{Z_n})| = \mathcal{O}_{\mathbb{P}}(1/p).$$

For the second term, recall that if F_1 and F_2 are CDFs supported on the interval I and $g : I \rightarrow \mathbb{R}$ is bounded and continuously differentiable, then

$$\left| \int g(t)(dF_1(t) - dF_2(t)) \right| \leq \left(\|g\|_{L^\infty(I)} + \|g'\|_{L^1(I)} \right) \cdot \|F_1 - F_2\|_{\text{KS}}.$$

Since both $\mathcal{Z}_+(F_{Z_n}), \mathcal{Z}_+(F_{n,k}^*) \xrightarrow{a.s.} \mathcal{Z}_+(F_Z)$, by Lemma 4, almost surely for large enough n , ,

$$|\varphi(T_\gamma(F_Z); F_{Z_n}) - \varphi(T_\gamma(F_Z); F_{n,k}^*)| = \mathcal{O}(k/p).$$

Acknowledgements

This research was made possible by the United States – Israel Binational Science Foundation (BSF) Grant 2016201 “Frontiers of Matrix Recovery” and partially supported by NSF DMS grants no. 1407813, 1418362, and 1811614. ER was supported by Israel Science Foundation grant no. 1523/16 and an Einstein-Kaye Fellowship from the Hebrew University of Jerusalem.

References

- [Achlioptas and McSherry, 2001] Achlioptas, D. and McSherry, F. (2001). Fast Computation of Low Rank Matrix Approximations. In *Proceedings of the thirty-third annual ACM symposium on Theory of computing*, pages 611–618.
- [Alter et al., 2000] Alter, O., Brown, P. O., and Botstein, D. (2000). Singular value decomposition for genome-wide expression data processing and modeling. *Proceedings of the National Academy of Sciences*, 97(18):10101–10106.
- [Azar et al., 2001] Azar, Y., Fiat, A., Karlin, A. R., McSherry, F., and Saia, J. (2001). Spectral Analysis of Data. In *Proceedings of the thirty-third annual ACM symposium on Theory of computing*, pages 619–626.
- [Bai and Silverstein, 2010] Bai, Z. and Silverstein, J. W. (2010). *Spectral analysis of large dimensional random matrices*, volume 20. Springer.
- [Bai and Yao, 2008] Bai, Z. and Yao, J.-f. (2008). Central limit theorems for eigenvalues in a spiked population model. *Annales de l’Institut Henri Poincaré (B) Probability and Statistics*, 44(3):447–474.
- [Bai and Silverstein, 2004] Bai, Z. D. and Silverstein, J. W. (2004). CLT for linear spectral statistics of large-dimensional sample covariance matrices. *Ann. Probab.*, 32(1A):553–605.
- [Bai et al., 1998] Bai, Z.-D., Silverstein, J. W., et al. (1998). No eigenvalues outside the support of the limiting spectral distribution of large-dimensional sample covariance matrices. *The Annals of Probability*, 26(1):316–345.
- [Baik et al., 2005] Baik, J., Ben Arous, G., and Pécché, S. (2005). Phase transition of the largest eigenvalue for nonnull complex sample covariance matrices. *The Annals of Probability*, 33(5):1643–1697.
- [Baik and Silverstein, 2006] Baik, J. and Silverstein, J. W. (2006). Eigenvalues of large sample covariance matrices of spiked population models. *Journal of Multivariate Analysis*, 97(6):1382–1408.
- [Benaych-Georges and Nadakuditi, 2012a] Benaych-Georges, F. and Nadakuditi, R. R. (2012a). The singular values and vectors of low rank perturbations of large rectangular random matrices. *Journal of Multivariate Analysis*, 111:120–135.
- [Benaych-Georges and Nadakuditi, 2012b] Benaych-Georges, F. and Nadakuditi, R. R. (2012b). The singular values and vectors of low rank perturbations of large rectangular random matrices. *Journal of Multivariate Analysis*, 111:120–135.
- [Bickel and Levina, 2008] Bickel, P. J. and Levina, E. (2008). Covariance regularization by thresholding. *The Annals of Statistics*, 36(6):2577–2604.

- [Cattell, 1966] Cattell, R. B. (1966). The scree test for the number of factors. *Multivariate Behavioral Research*, 1(2):245–276.
- [Chatterjee, 2015] Chatterjee, S. (2015). Matrix estimation by universal singular value thresholding. *Annals of Statistics*, 43(1):177–214.
- [Donoho et al., 2020] Donoho, D. L., Gavish, M., and Romanov, E. (2020). Code supplement for “ScreeNOT: Exact MSE-Optimal Singular Value Thresholding in Correlated Noise”. <https://purl.stanford.edu/py196rk3919>.
- [Edfors and Sandell, 1998] Edfors, O. and Sandell, M. (1998). OFDM channel estimation by singular value decomposition. *IEEE Transactions on Communications*, 46(7):931–939.
- [Gavish and Donoho, 2014] Gavish, M. and Donoho, D. L. (2014). The Optimal Hard Threshold for Singular Values is $4/\sqrt{3}$. *IEEE Transactions on Information Theory*, 60(8):5040–5053.
- [Hoff, 2006] Hoff, P. D. (2006). Model averaging and dimension selection for the singular value decomposition.
- [Hong et al., 2018] Hong, D., Balzano, L., and Fessler, J. A. (2018). Asymptotic performance of PCA for high-dimensional heteroscedastic data. *Journal of multivariate analysis*, 167:435–452.
- [Jackson, 1993] Jackson, D. A. (1993). Stopping rules in principal components analysis: a comparison of heuristical and statistical approaches. *Ecology*.
- [Johnstone, 2001] Johnstone, I. M. (2001). On the distribution of the largest eigenvalue in principal components analysis. *Annals of Statistics*, 29(2):295–327.
- [Jolliffe, 2005] Jolliffe, I. (2005). *Principal component analysis*. Springer, New York, 2nd edition.
- [Lagerlund et al., 1997] Lagerlund, T. D., Sharbrough, F. W., and Busacker, N. E. (1997). Spatial filtering of multichannel electroencephalographic recordings through principal component analysis by singular value decomposition. *Journal of clinical neurophysiology : official publication of the American Electroencephalographic Society*, 14(1):73–82.
- [Leeb and Romanov, 2018] Leeb, W. and Romanov, E. (2018). Optimal spectral shrinkage and PCA with heteroscedastic noise. *arXiv preprint arXiv:1811.02201*.
- [Nadler, 2008] Nadler, B. (2008). Finite sample approximation results for principal component analysis: A matrix perturbation approach. *The Annals of Statistics*, 36(6):2791–2817.
- [Owen and Perry, 2009] Owen, A. B. and Perry, P. O. (2009). Bi-cross-validation of the SVD and the nonnegative matrix factorization. *The Annals of Applied Statistics*, 3(2):564–594.
- [Paul, 2007] Paul, D. (2007). Asymptotics of Sample Eigenstructure for a Large Dimensional Spiked Covariance Model. *Statistica Sinica*, 17(4):1617–1642.
- [Perry, 2009] Perry, P. O. (2009). *Cross validation for unsupervised learning*. PhD thesis, Stanford University.
- [Price et al., 2006] Price, A. L., Patterson, N. J., Plenge, R. M., Weinblatt, M. E., Shadick, N. A., and Reich, D. (2006). Principal components analysis corrects for stratification in genome-wide association studies. *Nature genetics*, 38(8):904–9.
- [Shabalin and Nobel, 2013] Shabalin, A. A. and Nobel, A. B. (2013). Reconstruction of a low-rank matrix in the presence of Gaussian noise. *Journal of Multivariate Analysis*, 118:67–76.

- [Silverstein, 1985] Silverstein, J. W. (1985). The limiting eigenvalue distribution of a multivariate F matrix. *SIAM Journal on Mathematical Analysis*, 16(3):641–646.
- [Silverstein and Choi, 1995] Silverstein, J. W. and Choi, S.-I. (1995). Analysis of the limiting spectral distribution of large dimensional random matrices. *Journal of Multivariate Analysis*, 54(2):295–309.
- [Wachter et al., 1980] Wachter, K. W. et al. (1980). The limiting empirical measure of multiple discriminant ratios. *The Annals of Statistics*, 8(5):937–957.
- [Wold, 1978] Wold, S. (1978). Cross-Validatory Estimation of the Number of Components in Factor and Principal Components Components Models. *Technometrics*, 20(4):397–405.
- [Yin et al., 1983] Yin, Y., Bai, Z., and Krishnaiah, P. (1983). Limiting behavior of the eigenvalues of a multivariate F matrix. *Journal of Multivariate Analysis*, 13(4):508–516.

A Proof of Lemma 8

Define the probability distribution $d\tilde{H} = \gamma dH + (1 - \gamma)\delta_0$, so that, by definition, $\tilde{\varphi}_\gamma(y; H) = \varphi(y; \tilde{H})$. Since

$$\Psi(y; H) = y \cdot \frac{\mathcal{D}'(y; H)}{\mathcal{D}(y; H)} = y \cdot \left(\frac{\varphi'(y; H)}{\varphi(y; H)} + \frac{\varphi'(y; \tilde{H})}{\varphi(y; \tilde{H})} \right),$$

to show that Ψ is increasing, it suffices to show that $y \mapsto y \cdot \frac{\varphi'(y; H)}{\varphi(y; H)}$ is increasing for any CDF H and $y > \mathcal{Z}_+(H)$.

Introduce a change of variables $w = \log(y)$ and set $\psi(w) = \varphi(e^w; H)$. We have

$$y \cdot \frac{\varphi'(y; H)}{\varphi(y; H)} = y \cdot \frac{d}{dy} (\log \varphi(y; H)) = y \cdot \frac{d}{dw} (\log \varphi(e^w; H)) \cdot \frac{dw}{dy} = \frac{d}{dw} (\log \psi(w)).$$

Since w is strictly increasing in y , it remains to show that $w \mapsto (\log \psi(w))'$ is increasing, equivalently, that $w \mapsto \psi(w)$ is log-convex. Write

$$\psi(w) = \int \psi_z(w) dH(z), \quad \text{where} \quad \psi_z(w) = \frac{e^{zw}}{e^{2w} - z^2}.$$

Since a convex combination of log-convex functions is log-convex, it suffices to verify that each $\psi_z(w)$ is log-convex, whenever $y^2 = e^{2w} > z^2$. A straightforward calculation gives:

$$(\log \psi_z(w))' = 1 - \frac{2e^{2w}}{e^{2w} - z^2} = -\frac{z^2 + e^{2w}}{e^{2w} - z^2} = -1 - \frac{2z^2}{e^{2w} - z^2},$$

which is negative and clearly increasing in w . Thus, $\psi_z(w)$ is log-convex, and so we conclude that $y \mapsto \mathcal{D}(y; H)$ is strictly increasing. For the limit as $y \rightarrow \infty$, write

$$\varphi(y; H) = \int \frac{y}{y^2 - z^2} dH(z) = \frac{1}{y} + o\left(\frac{1}{y^2}\right), \quad \varphi(y; H) = - \int \frac{y^2 + z^2}{(y^2 - z^2)^2} dH(z) = -\frac{1}{y^2} + o\left(\frac{1}{y^3}\right),$$

as $y \rightarrow \infty$. Thus, $\Psi_\gamma(y; H) = -2 + o(1)$ as $y \rightarrow \infty$.

For part (2), observe that the additional assumption on H implies that $\frac{\varphi'(y; H)}{\varphi(y; H)} \rightarrow -\infty$ as $y \rightarrow \mathcal{Z}_+(H)$ from the right, hence $\Psi(y) \rightarrow -\infty$. Now, since $\Psi(y)$ is continuous on $y \in (\mathcal{Z}_+(H), \infty)$, it must attain $\Psi(y^*) = -4$ for some y^* . This y^* must be unique since, as we have proved in (1), $\Psi(y; H)$ is strictly increasing.

B Proof of Proposition 2

We provide a proof assuming $r = 1$ (in fact the case $j \leq r$ already follows from the result of [Benaych-Georges and Nadakuditi, 2012b]).

The argument below relies on ideas from [Nadler, 2008].

When $r = 1$, the measurement matrix Y_n has the form $Y_n = x_1 \mathbf{a}_{1,n} \mathbf{b}_{1,n}^\top + Z_n$. Of course, the eigenvectors of $Y_n^\top Y_n$ are exactly the right singular vectors of Y_n , namely, $\mathbf{v}_{1,n}, \dots, \mathbf{v}_{p,n}$. Let $P_n = I - \mathbf{b}_{1,n} \mathbf{b}_{1,n}^\top$ be the projection onto the orthogonal complement of $\mathbf{b}_{1,n}$, and let $\mathbf{q}_{2,n}, \dots, \mathbf{q}_{p,n}$

be an eigenbasis of $P_n Y_n Y_n^\top P_n$, corresponding to its restriction onto $\text{range}(P_n) = \{\mathbf{b}_{1,n}\}^\perp$ in \mathbb{R}^p . Of course, the ordered tuple $\mathcal{B} = (\mathbf{b}_{1,n}, \mathbf{q}_{2,n}, \dots, \mathbf{q}_{p,n})$ constitutes an orthonormal basis of \mathbb{R}^p .

We now write the matrix $Y_n^\top Y_n$ in terms of the basis \mathcal{B} (that is, we conjugate it by the appropriate orthogonal change-of-basis matrix). The resulting matrix has the form

$$\mathbb{M} = \begin{bmatrix} \alpha_n & \mathbf{w}^\top \\ \mathbf{w} & D \end{bmatrix},$$

where

- $\alpha_n = \mathbf{b}_{1,n}^\top Y_n^\top Y_n \mathbf{b}_{1,n}$.
- $\mathbf{w} \in \mathbb{R}^{p-1}$ is given by

$$\mathbf{w}^\top = [\mathbf{b}_{1,n}^\top Y_n^\top Y_n \mathbf{q}_{2,n}, \dots, \mathbf{b}_{1,n}^\top Y_n^\top Y_n \mathbf{q}_{p,n}].$$

Note that, using $\mathbf{b}_{1,n} \perp \mathbf{q}_{i,n}$, we can write, for $i = 2, \dots, p$,

$$w_{i,n} = \mathbf{b}_{1,n}^\top Y_n^\top Y_n \mathbf{q}_{i,n} = (x_1 \mathbf{a}_{1,n}^\top + \mathbf{b}_{1,n}^\top Z_n^\top) Z_n \mathbf{q}_{i,n} = x_1 \mathbf{a}_{1,n}^\top Z_n \mathbf{q}_{i,n} + \mathbf{b}_{1,n}^\top Z_n^\top Z_n \mathbf{q}_{i,n},$$

where $\mathbf{w} = (w_{2,n}, \dots, w_{p,n})$.

- D is a diagonal matrix, $D = \text{diag}(\mu_{2,n}, \dots, \mu_{p,n})$ where $\mu_{i,n}$ is the eigenvalue of $P_n Y_n^\top Y_n P_n = P_n Z_n^\top Z_n P_n$ corresponding to the eigenvector $\mathbf{q}_{i,n}$.

The matrix \mathbb{M} is a so-called arrowhead matrix. Recall that, by definition, its eigenvalues are $y_{1,n}^2, \dots, y_{n,n}^2$; the corresponding eigenvectors are known to have the form

$$\mathbf{p}_{j,n} \propto \left(1, \frac{w_{2,n}}{y_{j,n}^2 - \mu_{2,n}}, \dots, \frac{w_{p,n}}{y_{j,n}^2 - \mu_{p,n}} \right), \quad j = 1, \dots, p.$$

Of course, recall that $\mathbf{p}_{j,n}$ is simply $\mathbf{v}_{j,n}$ written in the basis \mathcal{B} . Now, the first entry of $\mathbf{p}_{j,n}$ is (up to the ambiguous sign) the inner product $\langle \mathbf{b}_{1,n}, \mathbf{v}_{j,n} \rangle$, since $\mathbf{b}_{1,n}$ is represented by \mathbf{e}_1 in the basis \mathcal{B} . Thus,

$$|\langle \mathbf{b}_{1,n}, \mathbf{v}_{j,n} \rangle| = \left(1 + \sum_{i=2}^n \frac{w_{i,n}^2}{(y_{j,n}^2 - \mu_{i,n})^2} \right)^{-1/2}.$$

We claim that for any fixed $j \geq 2$,

$$\sum_{i=2}^n \frac{w_{i,n}^2}{(y_{j,n}^2 - \mu_{i,n})^2} \xrightarrow{a.s.} \infty,$$

from which the claimed result follows. Recall that, by assumption, $\mathbf{a}_{1,n}$ is uniform on the unit sphere \mathcal{S}^{n-1} . Introduce a Gaussian random vector, $\mathbf{g} \sim \mathcal{N}(0, I)$, independent of Z_n and $\mathbf{b}_{1,n}$, such that $\mathbf{a}_{i,n} = \mathbf{g} / \|\mathbf{g}\|$. Note that the basis $\mathbf{q}_{2,n}, \dots, \mathbf{q}_{n,n}$ can be chosen such that $\mathbf{b}_{1,n}^\top Z_n^\top Z_n \mathbf{q}_{i,n} \geq 0$ for all $2 \leq i \leq n$; indeed assume that this is the case. Setting $\eta_i = (\mu_{i,n})^{-1/2} \mathbf{g}^\top Z_n \mathbf{q}_{i,n}$, the random variables η_2, \dots, η_p are standard Gaussians, independent of Z_n and $\mathbf{b}_{1,n}$, and independent of one another, as

$$\text{Cov}(\eta_i, \eta_k) = (\mu_{i,n} \mu_{k,n})^{-1/2} \mathbf{q}_{i,n}^\top Z_n^\top Z_n \mathbf{q}_{k,n} = \mathbb{1}_{\{i=k\}},$$

and this is true because the vectors $\mathbf{q}_{i,n}$ are eigenvectors of $P_n Y_n^\top Y_n P_n = P_n Z_n^\top Z_n P_n$, with eigenvalues $\mu_{i,n}$. Clearly,

$$w_{i,n}^2 = \left(x_1 \mathbf{a}_{1,n}^\top Z_n \mathbf{q}_{i,n} + \mathbf{b}_{1,n}^\top Z_n^\top Z_n \mathbf{q}_{i,n} \right)^2 = \left(\frac{x_1 \sqrt{\mu_{i,n}}}{\|\mathbf{g}\|} \eta_i + \mathbf{b}_{1,n}^\top Z_n^\top Z_n \mathbf{q}_{i,n} \right)^2 \geq \frac{x_1^2 \mu_{i,n}}{\|\mathbf{g}\|^2} \eta_i^2 \mathbb{1}_{\{\eta_i \geq 0\}}.$$

Since $\mu_{i,n}$ are the eigenvalues of $P_n Y_n Y_n' P_n = P_n Z_n Z_n' P_n$, with P_n being a projection of co-dimension one, the eigenvalue interlacing theorem gives

$$z_{p,n}^2 \leq \mu_{p,n} \leq z_{n-1,n}^2 \leq \dots \leq z_{2,n}^2 \leq \mu_{2,n} \leq z_{1,n}^2,$$

with $z_{1,n}^2, \dots, z_{n,n}^2$ being the eigenvalues of $Z_n^\top Z_n$. The empirical CDF of the $z_{i,n}$ -s is F_{Z_n} , and recall that by assumption, F_{Z_n} converges to F_Z weakly almost surely. Thus, the empirical CDF of $\sqrt{\mu_{2,n}}, \dots, \sqrt{\mu_{p,n}}$ also converges weakly almost surely to F_Z . Fixing any $\epsilon > 0$, we know that with probability 1, for large enough n , $y_{j,n}^2 \leq (\mathcal{Z}_+(F_Z) + \epsilon)^2$, since $y_{j,n} \xrightarrow{a.s.} y_{j,\infty} = \mathcal{Z}_+(F_Z)$ (and $j > r = 1$). Since $\mu_{2,n} \xrightarrow{a.s.} \mathcal{Z}_+(F_Z)^2$, we deduce that with probability 1, for large enough n ,

$$\sum_{i=2}^n \frac{w_{i,n}^2}{(y_{j,n}^2 - \mu_{i,n})^2} \geq \sum_{i=2}^n \frac{w_{i,n}^2}{\left((\mathcal{Z}_+(F_Z) + \epsilon)^2 - \mu_{i,n} \right)^2} \geq \frac{x_1^2}{\|\mathbf{g}\|^2} \sum_{i=2}^n \frac{\eta_i^2 \mathbb{1}_{\{\eta_i \geq 0\}} \cdot \mu_{i,n}}{\left((\mathcal{Z}_+(F_Z) + \epsilon)^2 - \mu_{i,n} \right)^2}.$$

Since $\mathbb{E}[\eta_i^2 \mathbb{1}_{\{\eta_i \geq 0\}}] = 1/2$, and $\|\mathbf{g}\|^2/n \xrightarrow{a.s.} 1$, appealing to the strong law of large numbers,

$$\frac{x_1^2}{\|\mathbf{g}\|^2} \sum_{i=2}^n \frac{\eta_i^2 \mathbb{1}_{\{\eta_i \geq 0\}} \cdot \mu_{i,n}}{\left((\mathcal{Z}_+(F_Z) + \epsilon)^2 - \mu_{i,n} \right)^2} \xrightarrow{a.s.} \frac{1}{2} x_1^2 \int \frac{t^2}{\left((\mathcal{Z}_+(F_Z) + \epsilon)^2 - t^2 \right)^2} dF_Z(t).$$

Thus, almost surely, for any $\epsilon > 0$

$$\liminf_{n \rightarrow \infty} \left\{ \sum_{i=2}^n \frac{w_{i,n}^2}{(y_{j,n}^2 - \mu_{i,n})^2} \right\} \geq \frac{1}{2} x_1^2 \int \frac{t^2}{\left((\mathcal{Z}_+(F_Z) + \epsilon)^2 - t^2 \right)^2} dF_Z(t).$$

To conclude the proof, recall that the quantity on the right tends to ∞ as $\epsilon \rightarrow 0$.

C Additional numerical experiments

In this section we provide extensive numerical experiments validating different aspects of our results under various noise distributions.

C.1 Noise distributions

We have conducted experiments using the following noise distributions:

- **Marcenko-Pastur**: the matrix Z is an i.i.d Gaussian matrix, so that F_Z is a Marcenko-Pastur with shape parameter γ .
- **Chi10**: A noise matrix with correlated columns, such that W is i.i.d Gaussian and F_S is the law of a χ -squared random variable with 10 degrees of freedoms, normalized to have variance 1: $T = \frac{1}{10} \sum_{i=1}^{10} g_i$ where $g_1, \dots, g_{10} \sim \mathcal{N}(0, 1)$.

- **Mix2**: A noise matrix with correlated columns, such that W is i.i.d Gaussian, and F_S is an equal mixture of two atoms: $dF_S = \frac{1}{2}\delta_1 + \frac{1}{2}\delta_{10}$.
- **Unif[1,10]**: A noise matrix with correlated columns, such that W is i.i.d Gaussian, and F_S is the uniform distribution on $[1, 10]$.
- **Fisher3n**: Z has the form $Z = W_1 S_2^{-1/2}$ where $W_1 \in \mathbb{R}^{n \times p}$ is i.i.d Gaussian $\mathcal{N}(0, 1/n)$, and $S_2 = W_2^\top W_2$ where $W_2 \in \mathbb{R}^{3p \times p}$ is an i.i.d Gaussian matrix with entries $\mathcal{N}(0, 1/(3n))$. Matrices of this form have been studied in the literature under the name F-matrices (also F-ratios, Fisher matrices). Their limiting singular value distribution is given by Wachter's law [Wachter et al., 1980], see also [Yin et al., 1983, Silverstein, 1985, Bai and Silverstein, 2010].
- **PaddedIdentity**: All the singular values of Z are 1, that is, $dF_Z = \delta_1$. Specifically, Z is the matrix $Z = [\mathbf{I}_{p \times p}, \mathbf{0}_{p \times (n-p)}]^\top$, that is, a p -by- p identity matrix, padded by zeros.

In the table below, one can find some useful quantities corresponding to the distributions above (with select choices of γ): the bulk edge $\mathcal{Z}_+(F_Z)$, the location of the BBP PT \mathcal{X}_+ , optimal threshold $T_\gamma(F_Z)$ and $x^* = \mathcal{Y}^{-1}(T_\gamma(F_Z))$. All these quantities are estimated by sampling a large noise matrix Z (specifically, we take $p = 3000$ and $n = p/\gamma$) and estimating all the necessary functionals by their plugin estimates, putting F_{Z_n} in place of F_Z , and rounding all numbers to 2 digits after the decimal point. Estimating \mathcal{X}_+ in this manner is especially problematic, since for any counting measure H , in our case $H = F_{Z_n}$, $\mathcal{X}_+(H) = \lim_{y \rightarrow \mathcal{Z}_+(H)} (D_{p/n}(y; H))^{-1/2} = 0$, since $\mathcal{D}(\cdot; H)$ has $1/y$ singularity near $\mathcal{Z}_+(H)$. For our purposes, we use the heuristic $\mathcal{X}_+ \approx (D_{p/n}(\mathcal{Z}_+(F_{Z_n}) + 0.01; F_{Z_n}))^{-1/2}$, which may be somewhat off from the true PT location.¹⁷ In the case of **PaddedIdentity**, it is obvious that $\mathcal{X}_+ = 0$, and this is what we give below.

Distribution:	γ	$\mathcal{Z}_+(F_Z)$	$\mathcal{X}_+(F_Z)$	$T_\gamma(F_Z)$	$\mathcal{Y}^{-1}(T_\gamma(F_Z))$
Marcenko-Pastur	0.5	1.7	0.91	1.98	1.48
	1.0	2.0	1.07	2.31	1.73
Chi10	0.5	2.11	1.59	2.17	1.7
	1.0	2.26	1.5	2.46	1.89
Fisher3n	0.5	1.99	1.19	2.23	1.7
	1.0	2.28	1.36	2.57	1.95
Mix2	0.5	4.76	2.73	5.34	4.16
	1.0	5.44	3.13	6.08	4.73
Unif[1,10]	0.5	4.4	2.48	4.96	3.79
	1.0	5.04	2.72	5.7	4.36
PaddedIdentity	0.5	1.0	0.0	1.62	1.11
	1.0	1.0	0.0	1.73	1.15

C.2 Description of experiments

For each noise distribution we conduct the following experiments:

- **Hist**: We give a histogram singular values of a large noise matrix, in the case where the description of F_Z is not trivial. We do this to get a some sense for how the noise bulk looks like. Specifically, the noise matrix we sample has dimensions $p = 3000$ and $n = p/\gamma$.

¹⁷For instance, when the noise is Marcenko-Pastur, exact expressions are available, see e.g. [Gavish and Donoho, 2014], and $\mathcal{X}_+ = \gamma^{1/4}$. This is quite off from the expression in the table!

- **R0-vs-R1:** We compare the functions $R_0(x)$ and $R_1(x)$ from Lemma 8, and demonstrate that $x^* = \mathcal{Y}^{-1}(T_\gamma(F_Z))$ is their unique crossing point $x > \mathcal{X}_+$; this is done in the following way: we consider a rank 1 signal $X = x\mathbf{a}\mathbf{b}^\top$ and $Y = X + Z$, where the signal directions \mathbf{a}, \mathbf{b} and noise matrix Z are sampled once, and we let the intensity x vary. The dimensions used are $p = 500$ and $n = p/\gamma$. We plot the quantities $R_0(x) = \|X\|_F^2 = x^2$ (the error of the estimator $\hat{X} = 0$) and $\hat{R}_1(x) = \|X - y_1\mathbf{u}\mathbf{v}^\top\|_F^2$, the error obtained by for estimating X using the principal component of Y . The theory states that $\hat{R}_1(x)$ converges to $R_1(x)$, and we also plot this, as well as show that x^* is the unique intersection point of $R_0(x)$ and $R_1(x)$. Thresholding at the intersection of $\bar{R}_1(x)$ and $R_0(x)$ is optimal (for this problem instance), and we see that indeed this intersection point is quite close to x^* .
- **SE-vs-ASE:** Our theory states that as n, p grow, the random function $\theta \mapsto \text{SE}_n[\mathbf{x}|\theta]$ tends to the deterministic function $\theta \mapsto \text{ASE}[\mathbf{x}|\theta]$, when $\theta > \mathcal{Z}_+(F_Z)$. We illustrate this phenomenon. We consider a single problem instance, corresponding to the rank $r = 5$ signal $\mathbf{x} = (0.5, 1.0, 1.3, 2.5, 5.2)$, and plot the function $\text{SE}_n[\mathbf{x}|\theta]$ and $\text{ASE}[\mathbf{x}|\theta]$ on top of each other (we plot $\text{SE}_n[\mathbf{x}|\theta]$ for very few thresholds $\theta \leq y_{r+1,n}$; as the rank of X_t grows, the MSE blows up quickly). We use dimensions $p = 500$ and $n = p/\gamma$. We indicate the locations of $z_+, T_\gamma(F_Z)$ and the estimates $T_{p/n}(F_{n,k}^\star)$ for $\star \in \{0, w, i\}$, where we use $k = 4r = 20$. We see that for a “typical” problem instance, $\text{ASE}[\mathbf{x}|\theta]$ is indeed a good proxy for $\text{SE}_n[\mathbf{x}|\theta]$.
- **OracleAttainment:** We test Theorems 2 and 3, whereby the probability that thresholding at $T_{p/n}(F_{n,k}^\star)$ attains oracle loss with probability tending to 1 as $n, p \rightarrow \infty$. For various choices of p , we run $T = 50$ denoising experiments, and report the fraction of experiments where each threshold $\in \{T_\gamma(F_Z), T_{p/n}(F_{n,k}^0), T_{p/n}(F_{n,k}^w), T_{p/n}(F_{n,k}^i)\}$ attains oracle loss ($T_\gamma(F_Z)$ is computed as described in experiment **R0-vs-R1**). In all experiments, we use the signal $\mathbf{x} = (0.5, 1.0, 1.3, 2.5, 5.2)$ which has rank $r = 5$ (the same signal as in experiment **SE-vs-ASE**), and the upper bound $k = 4r = 20$. Note that we have chosen the spikes x_i to be all far from $x^* = \mathcal{Y}^{-1}(T_\gamma(F_Z))$, in accordance with the condition in Theorem 2.
- **Regret:** We compare the oracle loss $\text{SE}_n^*[\mathbf{x}]$ with $\text{SE}_n[\mathbf{x}|\hat{\theta}]$ for the choices

$$\hat{\theta} \in \left\{ T_\gamma(F_Z), T_{p/n}(F_{n,k}^0), T_{p/n}(F_{n,k}^w), T_{p/n}(F_{n,k}^i) \right\},$$

in the single-spiked setup, as described in experiment **R0-vs-R1** above. We let the spike intensity x vary and plot $\text{SE}_n[\mathbf{x}|\hat{\theta}]/\text{SE}_n^*[\mathbf{x}]$ for each choice of estimator. We expect the choice of estimator to especially matter when x is close to $x^* = \mathcal{Y}^{-1}(T_\gamma(F_Z))$ (indicated in the plots by a dashed vertical line), and this can indeed be seen in the plots. The ratios we report are averages across $T = 20$ experiments.

- **ConvergenceRate:** We study the rate of convergence of $T_{p/n}(F_{n,k}^\star)$ towards $T_\gamma(F_Z)$. To that end, we consider a rank $r = 10$ signal $\mathbf{x} = (1, \dots, 10)$, set $k = 20$ and plots the relative absolute error $\left| T_{p/n}(F_{n,k}^\star) - T_\gamma(F_Z) \right| / T_\gamma(F_Z)$ as p varies and $n = p/\gamma$. We plot the error in a logarithmic scale, to get a sense of its polynomial rate of decay in p . Note that by Proposition 1, we expect the slope in most cases to be, roughly, $\lesssim 1$. We find that almost always, $T_{p/n}(F_{n,k}^i)$ (imputation) approximates $T_\gamma(F_Z)$ much better than $T_{p/n}(F_{n,k}^w)$ (winsorization) or $T_{p/n}(F_{n,k}^0)$ (transport to zero). All points on the plots are generated by averaging the error of $T = 50$ experiments.

C.3 Distribution: Marcenko-Pastur, $\gamma = 1.0$

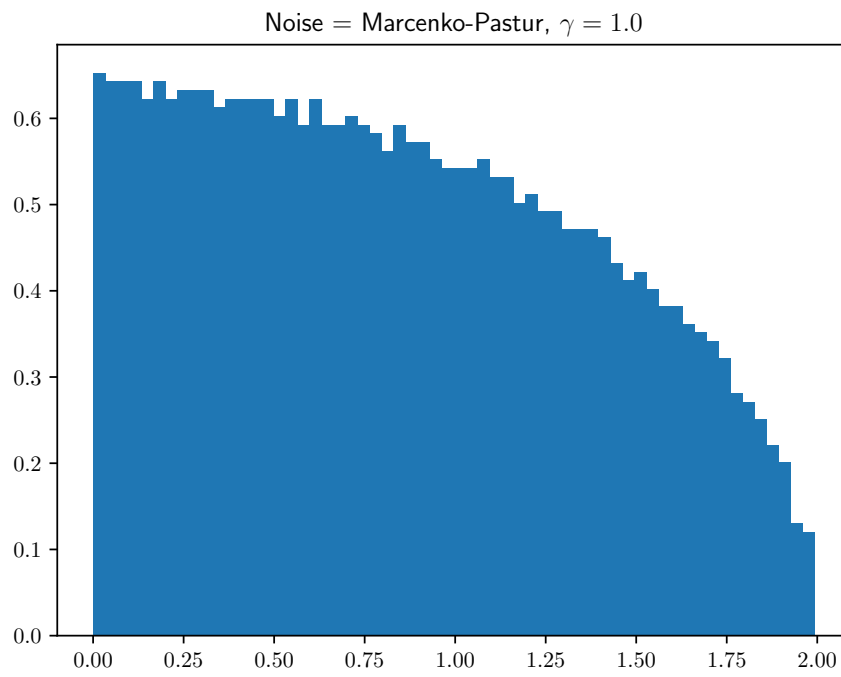


Figure 10: Experiment: **Hist**

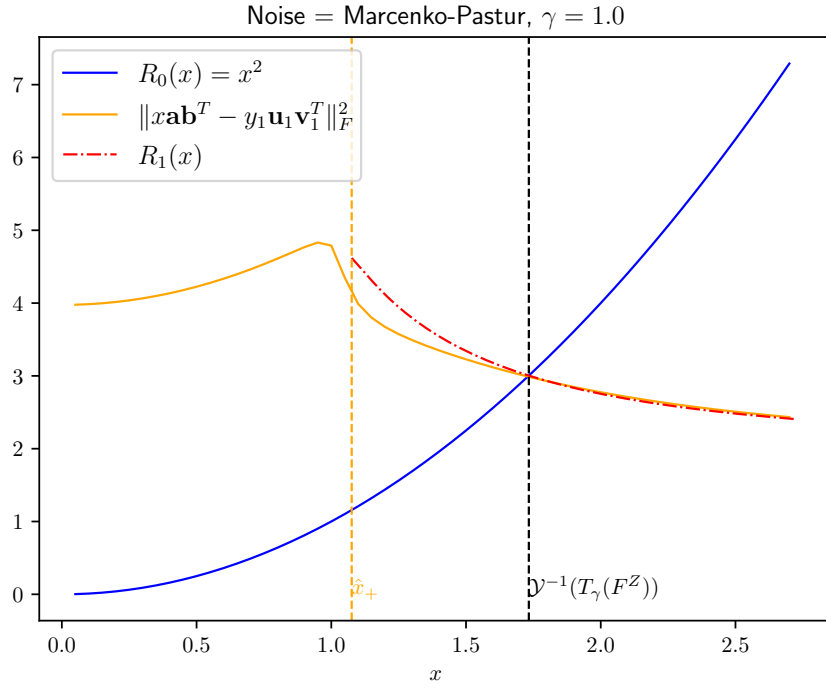


Figure 11: Experiment: **R0-vs-R1**

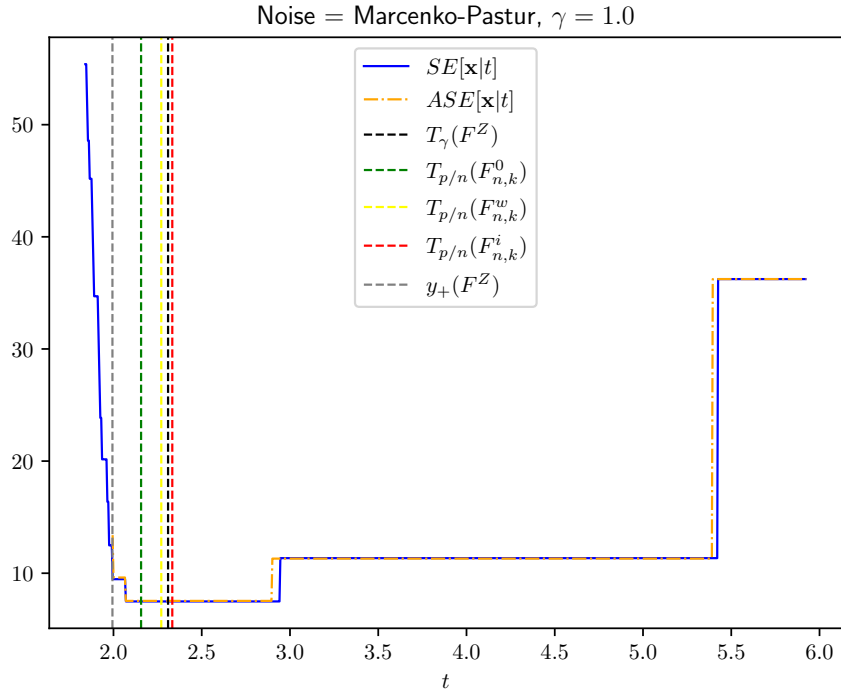


Figure 12: Experiment: **SE-vs-ASE**

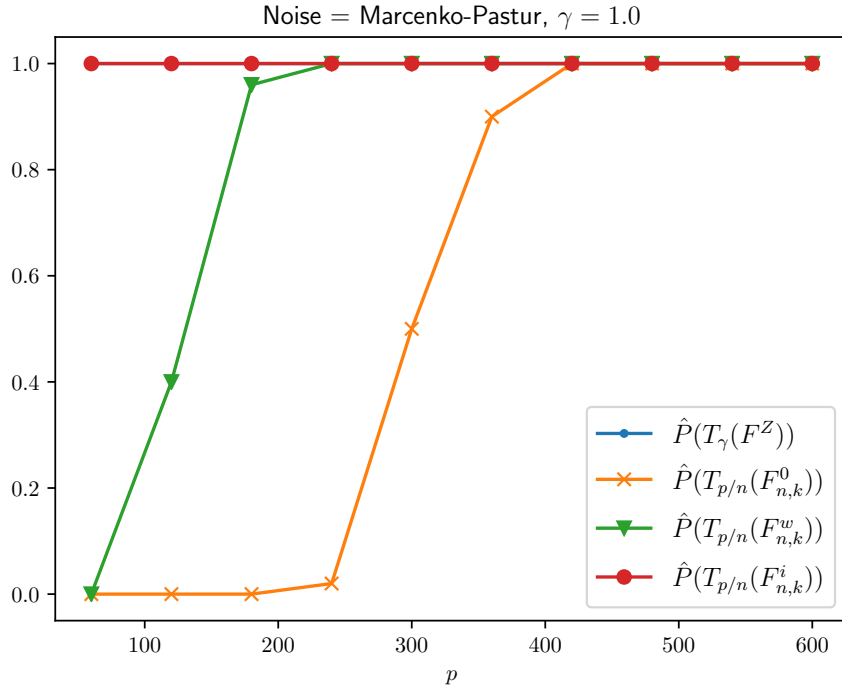


Figure 13: Experiment: **OracleAttainment**

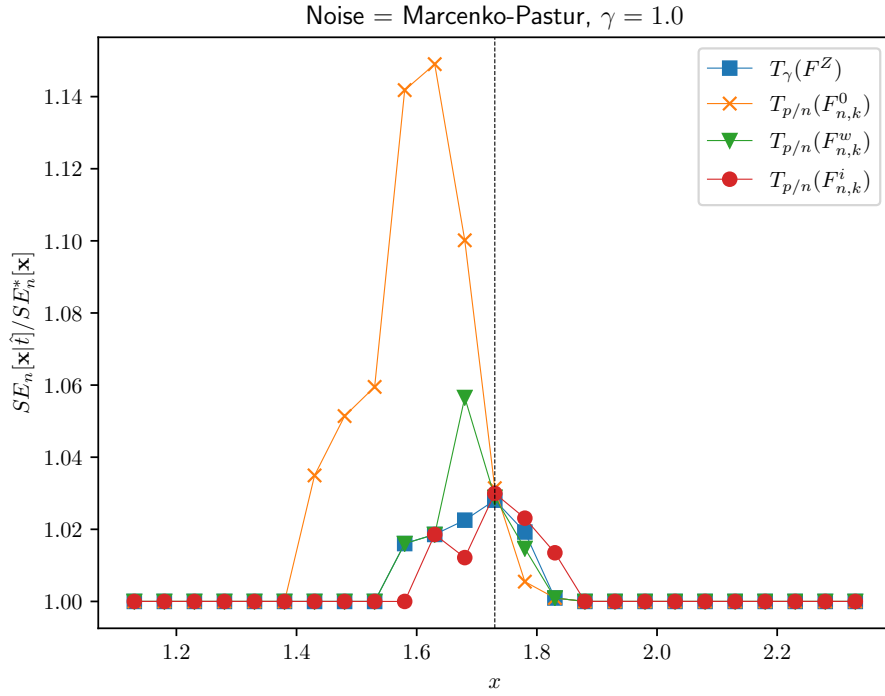


Figure 14: Experiment: **Regret**

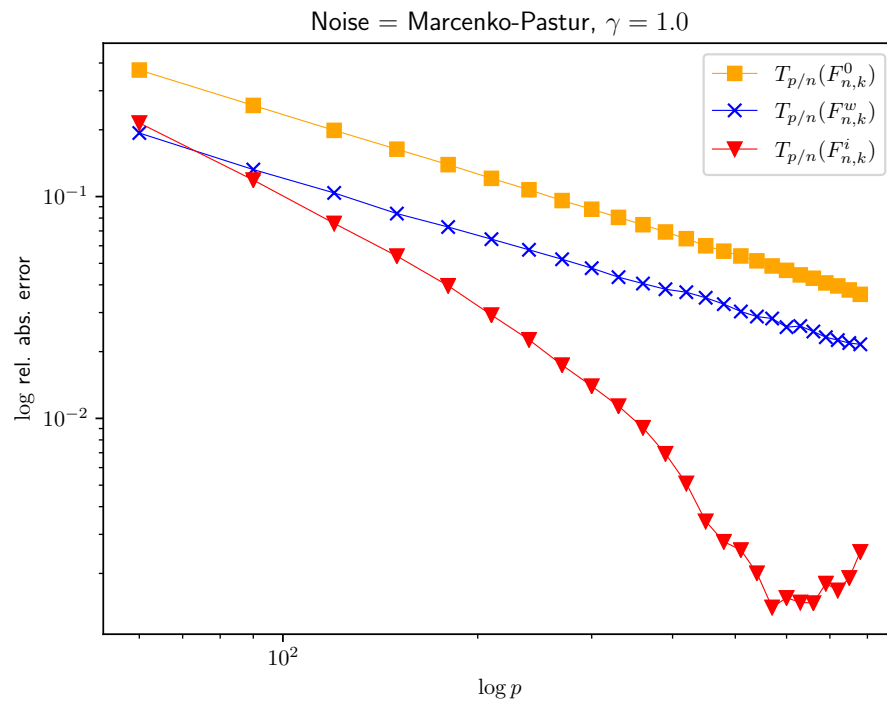


Figure 15: Experiment: **ConvergenceRate**

C.4 Distribution: Chi10, $\gamma = 0.5$

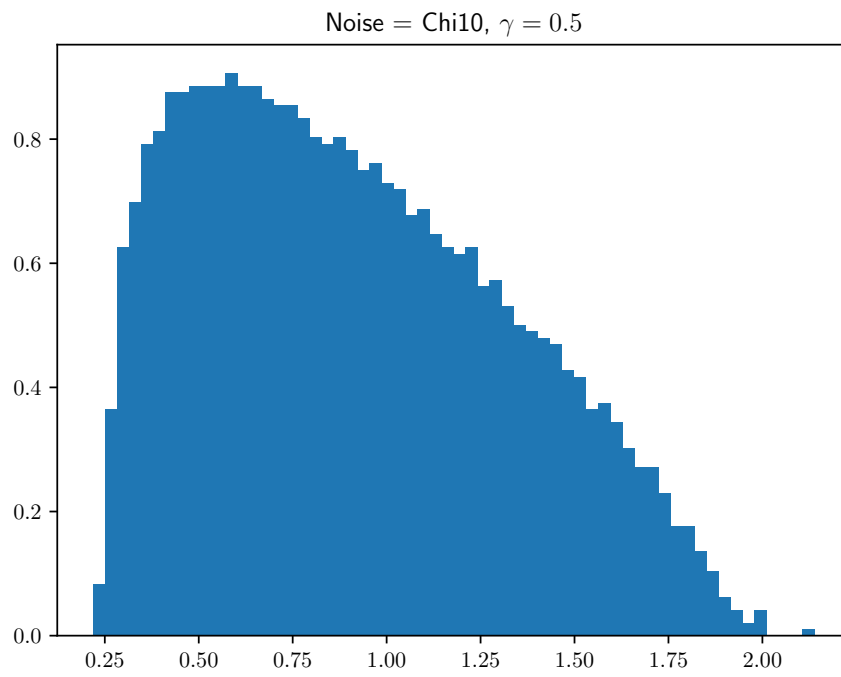


Figure 16: Experiment: **Hist**

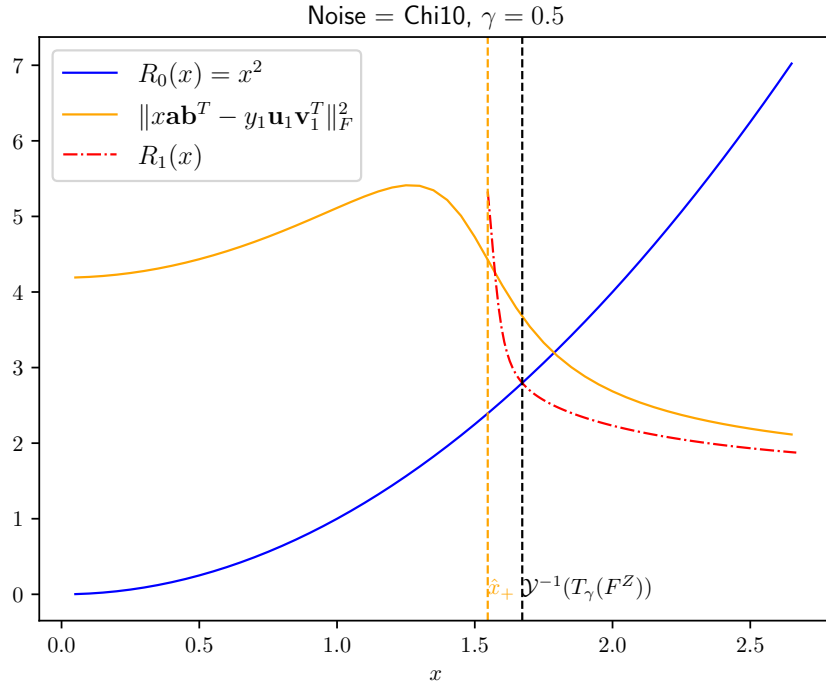


Figure 17: Experiment: **R0-vs-R1**

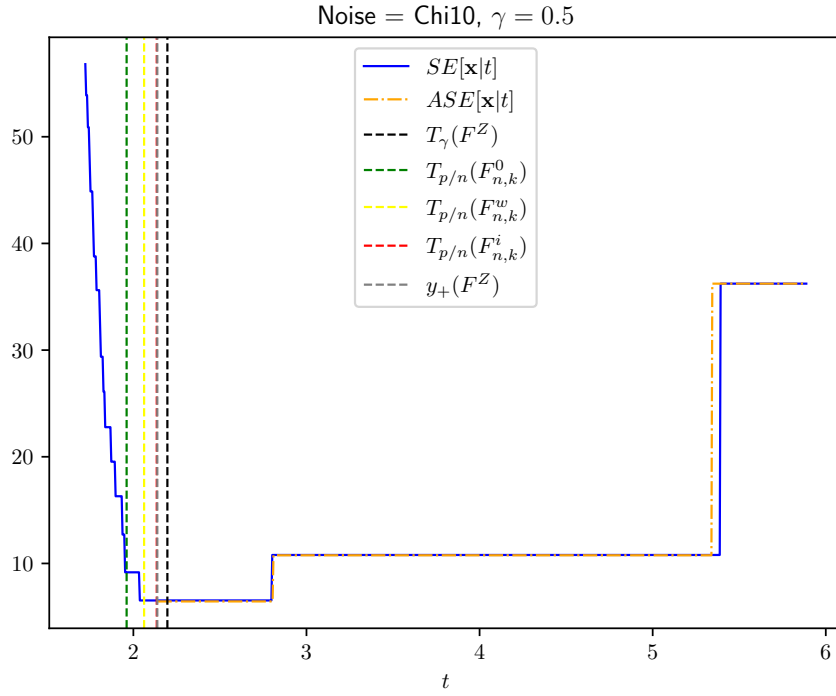


Figure 18: Experiment: **SE-vs-ASE**

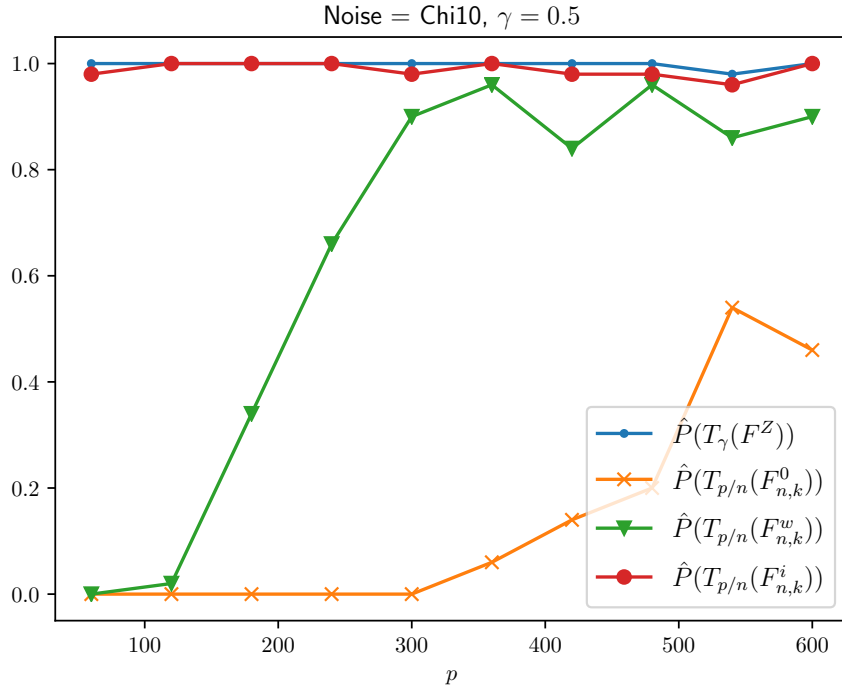


Figure 19: Experiment: **OracleAttainment**

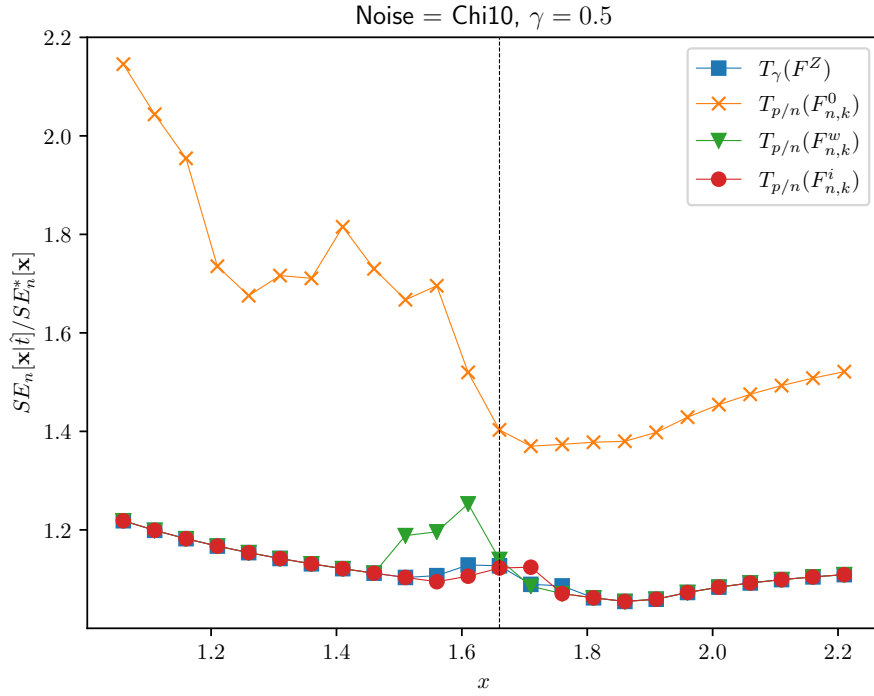


Figure 20: Experiment: **Regret**

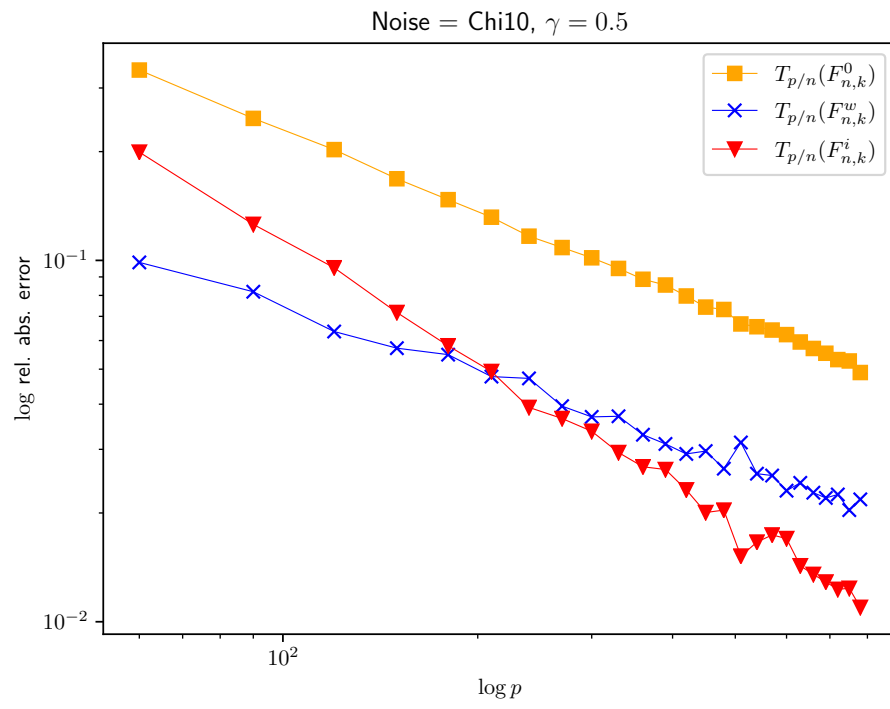


Figure 21: Experiment: **ConvergenceRate**

C.5 Distribution: Chi10, $\gamma = 1.0$

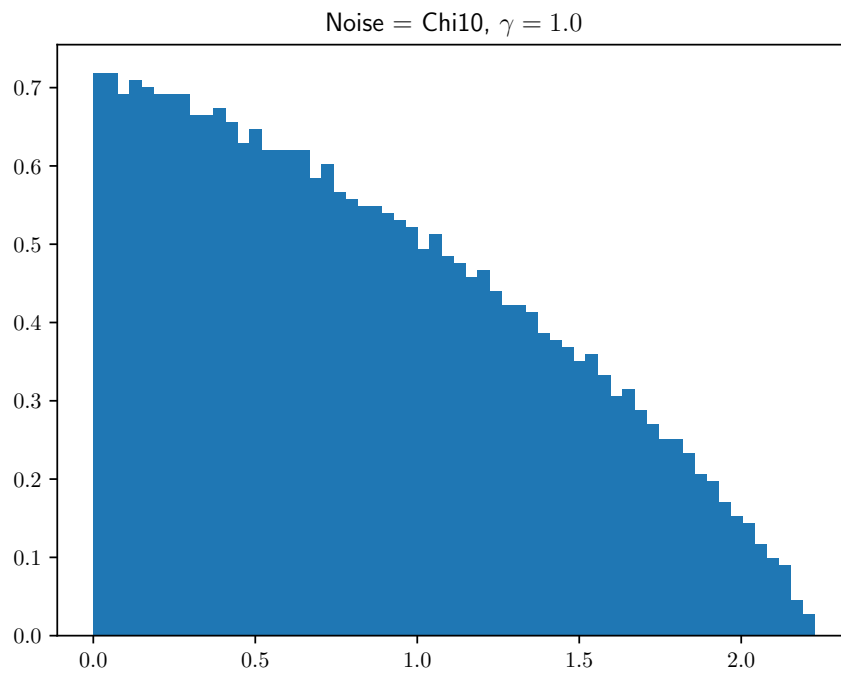


Figure 22: Experiment: **Hist**

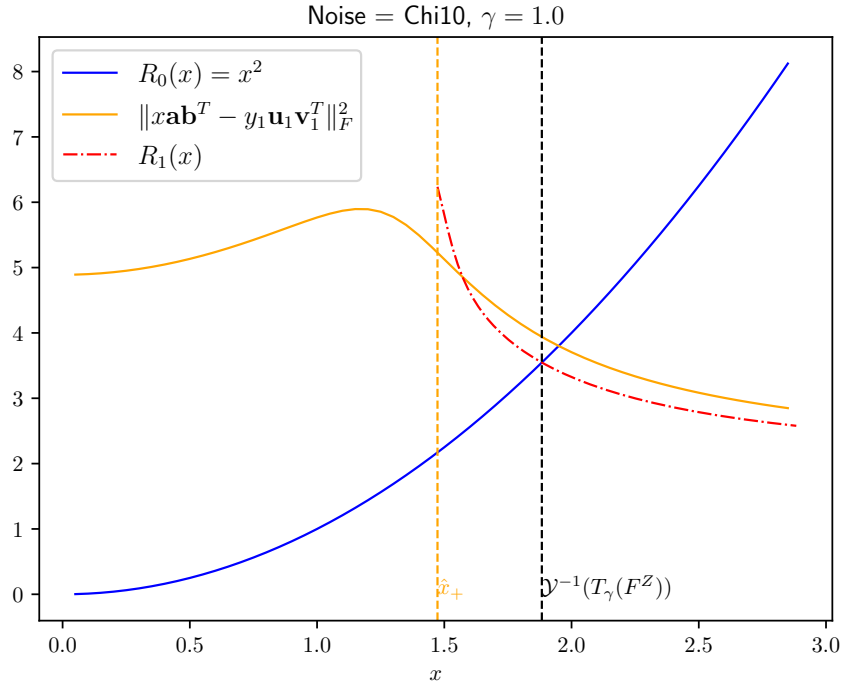


Figure 23: Experiment: **R0-vs-R1**

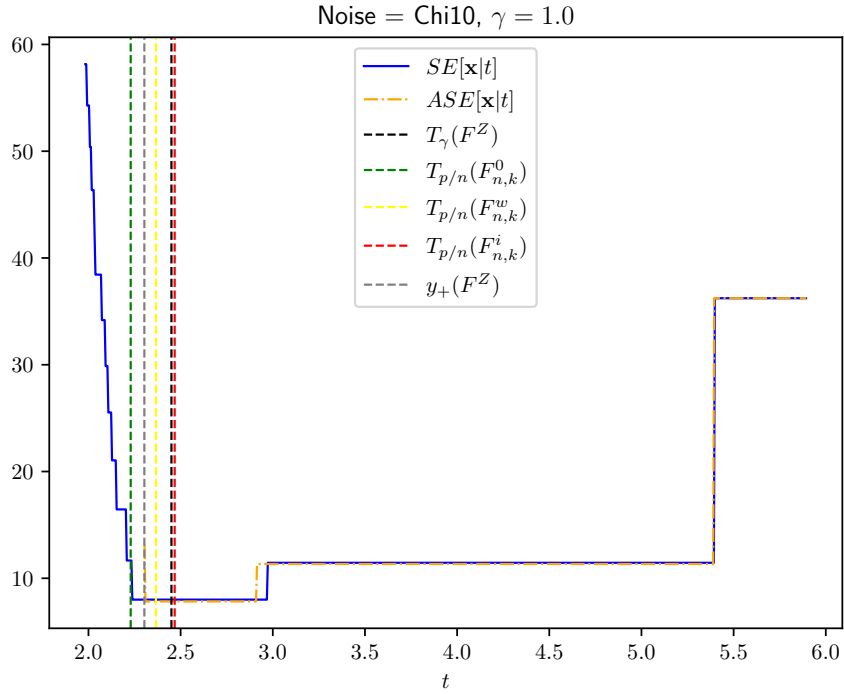


Figure 24: Experiment: **SE-vs-ASE**

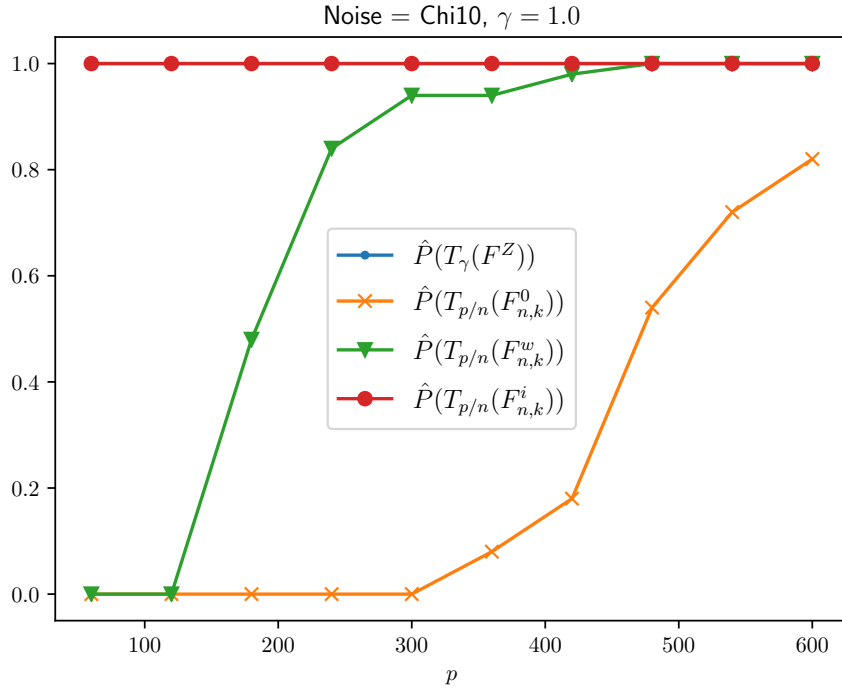


Figure 25: Experiment: **OracleAttainment**

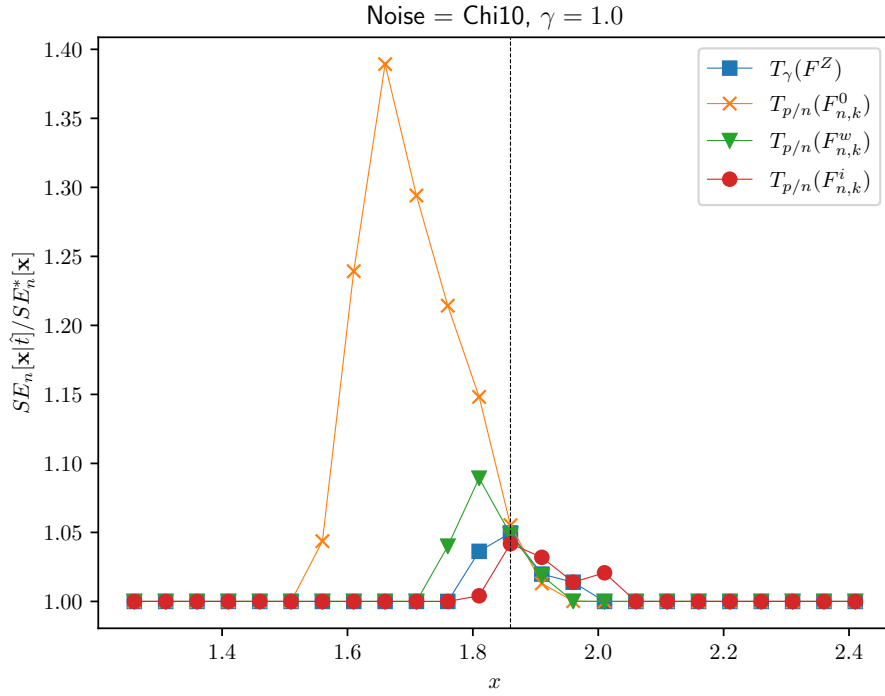


Figure 26: Experiment: **Regret**

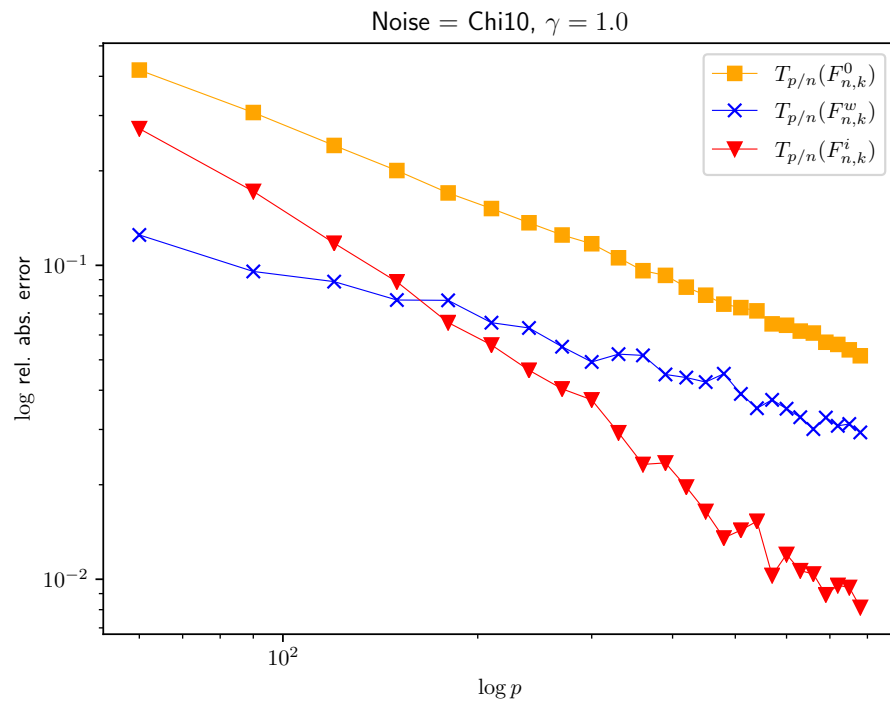


Figure 27: Experiment: **ConvergenceRate**

C.6 Distribution: Fisher3n, $\gamma = 0.5$

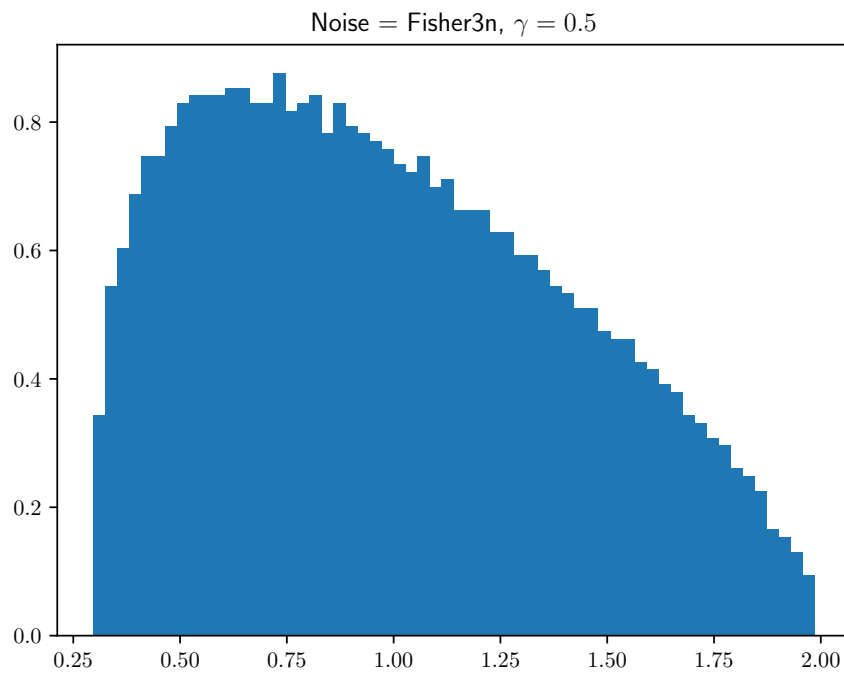


Figure 28: Experiment: **Hist**

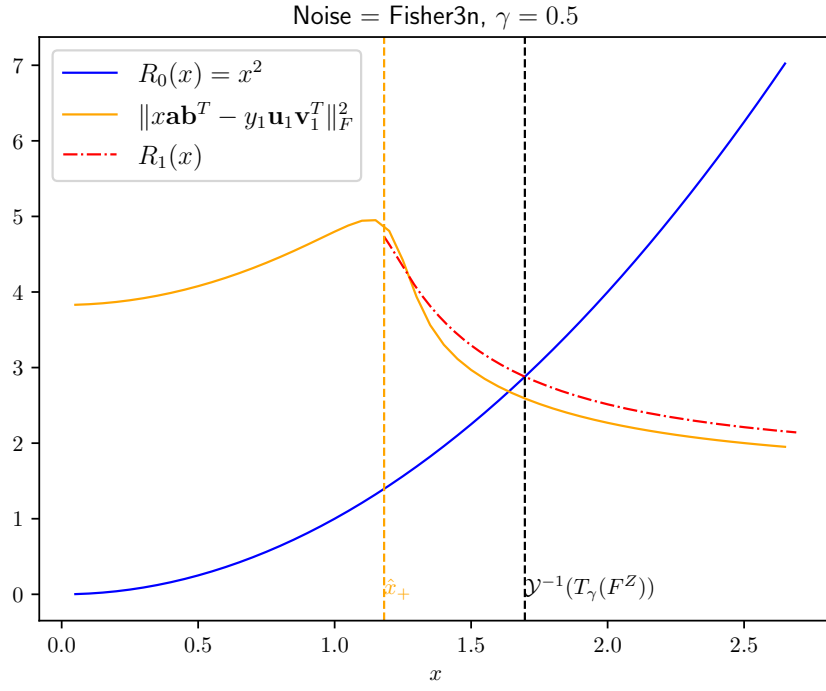


Figure 29: Experiment: **R0-vs-R1**

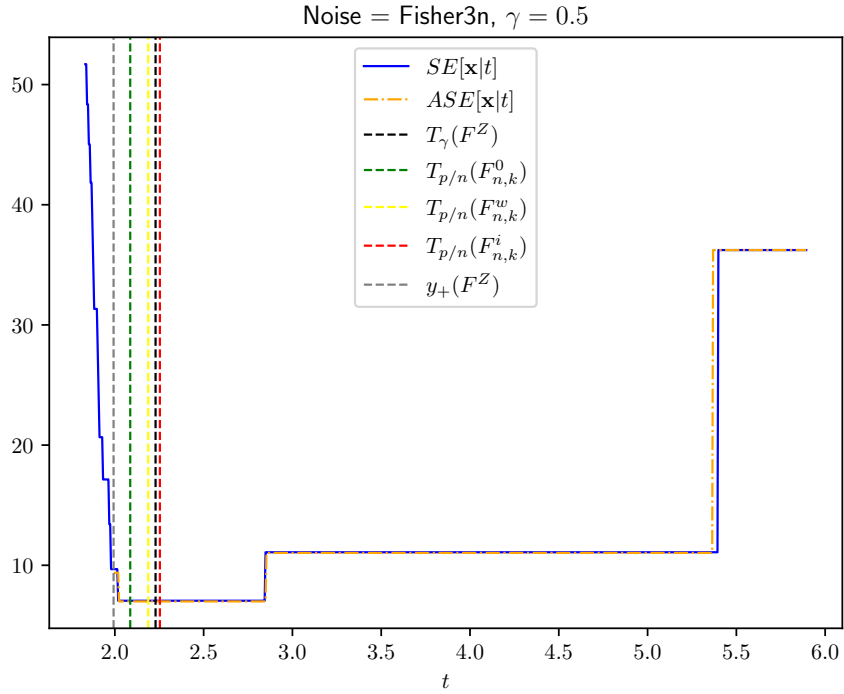


Figure 30: Experiment: **SE-vs-ASE**

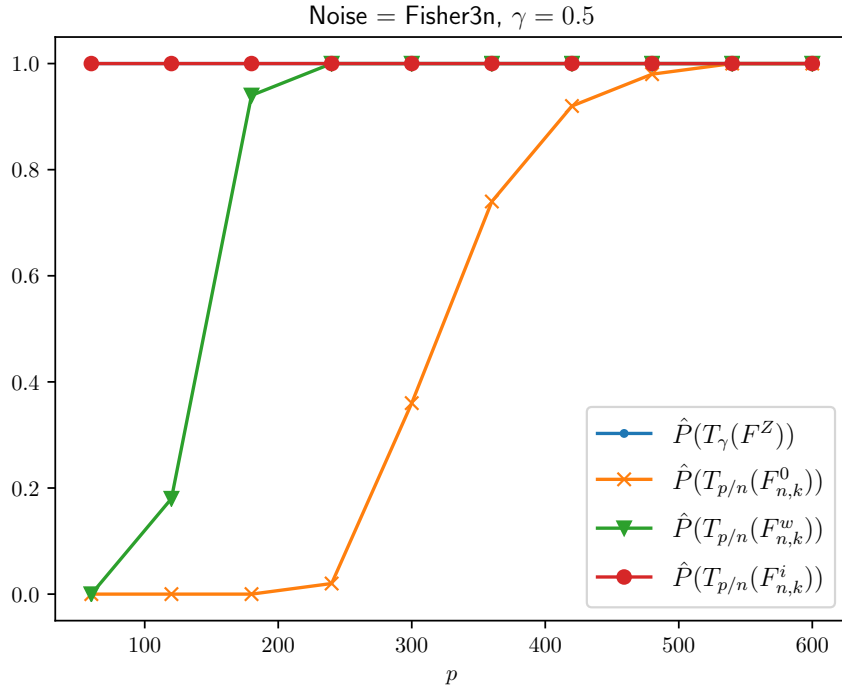


Figure 31: Experiment: **OracleAttainment**

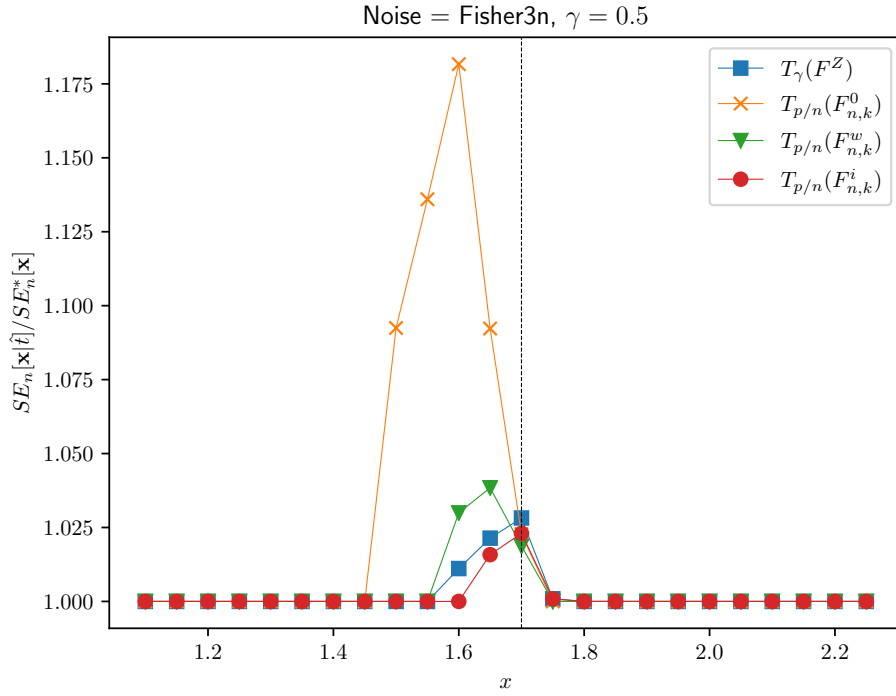


Figure 32: Experiment: **Regret**

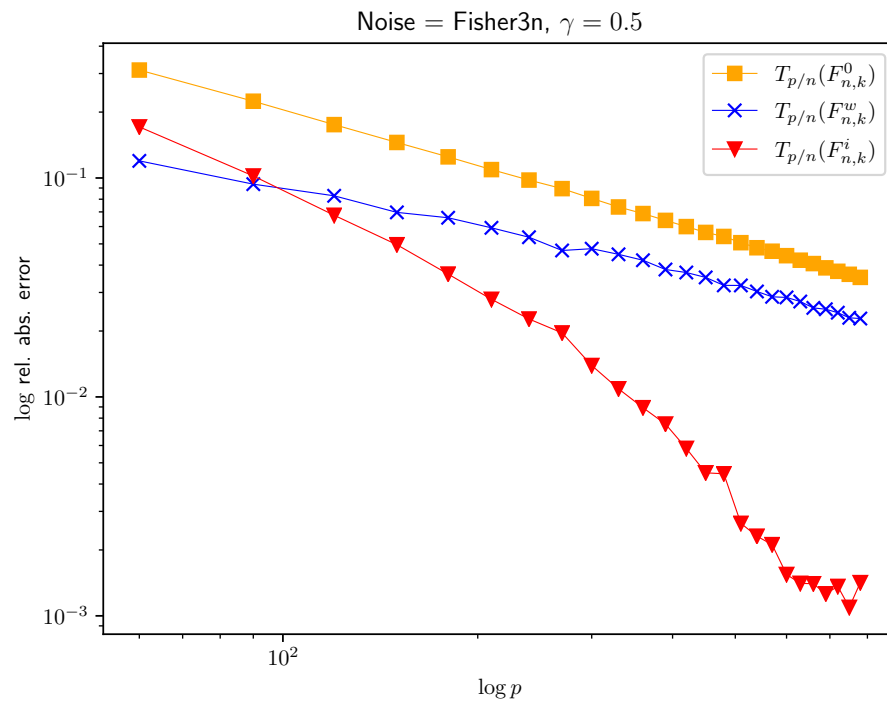


Figure 33: Experiment: **ConvergenceRate**

C.7 Distribution: Fisher3n, $\gamma = 1.0$

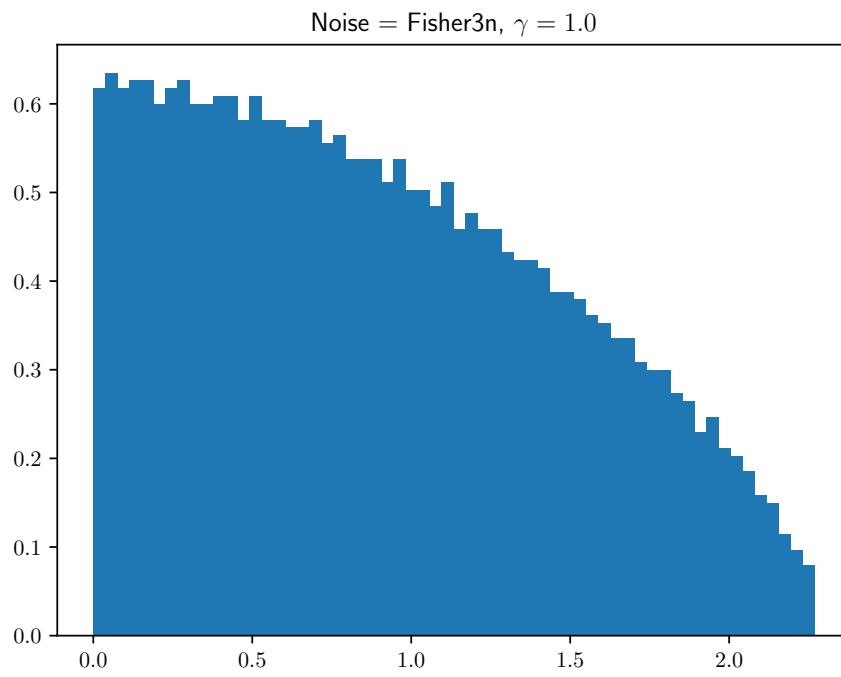


Figure 34: Experiment: **Hist**

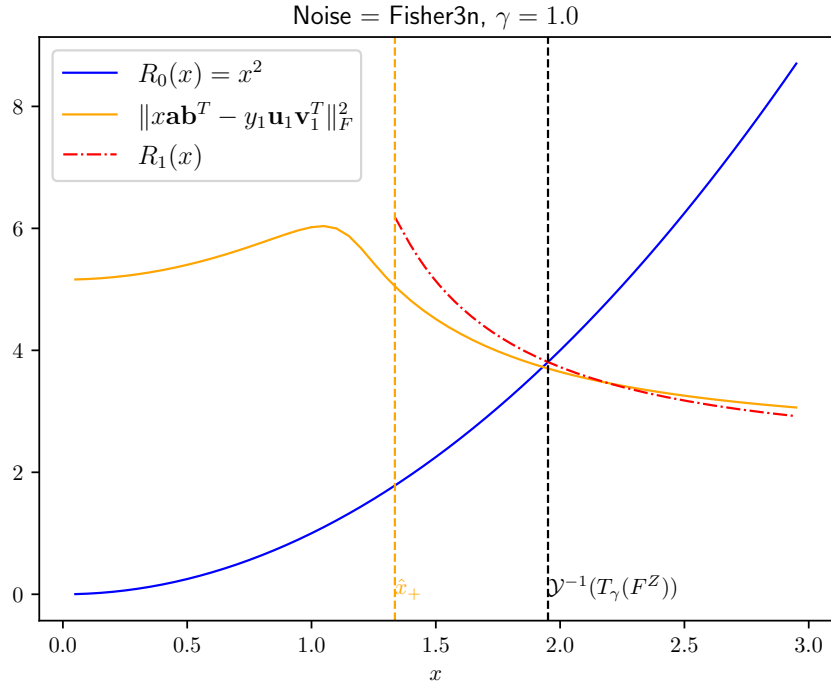


Figure 35: Experiment: **R0-vs-R1**

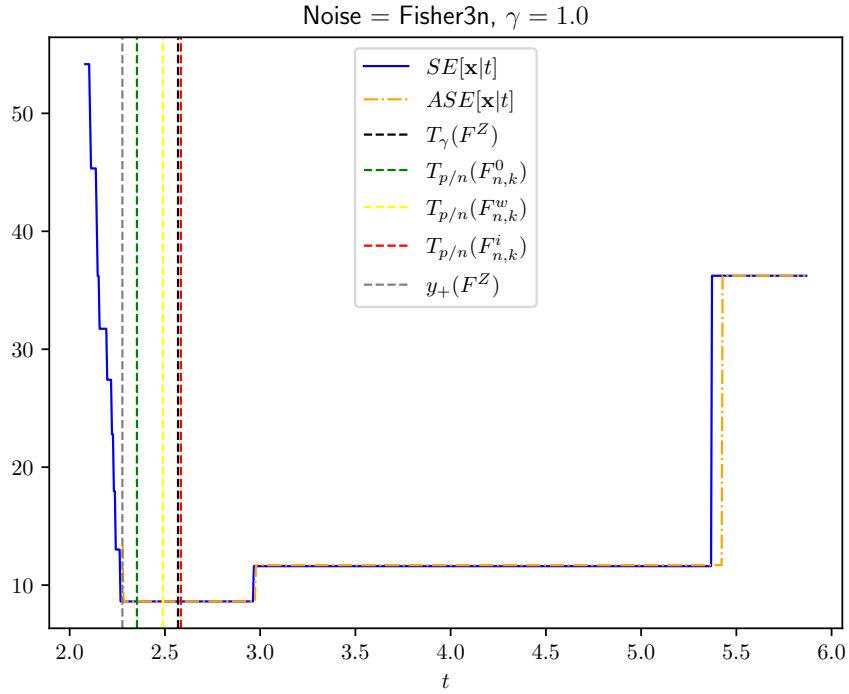


Figure 36: Experiment: **SE-vs-ASE**

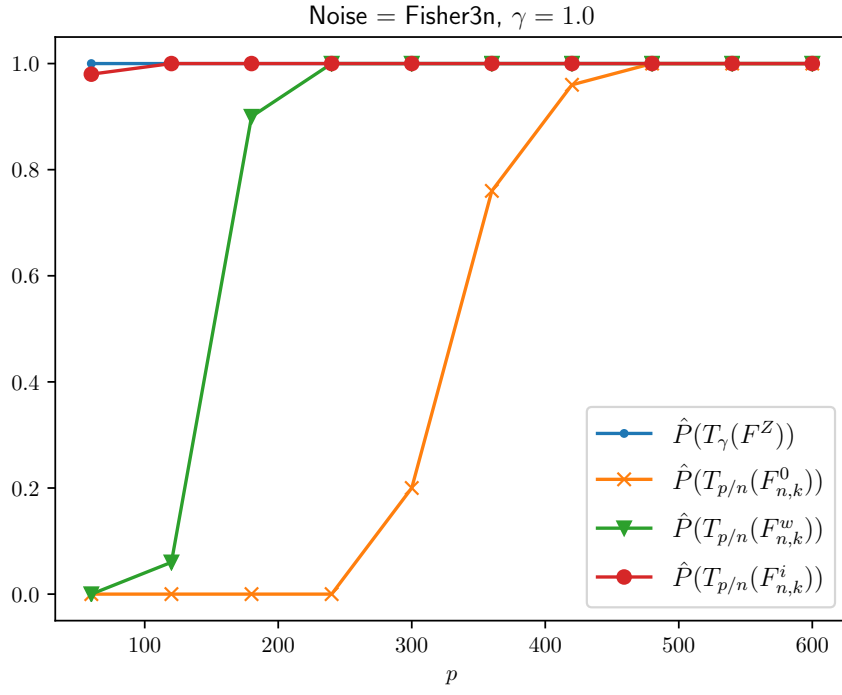


Figure 37: Experiment: **OracleAttainment**

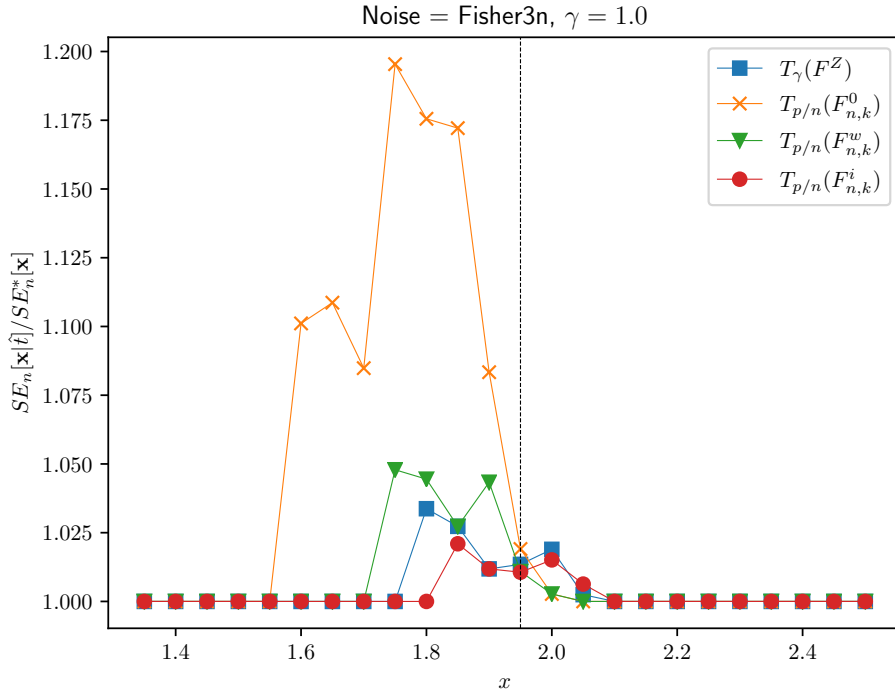


Figure 38: Experiment: **Regret**

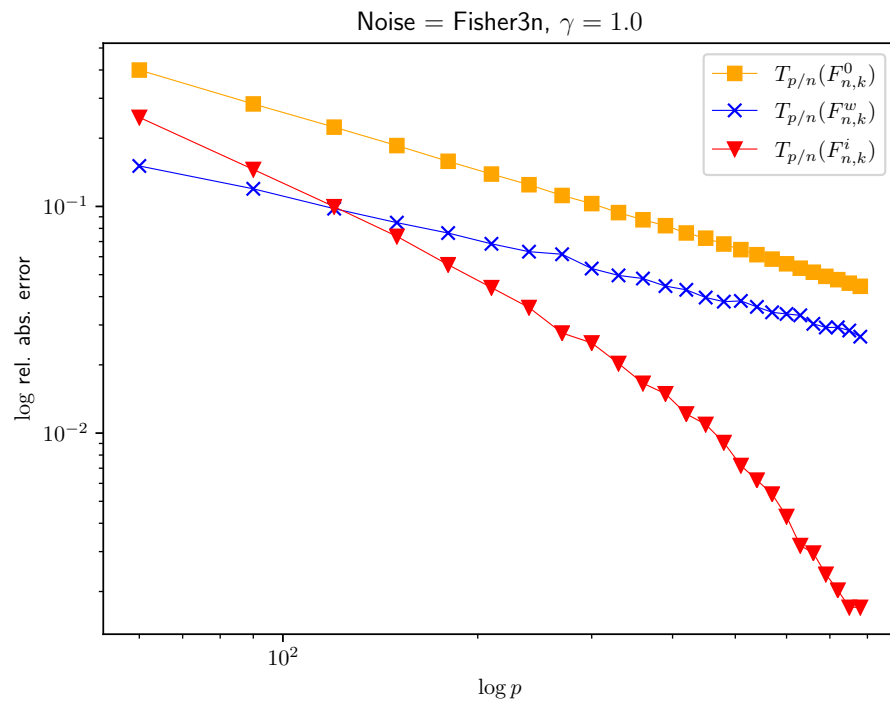


Figure 39: Experiment: **ConvergenceRate**

C.8 Distribution: Mix2, $\gamma = 0.5$

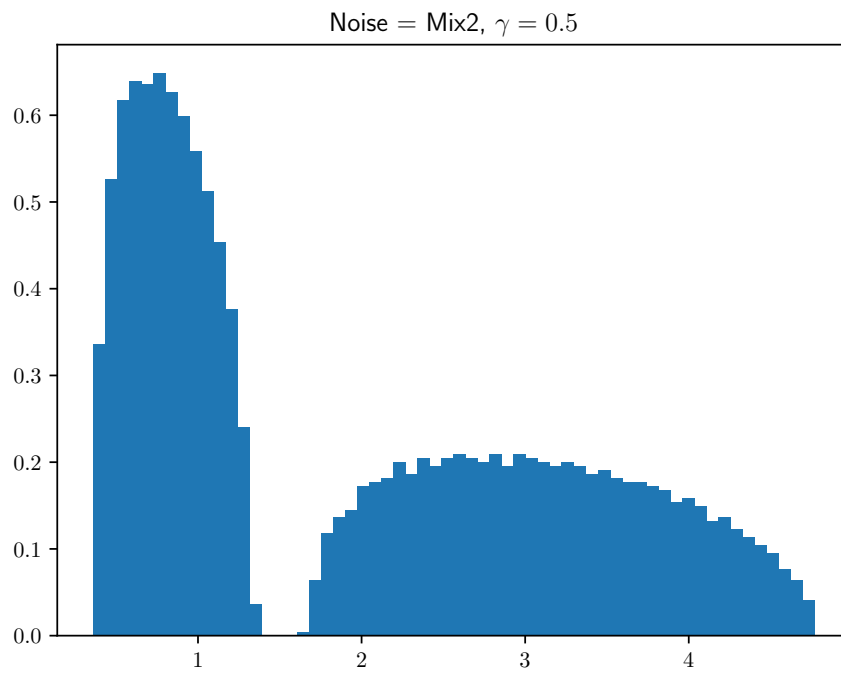


Figure 40: Experiment: **Hist**

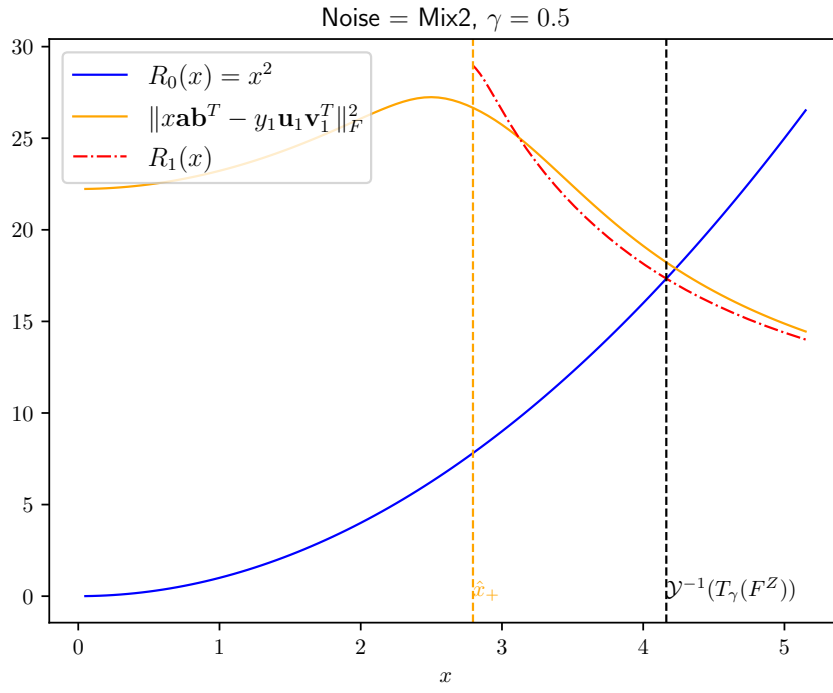


Figure 41: Experiment: **R0-vs-R1**

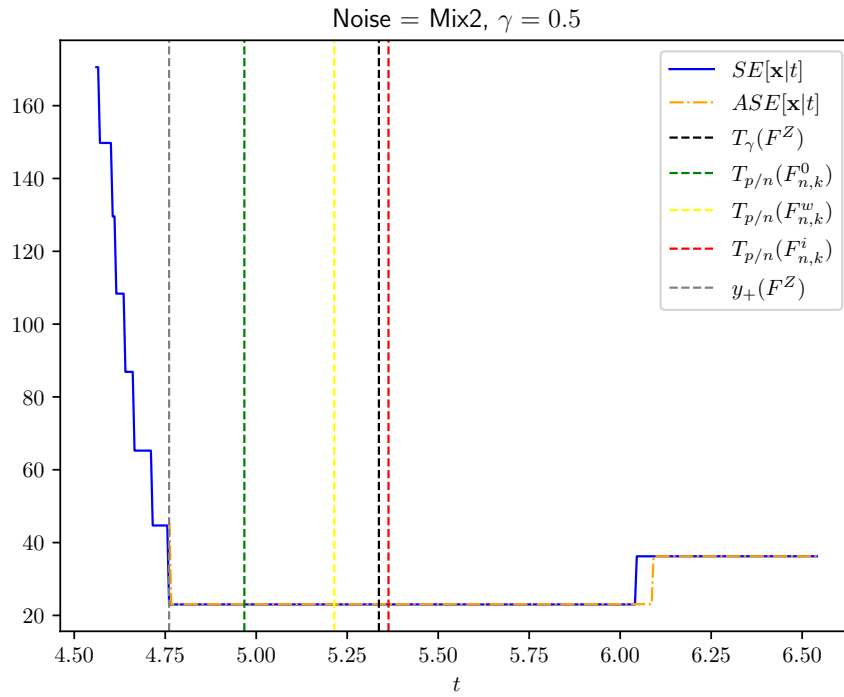


Figure 42: Experiment: **SE-vs-ASE**

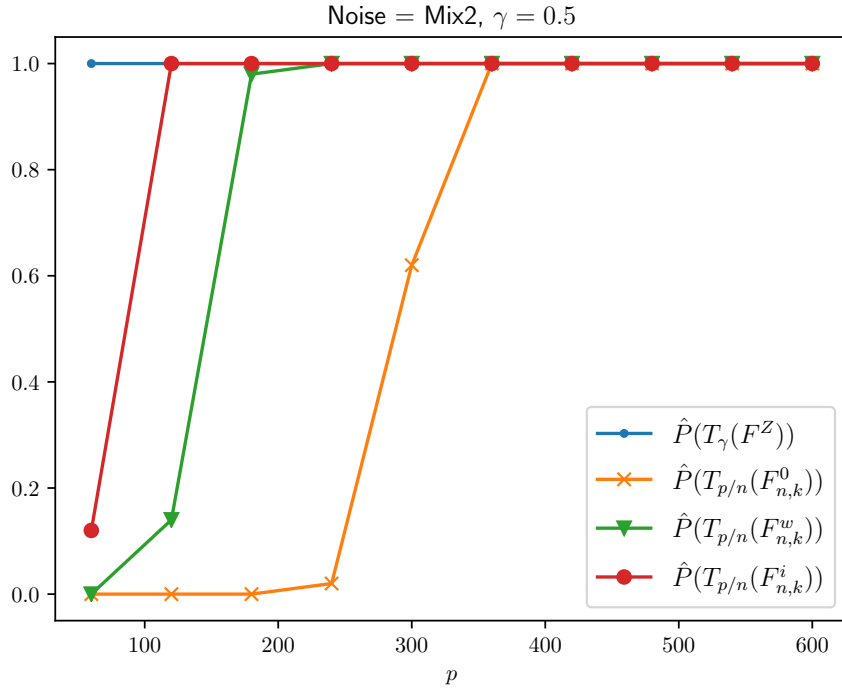


Figure 43: Experiment: **OracleAttainment**

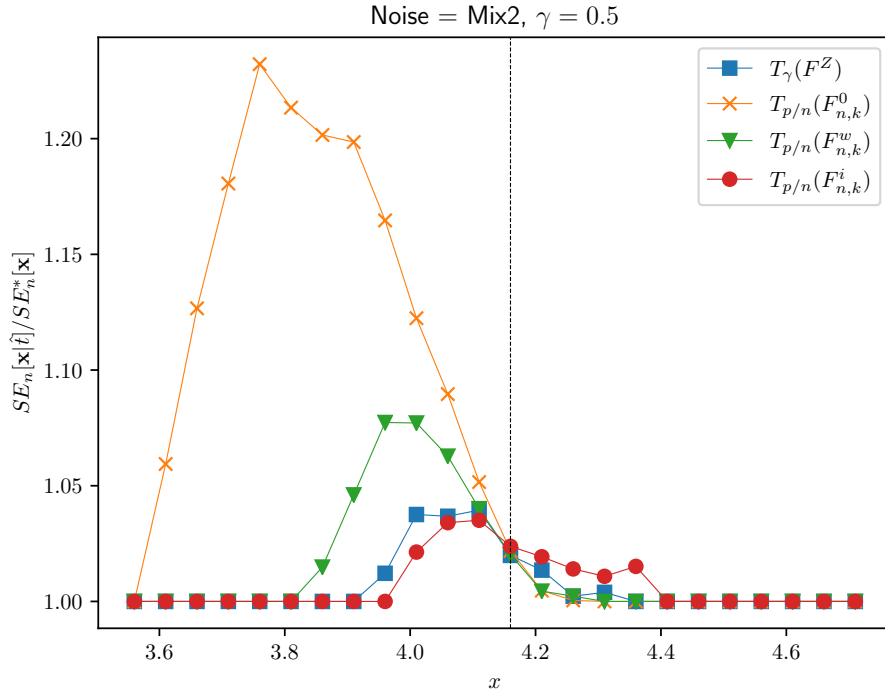


Figure 44: Experiment: **Regret**

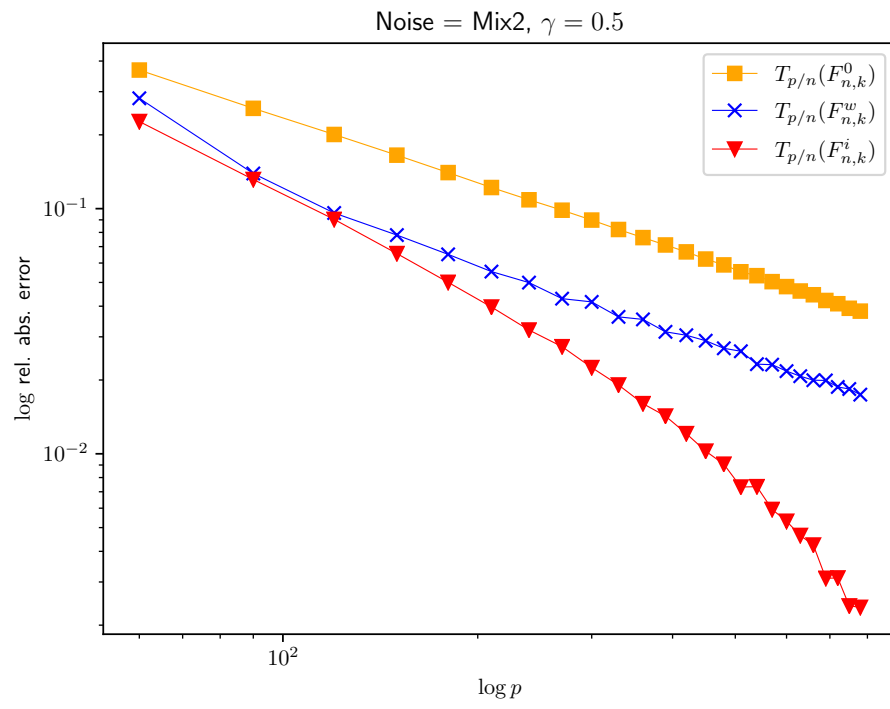


Figure 45: Experiment: **ConvergenceRate**

C.9 Distribution: Mix2, $\gamma = 1.0$

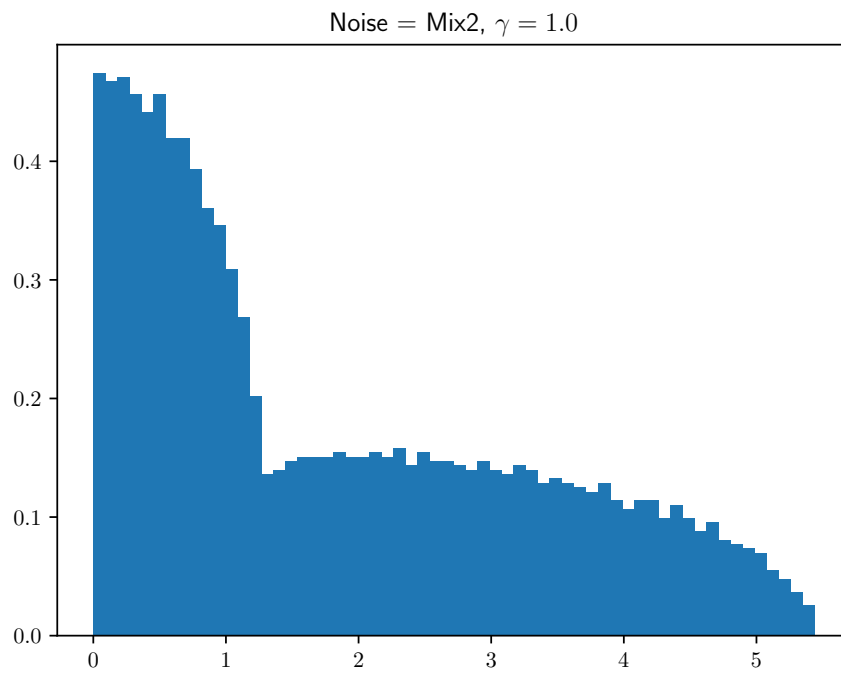


Figure 46: Experiment: **Hist**

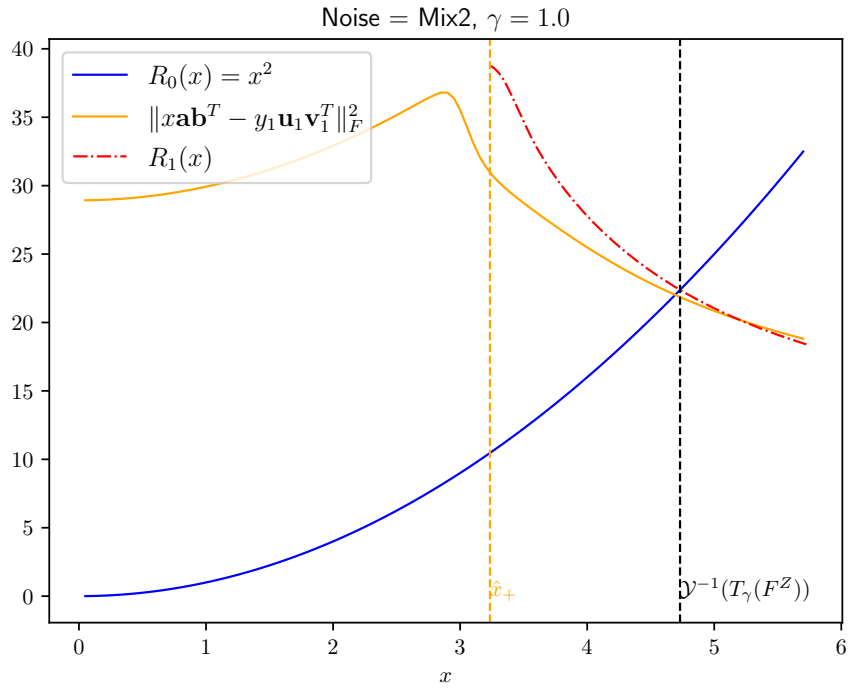


Figure 47: Experiment: **R0-vs-R1**

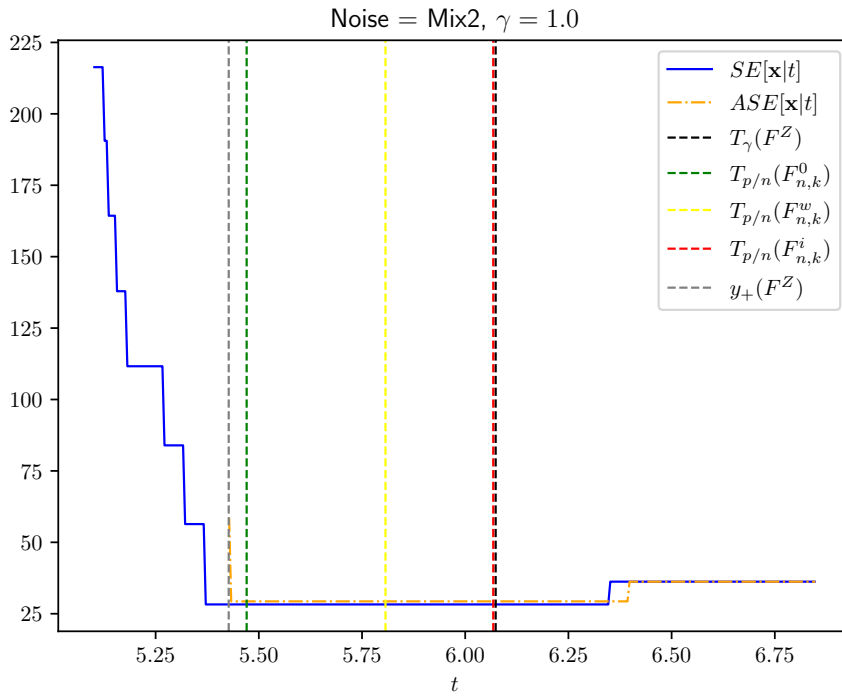


Figure 48: Experiment: **SE-vs-ASE**

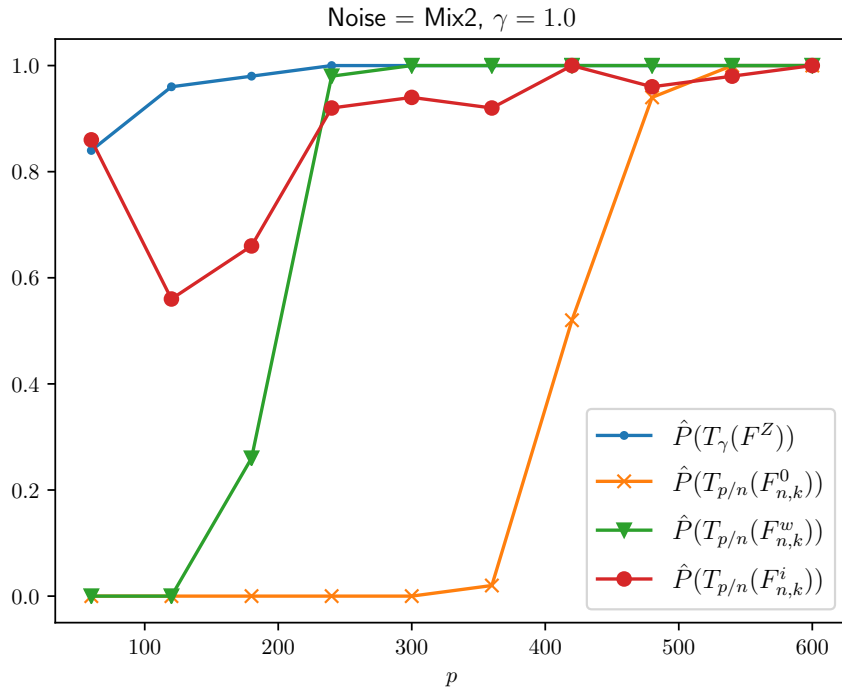


Figure 49: Experiment: **OracleAttainment**

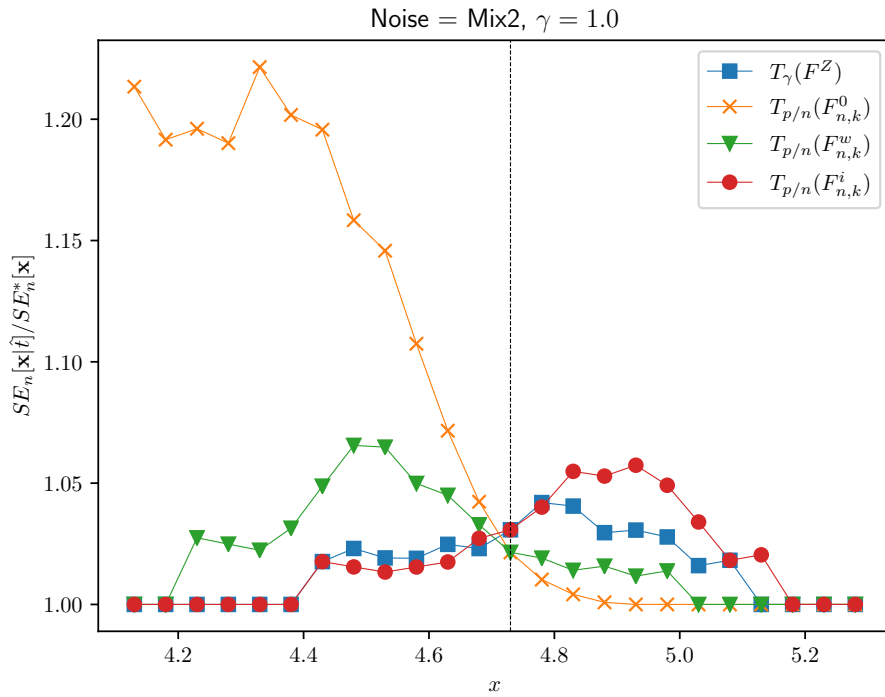


Figure 50: Experiment: **Regret**

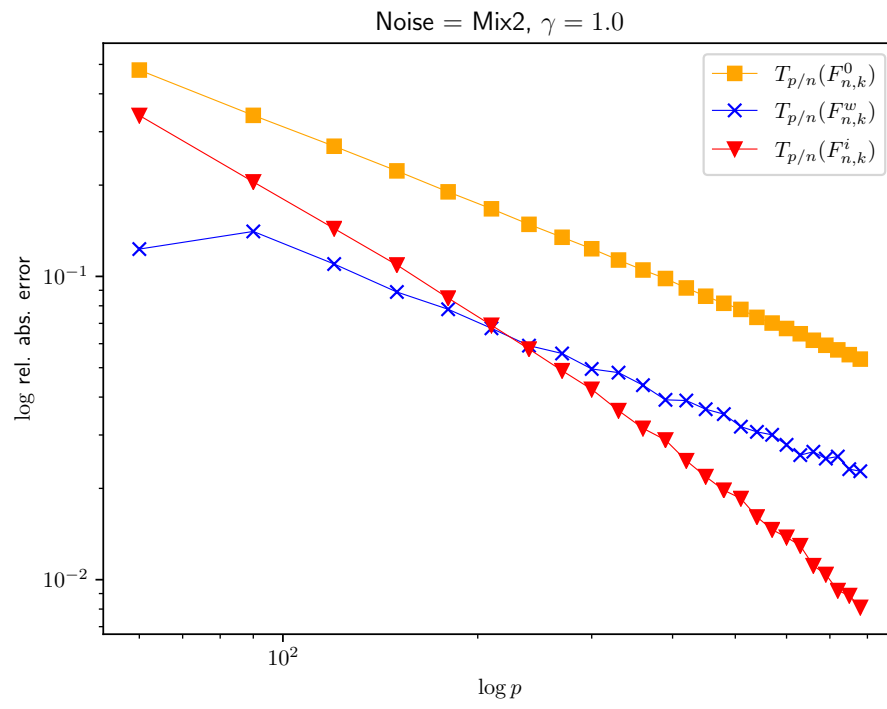


Figure 51: Experiment: **ConvergenceRate**

C.10 Distribution: Unif[1,10], $\gamma = 0.5$

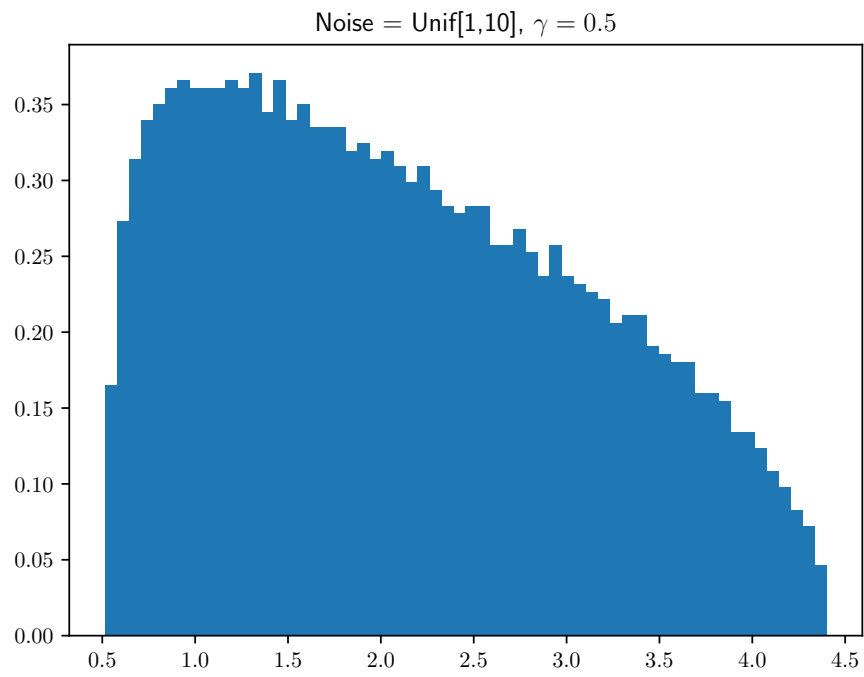


Figure 52: Experiment: **Hist**

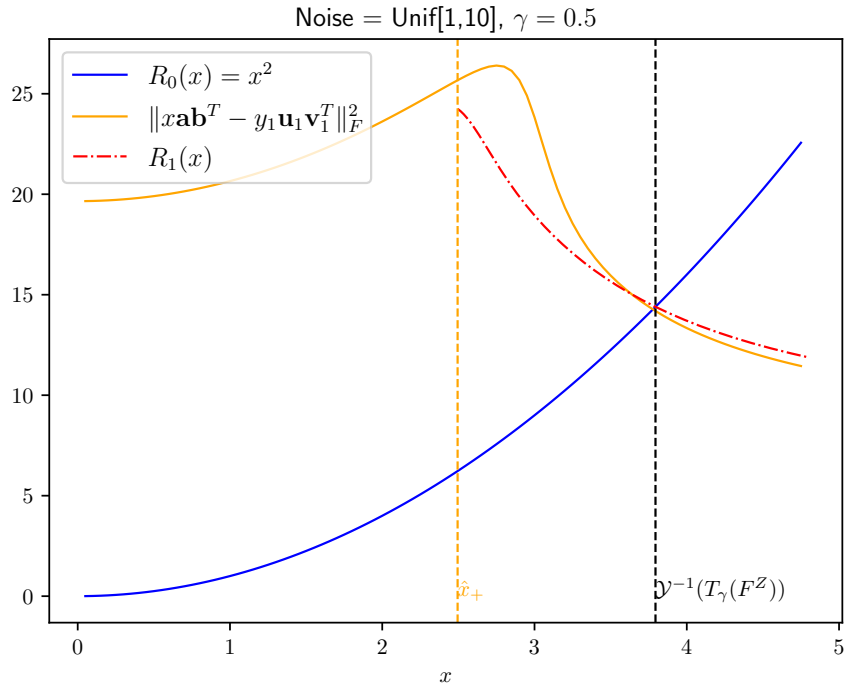


Figure 53: Experiment: **R0-vs-R1**

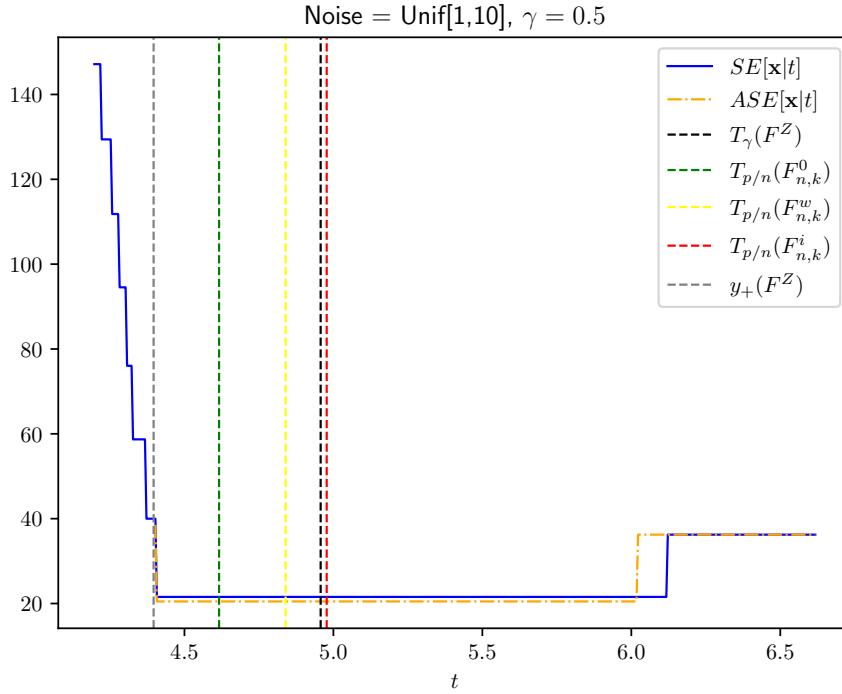


Figure 54: Experiment: **SE-vs-ASE**

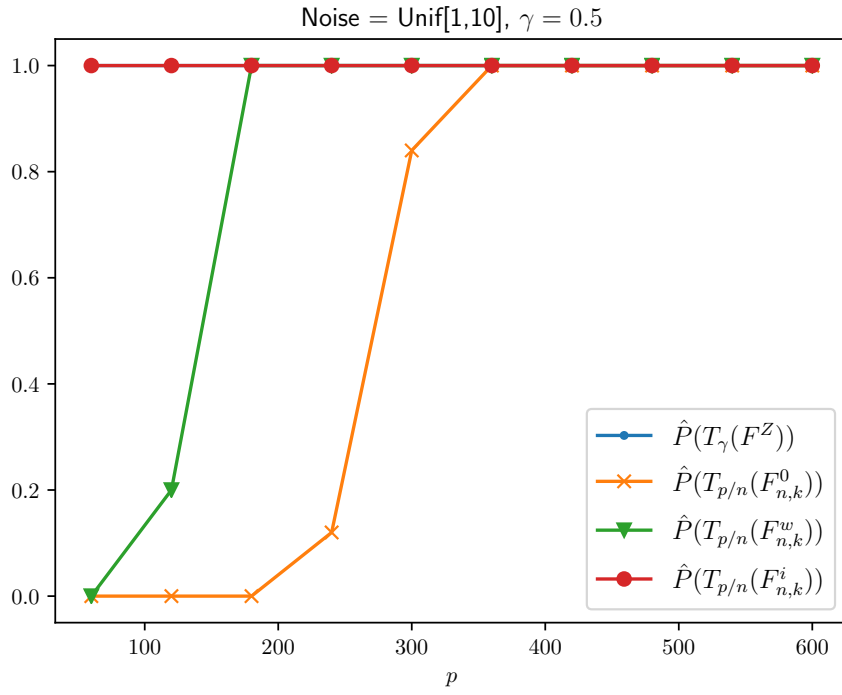


Figure 55: Experiment: **OracleAttainment**

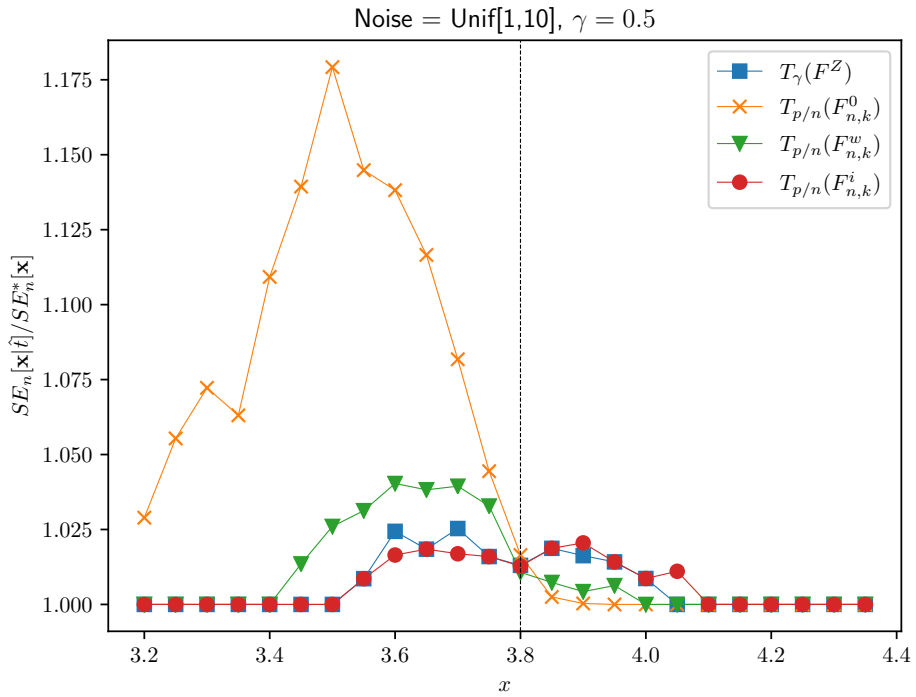


Figure 56: Experiment: **Regret**

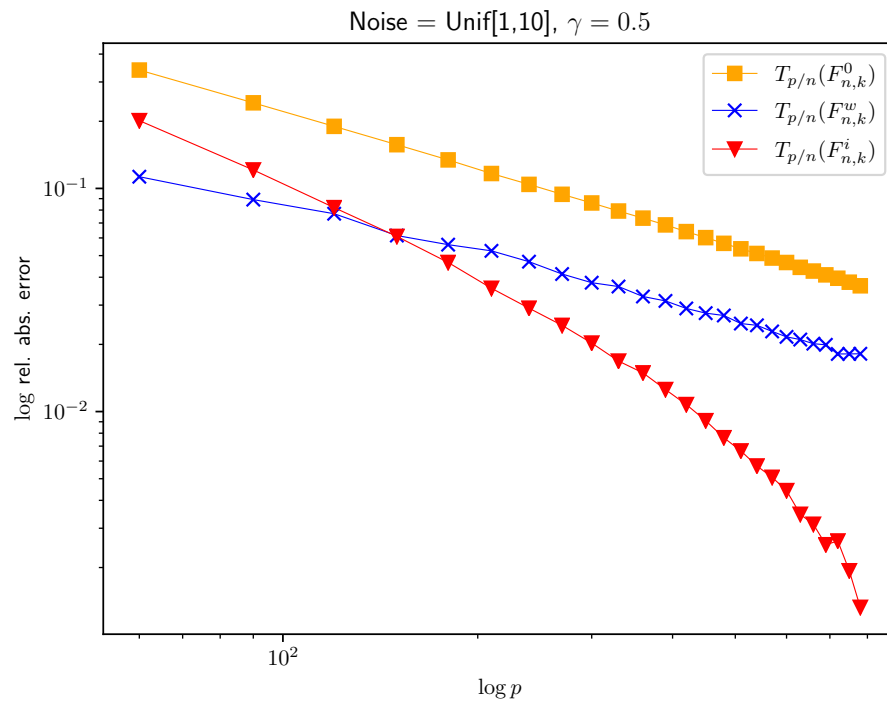


Figure 57: Experiment: **ConvergenceRate**

C.11 Distribution: Unif[1,10], $\gamma = 1.0$

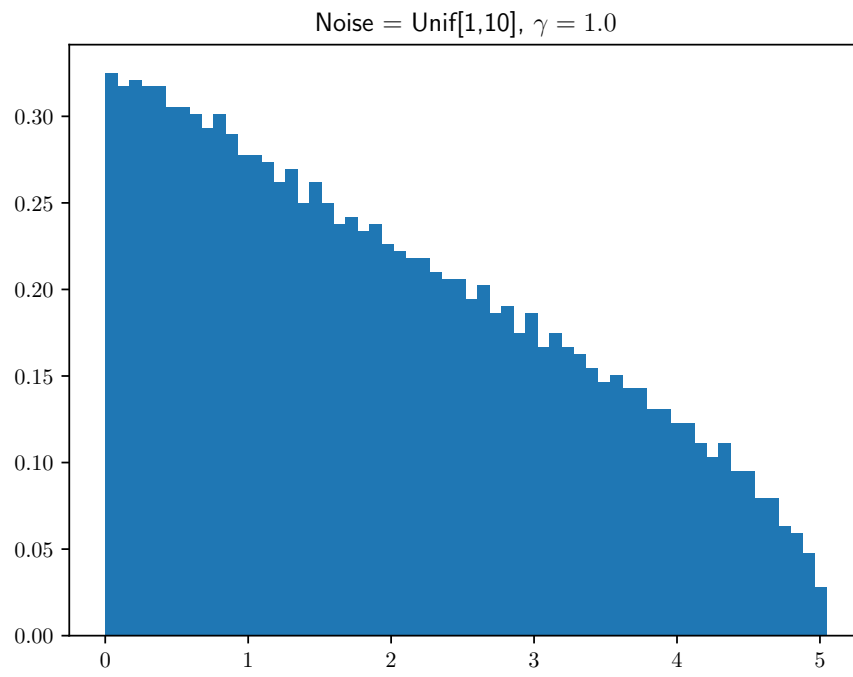


Figure 58: Experiment: **Hist**

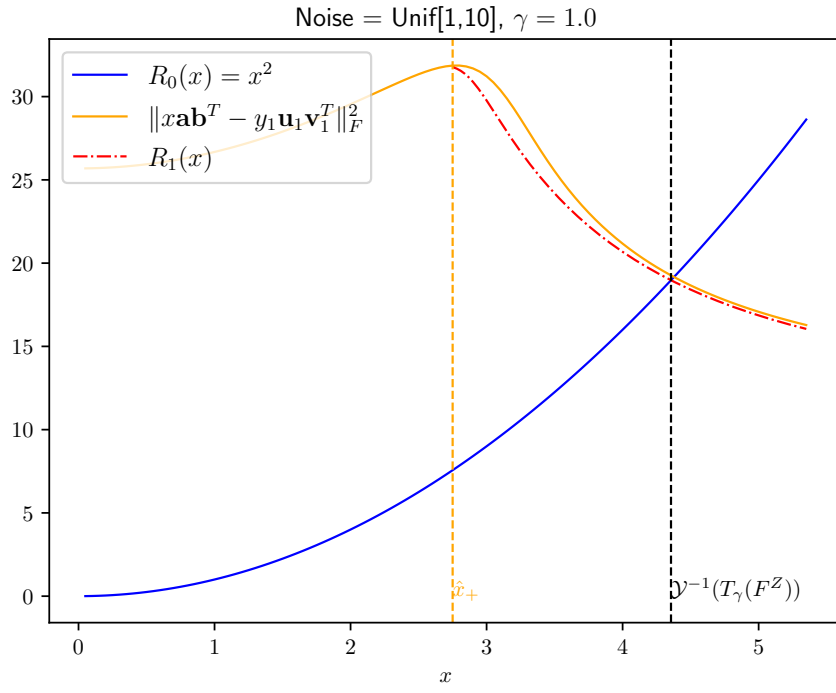


Figure 59: Experiment: **R0-vs-R1**

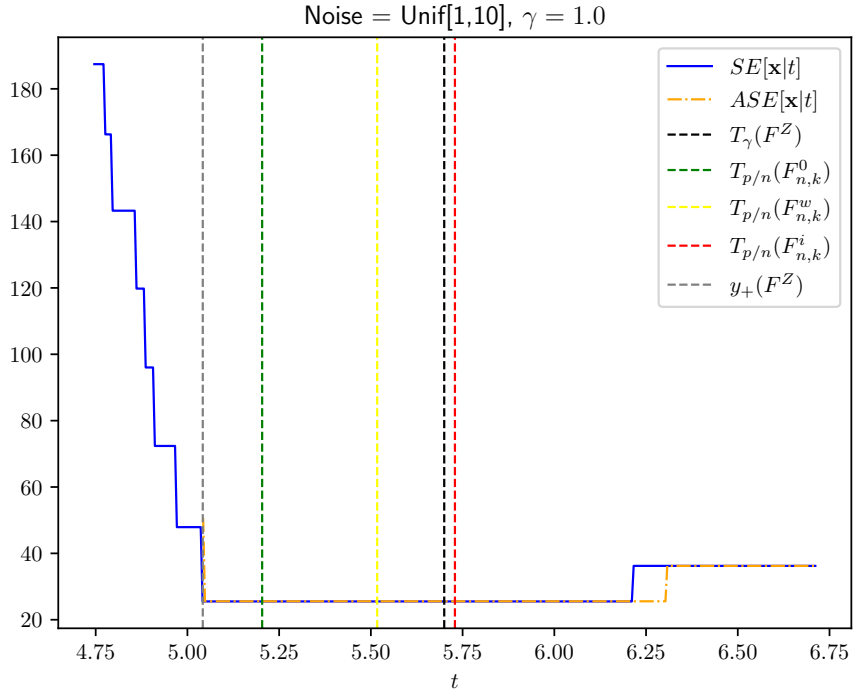


Figure 60: Experiment: **SE-vs-ASE**

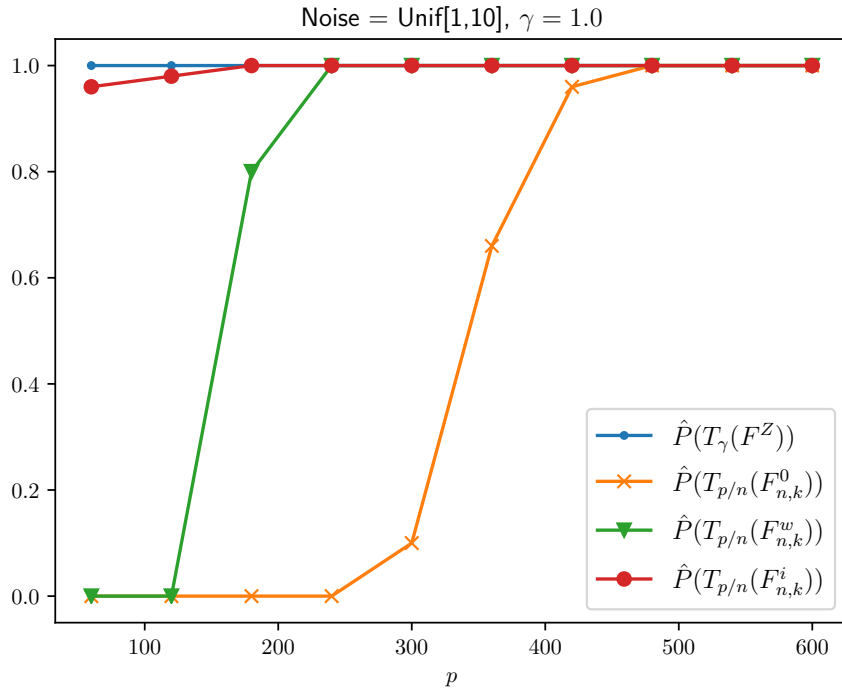


Figure 61: Experiment: **OracleAttainment**

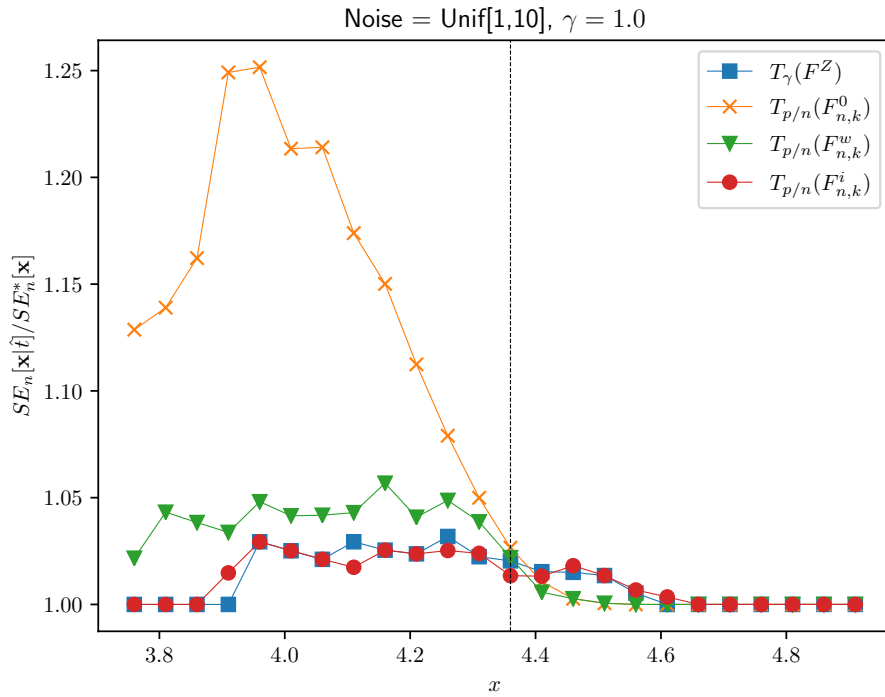


Figure 62: Experiment: **Regret**

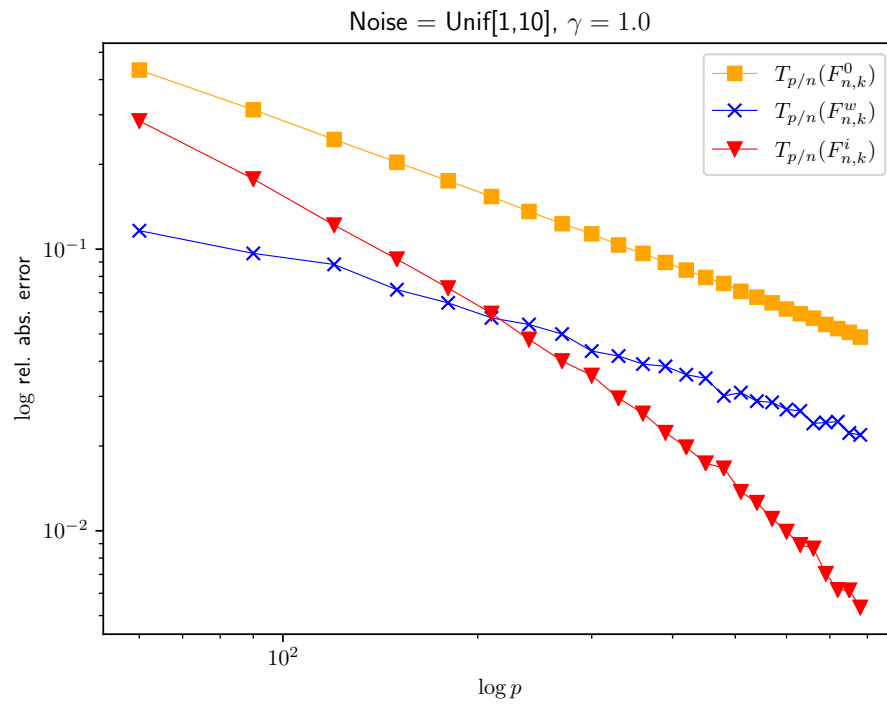


Figure 63: Experiment: **ConvergenceRate**

C.12 Distribution: PaddedIdentity, $\gamma = 0.5$

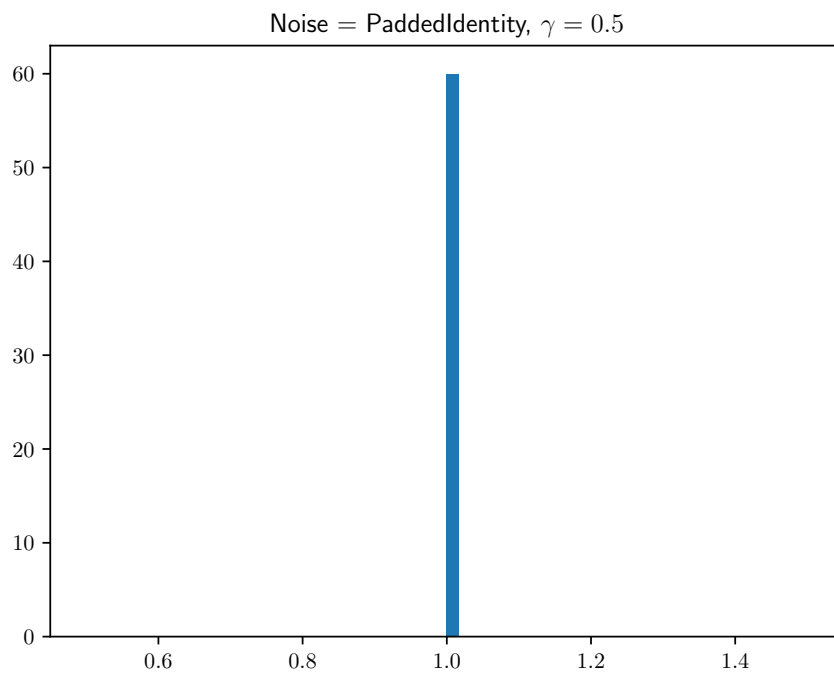


Figure 64: Experiment: **Hist**

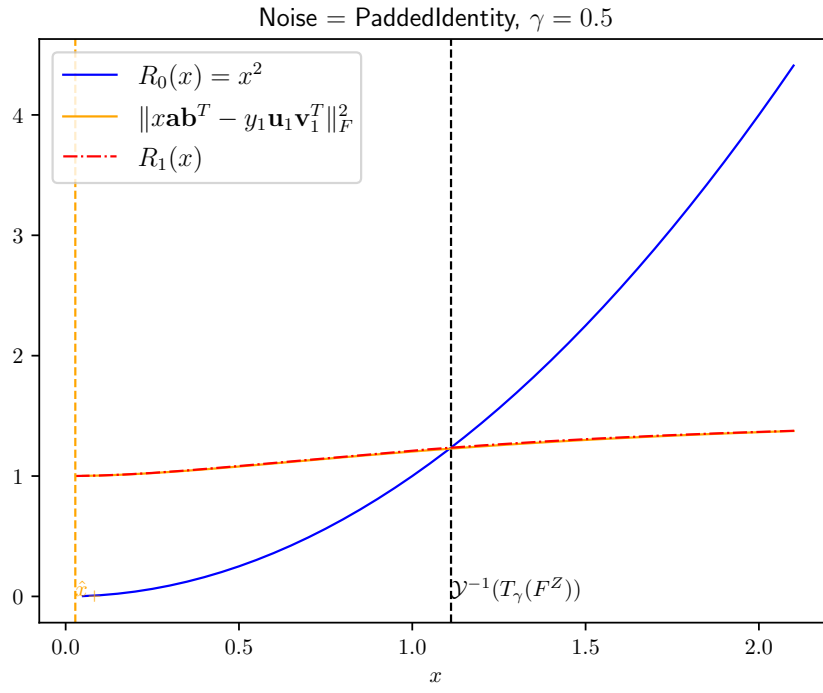


Figure 65: Experiment: **R0-vs-R1**

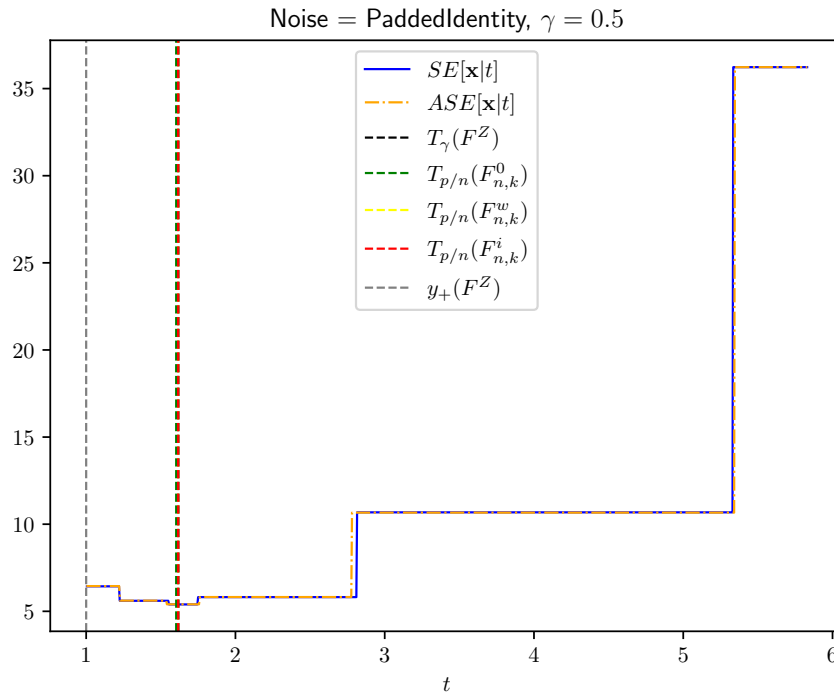


Figure 66: Experiment: **SE-vs-ASE**

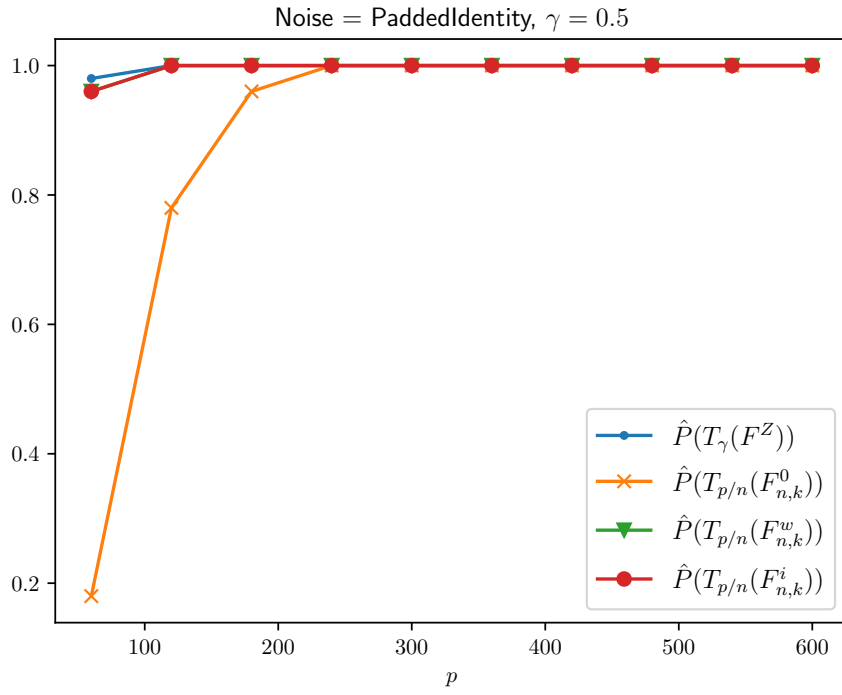


Figure 67: Experiment: **OracleAttainment**

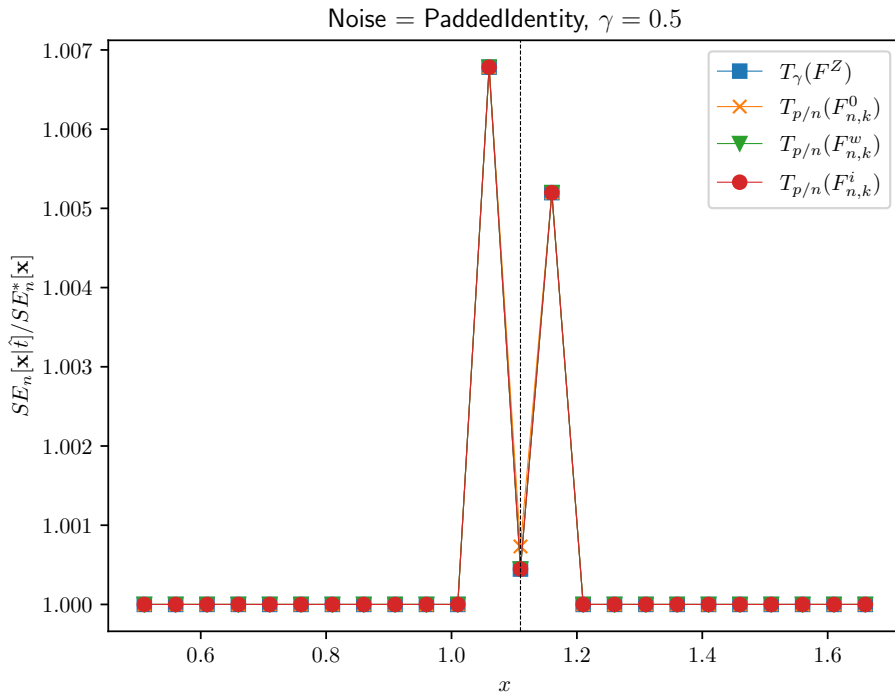


Figure 68: Experiment: **Regret**

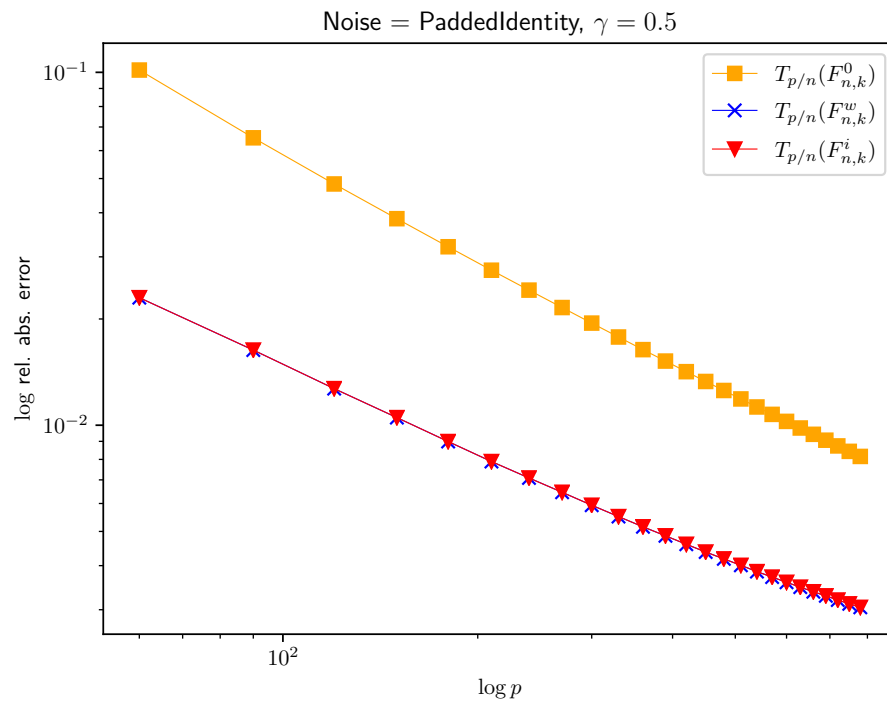


Figure 69: Experiment: **ConvergenceRate**

C.13 Distribution: PaddedIdentity, $\gamma = 1.0$

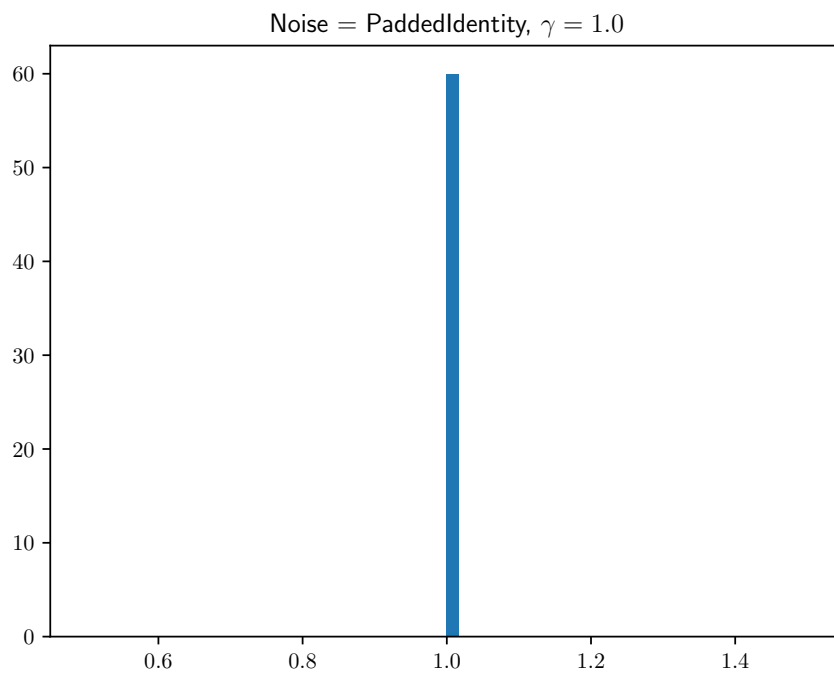


Figure 70: Experiment: **Hist**

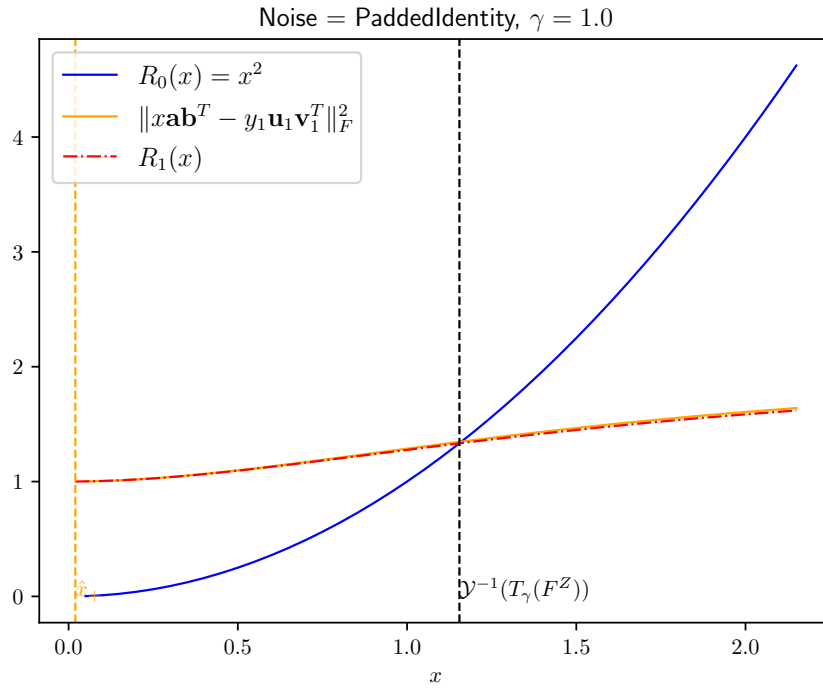


Figure 71: Experiment: **R0-vs-R1**

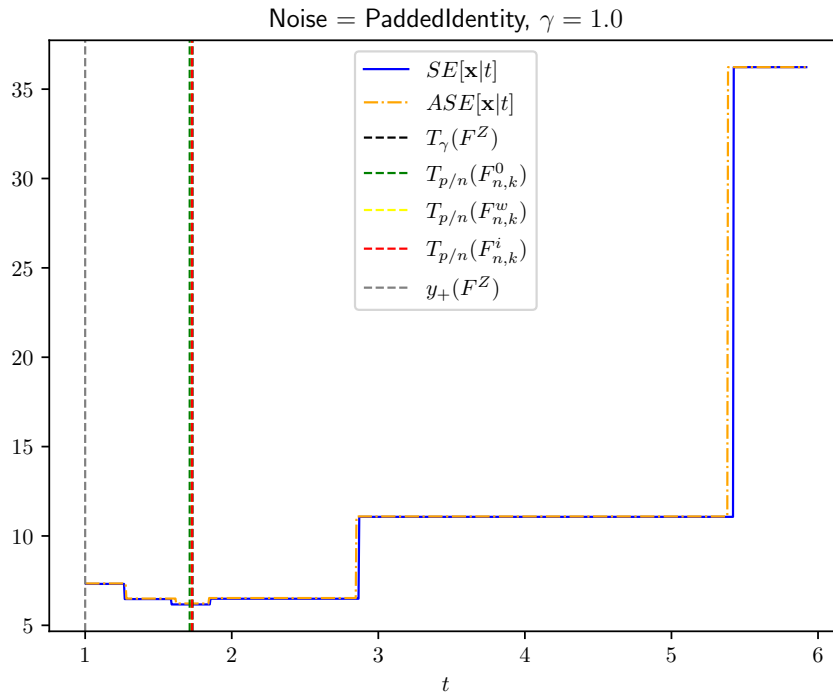


Figure 72: Experiment: **SE-vs-ASE**

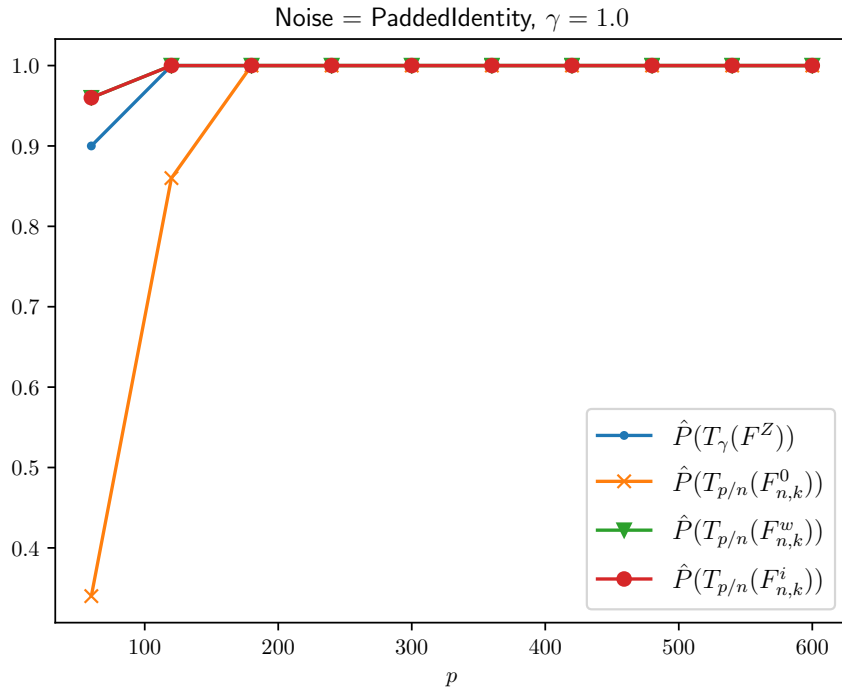


Figure 73: Experiment: **OracleAttainment**

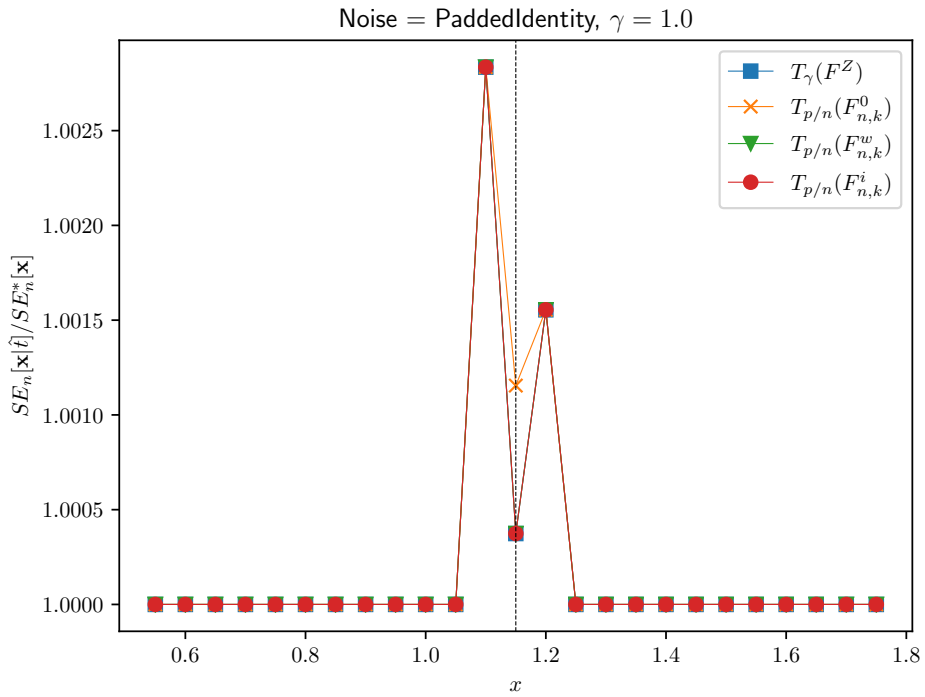


Figure 74: Experiment: **Regret**

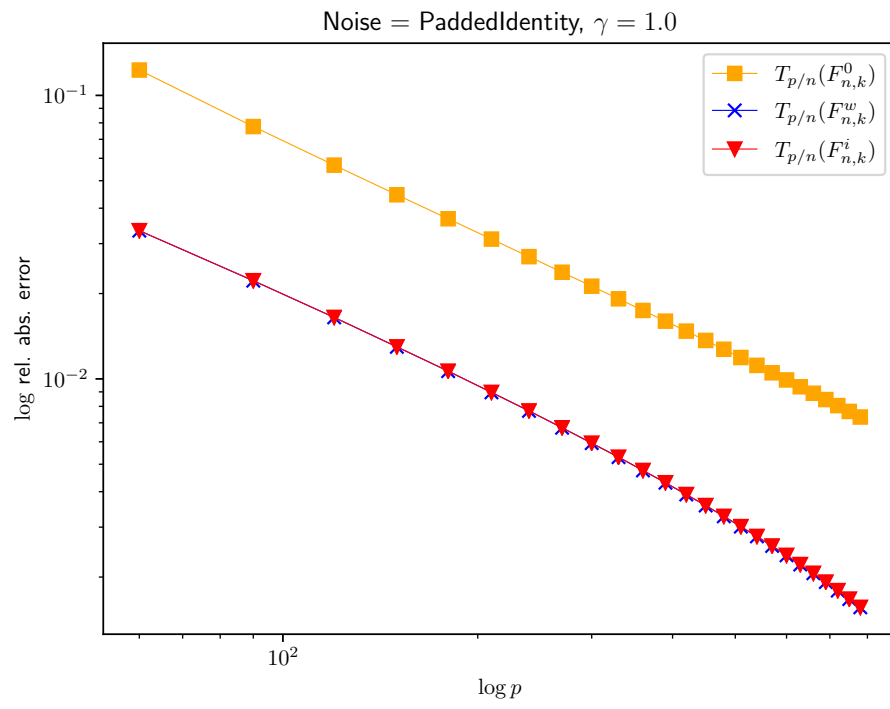


Figure 75: Experiment: **ConvergenceRate**